IJEST

ISSN: 0973-6255
Vol. 7 No. 2
July - December 2013

Indian Journal of Engineering, Science, and Technology

A Refereed Research Journal

Published by

BANNARI AMMAN INSTITUTE OF TECHNOLOGY

(Autonomous Institution Affiliated to Anna University of Technology, Coimbatore - Approved by AICTE - Accredited by NBA and NAAC with "A" Grade)
Sathyamangalam - 638 401 Erode District Tamil Nadu India
Ph: 04295-226340 - 44 Fax: 04295-226666
www.bitsathy.ac.in E-mail: ijest@bitsathy.ac.in

BANNARI AMMAN INSTITUTE OF TECHNOLOGY
Stay Ahead

TÜV NORD ISO 9001

Indian Journal of Engineering, Science, and Technology

IJEST is a refereed research journal published half-yearly by Bannari Amman Institute of Technology. Responsibility for the contents rests upon the authors and not upon the IJEST. For copying or reprint permission, write to Copyright Department, IJEST, Bannari Amman Institute of Technology, Sathyamanagalam, Erode District - 638 401, Tamil Nadu, India.

Indian Journal of Engineering, Science, and Technology

ISSN: 0973-6255

Volume 7 Number 2 **July - December 2013**

CONTENTS

Excerpt from the Proceeding of National Conference

Physical, Mechanical and Electrical Characterization of Composites Made Out of Waste CD

Shivanand Yali
Assistant Professor, Department of Mechanical Engineering, Basaveshwar Engineering College, Bagalkot-587102, Karnataka

Abstract

Compact disc is one of the electronic wastes increasing tremendously in recent years. There is a need of recycling of compact disc for making composites. So composite materials which can combine the metal with polymers were investigated. The present work aims at fabrication of polymer composites with polycarbonate as matrix and Aluminium as reinforcement both recovered from waste Compact Discs. It also aims at studying the properties like electrical conductivity, tensile strength and bending strength of the composites obtained from waste CDs.

Keywords: *Aluminium Reinforcement, Aluminium whiskers, Compact Discs, Composite materials, Polycarbonate, Polymer composites.*

1. INTRODUCTION

Materials have been very important in the history of humans. One of the more important groups of materials in our lives today is composites. The recent times have seen an additional emphasis where efforts are directed at developing cost- effective materials and then in the recycling of /salvaging the damaged-while-in-use materials. From the literature survey, it is obvious that every year huge amounts of compact discs are discarded all over the world. The non-biodegradable polycarbonate, heavy metals and harmful dyes of the discs lead to serious pollution problems. Hence there is a need to recycle the CD'S to make composite and study the properties. Present work aims at recycling compact disc to make less expensive, more efficient composite. The study encompasses factors such as effect of volume fraction and whisker size of the Aluminium reinforcement.

2. OBJECTIVES

- Making polymer whisker composites by recycling the compact disc.
- To study the mechanical properties of the composite.
- To study the electrical conductivity of the composite.
- To evaluate the effect of volume fraction of Aluminium on mechanical property of the composite.
- To study the density variation in the composite.

3. EXPERIMENTAL

3.1 Materials

Polycarbonate as a matrix: Polycarbonates are a particular group of thermoplastic polymers. They are easily worked, molded, and thermoformed. Their interesting features are temperature resistance, impact resistance and optical properties. Polycarbonate plastic used is recycled from waste CD.

Aluminium Whisker as Reinforcement: Aluminium is Silvery-white to grey having density of 2.7 g/cm^3 and melting temperature of 660^{0}C. Aluminium whiskers used as reinforcement in the composite are taken from recycled compact disc.

3.2. Preparation of Specimens

Open moulds for tensile and bending specimens are selected. Teflon coating was made to the mould surface for easy releasing of composite specimens. Weighed amount of polycarbonate granules and Aluminium whiskers of specified sizes are mixed and poured in the mould, then the mould with composite mixture kept in vacuum oven to temperature of 270^{0}C. Once it reaches to 270^{0}C it kept for slow cooling in the vacuum oven only.

3.3. Experimental Setup

Electrical conductivity: Electrical conductivity is measured by resisitivity meter. So initially resisitivity measured and then converted to electrical conductivity. Electrical conductivity is the reciprocal of the resisitivity.

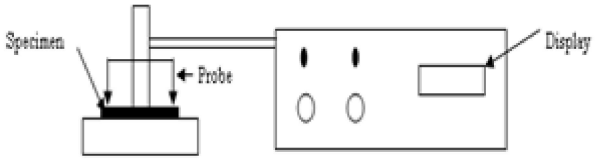

Fig.1 Setup for measuring conductivity

Tensile & Bending Strength: The tensile strength and bending strength tests were carried out using UNITEK electronic universal testing machine of model universal 2001 panel and loading ranges up to 50 KN.

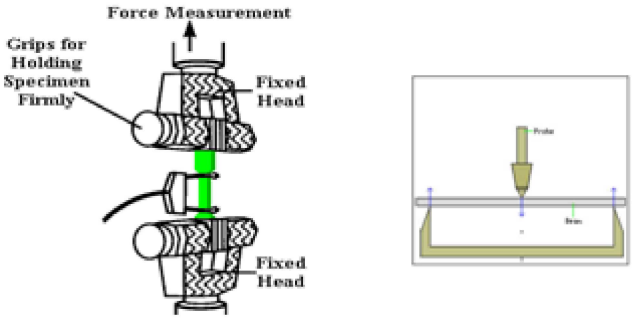

Fig.2 Setup for mechanical testing

4. RESULTS & DISCUSSIONS

4.1Results of screening experiments: The following Figure 3, 4, 5 and 6 describes the screening results of an experiment.

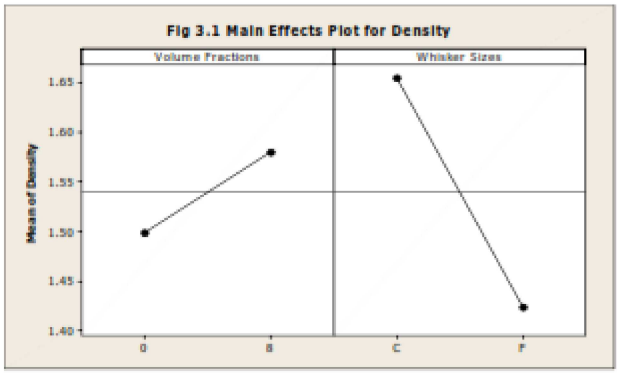

Fig.3 Screening design for density

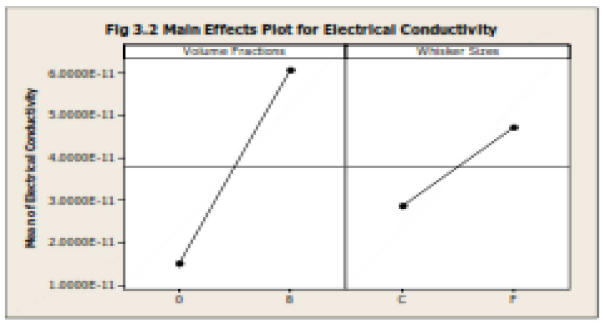

Fig.4 Screening design for electrical conductivity

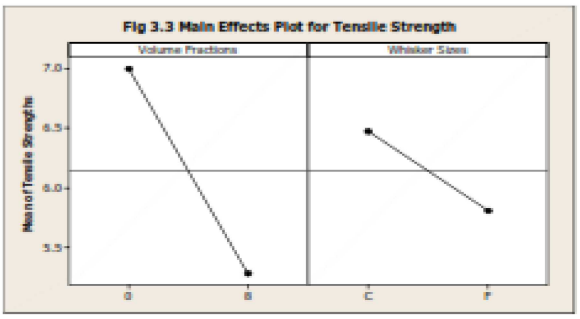

Fig.5 Screening design for tensile strength

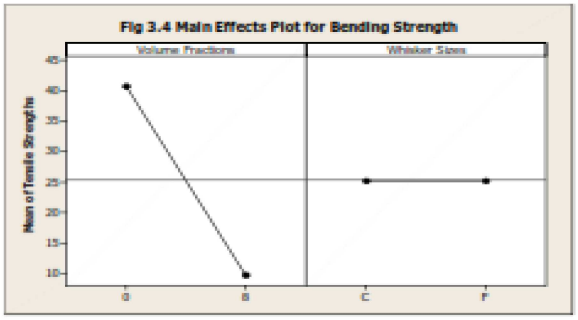

Fig. 6 Screening Design for Bending Strength

From Figure 3, 4, 5 and 6 it was found that the volume fraction is more dominant factor

4.2Results of Full Factorial Experiments:

4.2.1 Physical Properties: The physical properties of the experiment were discussed in this section.

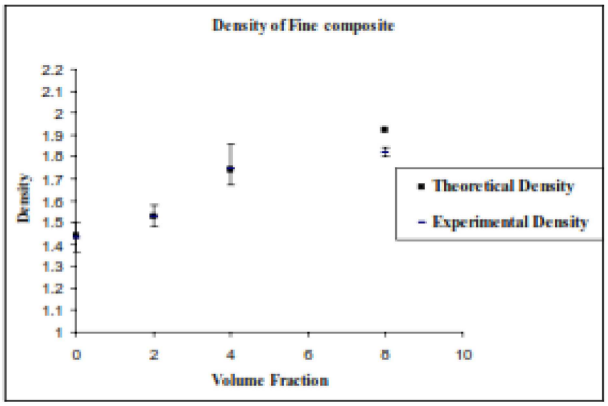

Fig.7 Density of composite with fine aluminium reinforcement

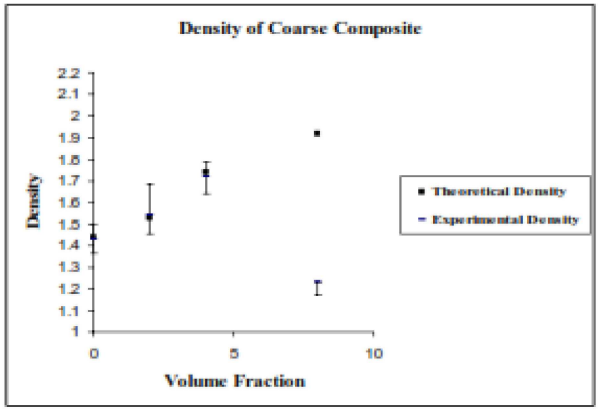

Fig.8 Density of composite with coarse aluminium reinforcement

From Figure 7 and 8, it can be noticed that experimental values of density are almost matching with the theoretically computed values for lower volume fractions. It may also be observed that at higher volume fraction density is decreasing which could be attributed to lack of filling filler (Aluminium) in the composites.

4.2.2 Electrical Properties:

The electrical properties of the experiment were discussed in this section.

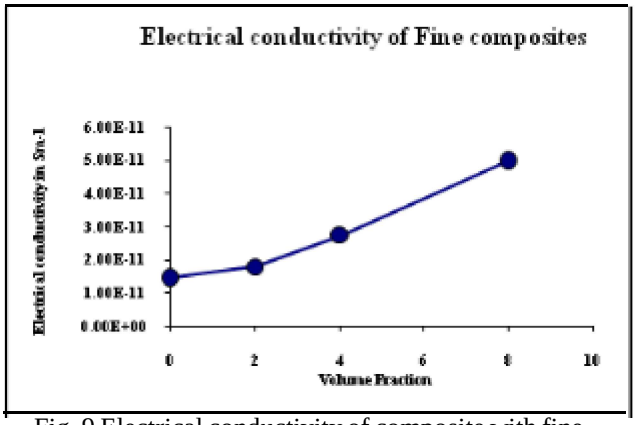

Fig. 9 Electrical conductivity of composite with fine aluminium reinforcement

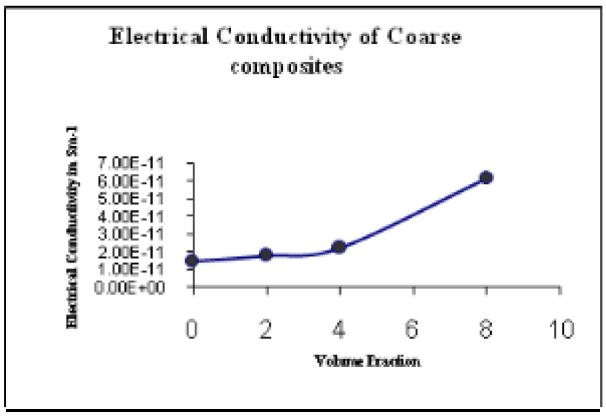

Fig.10 Electrical Conductivity of Composite with Coarse Aluminium Reinforcement

From Figure 9 and 10 describes the electrical conductivity of an experiment, it can be noticed that the electrical conductivity increases with volume fraction in both cases.

4.2.3 Mechanical Properties: The mechanical properties of the experiment are discussed in this section.

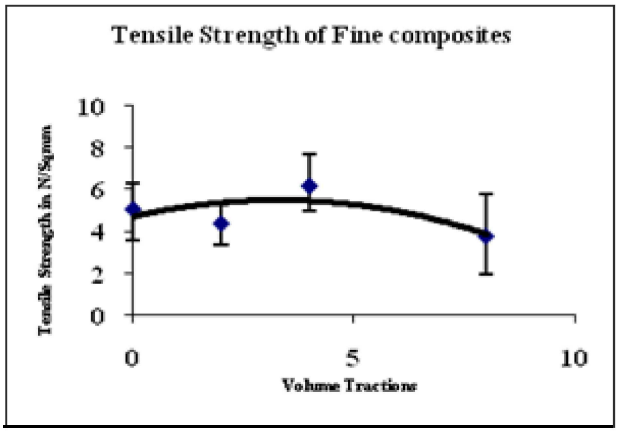

Fig.11 Tensile strength of fine composites

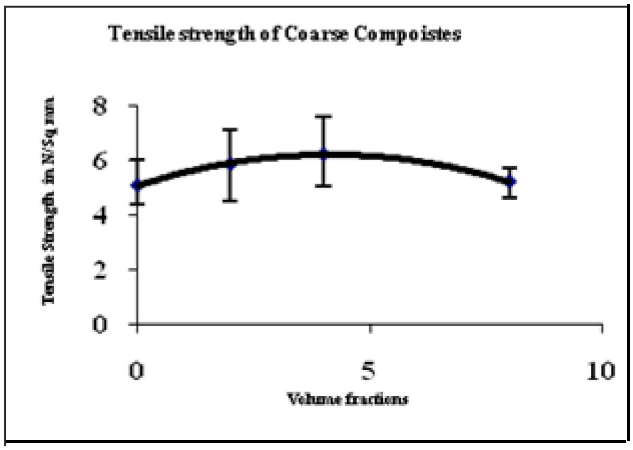

Fig.12 Tensile strength of coarse composite

From Figure 11 and 12, it is observed that, the strength shows initial increment but decline with a further increase in volume fraction of fillers.

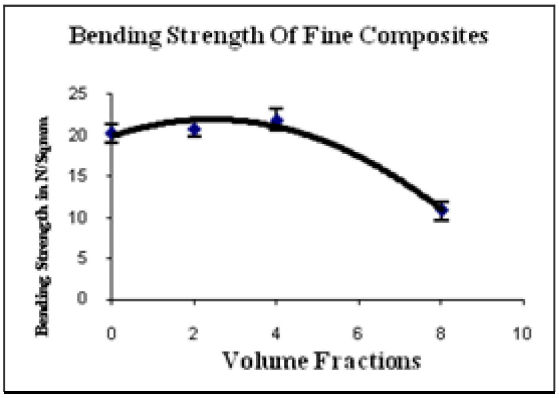

Fig.13 Bending strength of fine composites

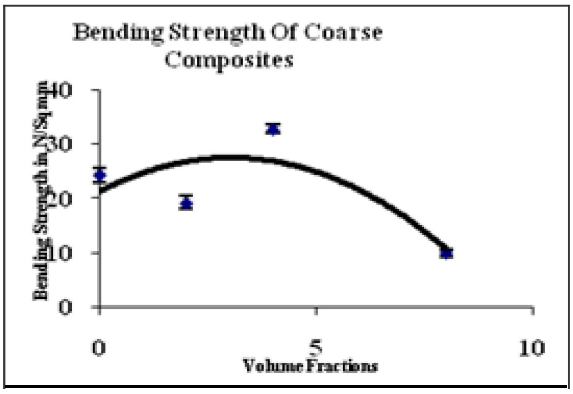

Fig.14 Bending strength of course composite

From Figure 13 and 14, it can be observed that the strength shows initial increment but decline with a further increase in volume fraction of fillers.

5. CONCLUSIONS

From the experimental results it is concluded as follows:

- Theoretical and experimental densities which are matching at lower volume fractions and is showing deviations at higher volume fractions due to lack of filling the filler.
- Electrical conductivity of the coarse and fine composites increases with increase in volume fraction of filler.
- Tensile strength shows initial increment but decline with a further increase in volume fraction of fillers.
- Bending strength shows initial increment but decline with a further increase in volume fraction of filler.

REFERENCES

[1] B. M.Daniel and L. D.Steven, "Introduction to Composites", Air Force Research Laboratory

[2] J. Riihimδki, "CD - Scrap Recycling Internal Report", Helsinki Univ. of Technol, Energy Engineering and Environmental Protection, Vol.27, 2001.

[3] K.C. Pohimann, "The Compact Disc: A Handbook of Theory and Use", MADISON, Wisconsin, 1989.

[4] J. Scheirs, "Polymer Recycling", CHICHESTEFR, UK: John Wiley & Sons 1998.

[5] C. Douglas, "Montgomery, Design and Analysis of Experiments", WILE PUBLICATION, 5th edition, 2001.

[6] K.A. Boudreau and R.A. Malloy, "A Method for the Recovery and Recycling of Polycarbonate from Optical Media Disc Application", Polymeric Materials Science and Engineering, Proceedings of the ACS Division of Polymeric Materials Science and Engineering, Washington, DC, USA, 67, 1992, pp.401-403.

Application of Non-Traditional Optimization Techniques in Measuring the Profitability of Banks

K.Venkatesh[1], R.Muruganandham[2] and K.Ravichandran[3]

[1&2]Department of Mechanical Engineering, Thiagarajar College of Engineering, Madurai – 625 015, Tamil Nadu

[3]Professor and Head, Department of Entrepreneurship Studies, School of Business Studies, Madurai Kamaraj University, Madurai - 625 021, Tamil Nadu

Abstract

Amidst jam-packed economic scenario, every month the financial institutions used to launch several schemes to be competitive. Although some of the banking sectors are failing to sit above the salt. They are failing may be of high liabilities, low profits, low interest rates and so on. The objective of this paper is to identify the highly profitable bank from both commercial banks of India. With the help of Ratio Analysis, financial status could be easily analyzed and judged. In order to study the profitability of the banks, Multi Criteria Decision Making (MCDM) tool called Fuzzy Logic Decision Making (FLDM) approach is applied in the paper. Finally, the suggestions are also given to enhance the profitability.

Keywords: *FLDM, Profitable and Commercial banks.*

1. INTRODUCTION

The banking industry is undergoing a dramatic change in the global economy. Banks seeking to delve new ideas to reduce their exposure and related risk-based capital requirement to corporate credit have found derivatives to be more efficient than securitization. The challenges and competitions in the Indian banking sector is conspicuously high. Some tremendous challenges have been occurred after liberalization. Banking sector broadly classified into commercial banks and co- operative banks. Commercial banks further divided into nationalized banks and private and foreign banks. While nationalized banks lead in their role in deposits and advances, private and foreign banks has brought the real action in this industry where co-operative banks focussing on services to revamp the growth of the people of India and make them more accessible to their target audience. Every split second, banking sector focussing on recording the issues and the needs of customers. The term profit is an accounting concept which shows the excess of income over expenditure viewed during a specified period of time. Profit is the main reason for the continued existence of every commercial organization. On the other hand, the term profitability is a relative measure where profit is expressed as a ratio, generally as a percentage.

Profitability (Yogesh Maheswari, 2005) depicts the relationship of the absolute amount of profit with various other factors. Profitability is a relative concept which is quite useful in decision making. Profitability is the most important and reliable indicator as it gives a broad indicator of the ability of a bank to raise its income level. Another main issue here is profit planning, which consists of various steps to be taken to improve the profitability of the bank. Introducing a new scheme to the people by considering the profitability on one hand and their growth on the other hand are little bit tedious task. Marketing a latest scheme to the people through dead tree media, advertisements in televisions and radios will create an immovable move. The nationalized banks, (Narinder Kaur and Reetu Kapoor, 2007) in spite of being played a major role in deposits and advance, private banks are highly profitable compared to other banks.

2. METHODOLOGY

The methodology of the paper is presented below,

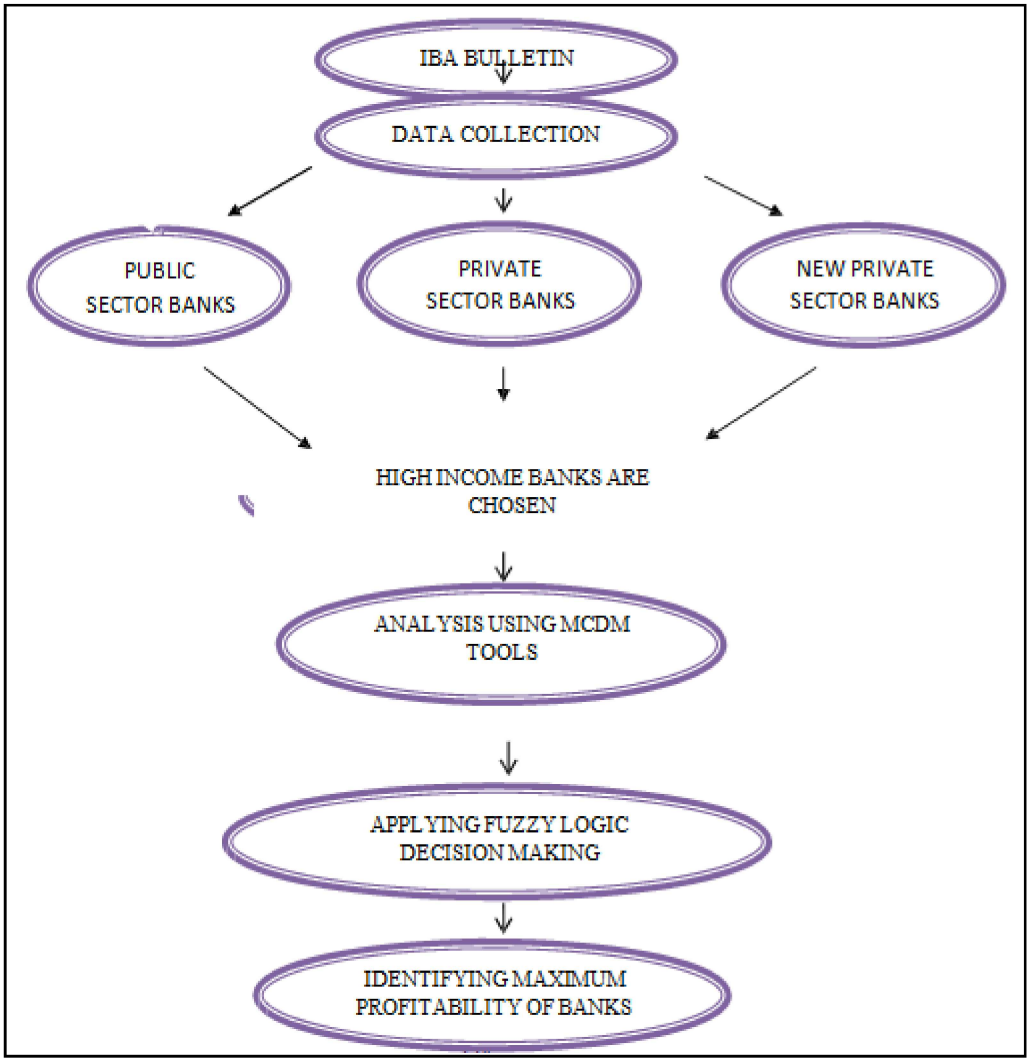

Fig.1 Methodology

The methodology of the paper is the data collection from IBA bulletin (As on March'31, 2011), then this data is proselytized into independent fuzzy sets and finally obtaining the fuzzy membership grade. The data were identified by considering the high total income.

3. FINANCIAL INSTITUTION

A bank is nothing but a financial institution that accepts deposits from the customers and the channels those deposits into lending activities. Banks borrows money through funds deposited on current accounts by accepting term deposits, and by issuing debt securities such as banknotes, bonds etc. Financial institutions also enable customer payments through various payment methods such as Automated Teller Machine (ATM), Wire transfers, Automated Clearing House (ACH) etc. Financial institution (Prasanna Chandra, 2007) plays an important role in economic development of the country.

The contributions of banking sector in economic development are capital formation, acts as a link between organized and unorganized sector, acts as a catalyst in social change, regulate the flow of national savings. Banking not only helps in capital formation but also in effective implementation of the monetary policy, development of industries, entrepreneurship and maintaining the balancing between the trade. A country with a financial institution (Sundaram, 2009) has a secure foundation for the economic development. It plays a major role in all sectors. It is becoming a major part of the country. The objective of the financial institution is to generate revenue by proffering loans which includes secured and unsecured loans, demand loan and subsidized loans because for the economic development, financial institution is necessary. It seems that Indian banking history is full of competition due to liberalization. Due to obsessed pace, financial institutions are performing well to a great extent by providing many

features to the invaluable customers. The financial institution is highlighted only because of high customers in numbers, high non-interest income, low expenditure, profit per employee and so on. The per employee includes deposit per employee, advance per employee, business per employee, total expenditure per employee, total income per employee, spread per employee, net profit per employee and burden per employee.

3.1 Services Offered By Financial Institutions

The major services offered by the financial institutions are cashless cards, insurance products, accepting deposits, granting loans, providing lockers and sell investment products.

3.2 Net Profit

Every business exists in order to earn profit. Without profit no commercial activity can sustain for a long period. Similarly, profit earning has become the main motive of commercial banks operating in India. Profit earning and timely growth in the profit earning is an essential feature for the continued success of a bank.

3.3 Total Expenditure

As far as the expenditure of public/private sector banks is concerned, it is fixed to a large extent because these banks cannot reduce labour force as the other industries can do in order to minimize their expenditure but in the recent years banks have taken some steps in this respect. The main components of the bank expenditure are interest on deposit, establishment expenditure and other expenditure.

3.4 Profit per Employee

It is used to identify the higher productivity of a bank. It looks at a company's sales in relation to the number of employees they have.

Above three parameters plays a major role in identifying the profitability.

4. FUZZY LOGIC DECISION MAKING

The concept of fuzzy logic was first coined by Lofti Zadeh in 1965. The concept of fuzzy set helps us to unravel the quantum of uncertainty associated with events. These events may be well defined engineering problems, such as design and development, control system design or fabrication of machine tools. The inputs may be time-varying, interactive in nature leading to multi input, multi output system. Thus each system possesses a degree of uncertainty associated with them. There are different faces of uncertainty. They are Inexactness – Inability to measure variables in precise manner. Semantic ambiguity – Property of possessing several distinct, but plausible and reasonable, interpretations of a particular state. Visual ambiguity – Refers to or arises due to the position or location or trajectory of an object or a system due to the representation of the object or observer position with reference to object. Structural ambiguity – The interconnections and interactions of different components can cause a high level of vagueness. Undecidability – This originates from our responsibility of discriminating different systems of an event.

4.1 Fuzzy Sets

To overcome above limitations fuzzy sets (Mohanty, 2005) could be used.

A variable in a fuzzy set will have a minimum value and a maximum value, the two values encompassing all values between. The range of values covered by a particular fuzzy set is termed as a domain of fuzzy set.

4.2 Fuzzy Decision Making Method

Classical decision making involves the notion that the uncertainty in future can be characterized probabilistically. If we knew about the states of future with certainty there is no problem. But it is not so. In many cases there is a high uncertainty about
the states in future. So we make use of classical Bayesian decision methods in which we make use of prior probabilities or weightings.

Fuzzy logic decision making is based on the following equation,

$\mu Z\text{-}p\ Wi\mu i$
(1) Where i= 1 to n

W_i – weightings

μi – Membership grade for each individual input
μ – Output membership grade

5. DATA COLLECTION

The data with regards to total income are collected from recently published IBA bulletin (IBA BULLETIN). A lot of multi criteria decision making (MCDM) tools like Analytical Hierarchy Process (AHP), Simple Additive Weighting (SAW), Graph Theory and Matrix Approach (GTMA) etc. were considered. However, Fuzzy logic decision making (Sundareswaran, 2008) approach has been successfully applied to analyze and rank the banks. The data collection is as follows,

Table 1 Data Collection (As on March'31, 2011) (in Crores)

Banks	Total Income	Operating Expenses	Business per Employee	Profit per Employee	Net NPA to Net Advances (in %)
Canara Bank	25752	4419	11.99	0.0976	1.10
Punjab National Bank	30599	6364	10.18	0.0835	0.85
State Bank of India	97219	23015	7.04	0.0384	1.63
The Federal Bank Ltd.	4569	836	9.23	0.0726	0.60
ICICI Bank Ltd.	32622	6617	7.35	0.1000	1.11
HDFC Bank Ltd.	24263	7153	6.53	0.0737	0.19
Axis Bank Ltd.	19787	4779	13.66	0.1400	0.29

From the above table, the data collected from the IBA bulletin is displayed based on High Total Income (As on March'31, 2011).

6. FUZZY ANALYSIS

Fuzzy logic decision making approach is applied and the membership grades are shown below,

Table 2 Membership Grades

Banks	Membership Grades
Canara Bank	0.2648
Punjab National Bank	0.3147
State Bank of India	0.2743
The Federal Bank Ltd.	0.0469
ICICI Bank Ltd.	***0.3355***
HDFC Bank Ltd.	0.2496
Axis Bank Ltd.	0.2035

According to the above table, it delineates the membership grades for the selected banks. It is identified that the ICICI Bank Ltd. is highly profitable compared to all selected banks based on Income.

The challenges (Ravichandran *et al*., 2013) are,

Finally it is evident that the banks have to overcome the challenges like,

1. Quickly changing environment
2. Competitors
3. Consumer trust
4. Technology updating
5. Financial Services delivery
6. Poor marketing strategies adopted by nationalized banks.

7. CONCLUSION

The paper has made a mathematical and scientific approach to identify the highly profitable bank among

selected banks based on high total income. The result reveals that the ICICI bank is highly profitable than SBI, Axis, HDFC, The Federal Bank Ltd., Punjab National Bank and Canara bank.

8. FUTURE WORK

The analysis will be extended to foreign banks too. The parameters considered for these will be validated using other Multi Criteria Decision Making (MCDM) tools. The other parameters might be considered in future to analyze the profitability.

REFERENCES

[1] IBA bulletin
[2] B.K. Mohanty, "Product classification in Internet business- A fuzzy approach", International Journal in Decision Support Systems, 2005.
[3] B.K. Mohanty, "Tranquility and Anxiety in E-Business - A fuzzy approach", International conference on Advanced Computer Theory and Engineering, 2005.
[4] Narinder Kaur and Reetu Kapoor, "Profitability Analysis of Public Sector Banks in India", Indian Management Studies Journal, Vol.11, 2007.
[5] Prasanna Chandra, "Financial Management", Tata McGraw-Hill, 2007.
[6] N. Rajshekar, "Banking in the New Millennium", ICFAI Books, 2001.
[7] V. Sundaram, "Money Banking and Public Finance", Alfa Publications, 2009
[8] K. Sundareswaran, "A Learner's Guide to Fuzzy Logic", Jaico Books. Delhi, 2008.
[9] J. Timothy Ross, "Fuzzy Logic with Engineering Applications", Wiley India, Delhi, 2010.
[10] Yogesh Maheswari, "Managerial Economics", Prentice Hall of India Private Limited. New Delhi, 2005.
[11] K. Ravichandran, K.Venkatesh and R. Muruganandham, "Fuzzy Logic Based Profitability Analysis And Marketing Challenges In Commercial Banks", "Marketing Dynamics", Aruna Publications, Chennai, 2013, pp. 230-237.

Drag Force Reduction in Bus Using Computational Fluid Dynamics

T.V. Nageswaran[1] and P. Vijian[2]

[1] P.G. Scholar, [2] Head of the Department, Department of Mechanical Engineering, A.C.College of Engineering and Technology, Karaikudi - 630 004, Tamil Nadu

Abstract

There are millions of light trucks on the road today with suboptimal aerodynamic forms. Aerodynamics of trucks and other high sided vehicles is of significant interest in reducing road side accidents due to wind loading and in improving fuel economy. Previous research has found that several kilometres per litre can be saved by specifically tailoring vehicle bodies for reduced aerodynamic drag. In vehicle body development, reduction of drag is essential for improving fuel consumption and driving performance. One of the main causes of aerodynamic drag for vehicles is the separation of flow near the vehicle's rear end.

Since most of the work done has been predominantly on optimization of design of vehicles such as cars and trucks, it is a great challenge to look at other vehicle geometries, such as those of buses, where there has been significantly less work done. In this study, both two dimensional and three-dimensional near field flow analysis has been performed to understand the airflow characteristics surrounding a bus like bluff body.

Keywords: *Aerodynamic drag, Boundary layer, Computational Fluid Dynamics (CFD).*

1. INTRODUCTION

Automotive industries are growing exponentially all around the world. All the vehicles are striving to achieve better mileage along with the appearance. Heavy vehicles like trucks and buses face these kind of problems. To save energy and to protect the global environment, fuel consumption reduction is primary concern of automotive development.

Generally there are two ways to reduce the fuel consumption of a vehicle. One can improve the efficiency of the available power which means an increase of the power delivered by the engine or, on the other hand, the required power that is needed to overcome the forces needs to be lowered. Considering the latter, it signifies achieving a reduction of fuel consumption by minimizing the weight of the vehicle or reducing its aerodynamic drag.

Aerodynamic drag is the force opposite to the direction of motion that acts on a body moving through air say an automobile or a truck and retards its movement. The reduction of fuel consumption of heavy vehicles like trucks and buses by aerodynamic means has become an accepted practice in the last decades. Modifications of the main shape of the vehicle improved the aerodynamic efficiency in a positive way. Aerodynamic drag on vehicles can be reduced either by streamlining the body or by controlling the boundary layer separation.

2. DESIGN PROCEDURE

2.1 Modelling

The vehicle chosen for my project work is TATA STARBUS. Modelling was done according to the dimensions using the software GAMBIT 2.4.6. GAMBIT is a general-purpose pre-processor for CFD Analysis, which allows easier access into the CFD world. GAMBIT allows you to construct and mesh models by means of its graphical user interface (GUI).

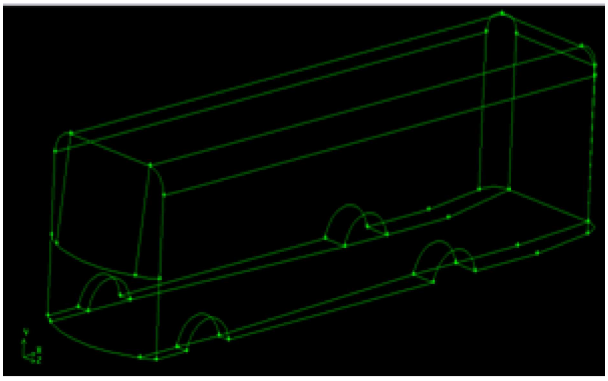

Fig.1 Isometric view of the vehicle

2.2 Meshing

A key step of the finite element method for numerical computation is mesh generation. One is given a domain and must partition it into simple "elements" meeting in well-defined ways. The grid designates the cell or elements and it is a discrete representation of the geometry of the problem. Meshing was done with the help of the software GAMBIT 2.4.6. It offers the unique advantage of both structured and unstructured meshing, so while idealized geometries can be created very quickly, innovative design features may also be incorporated and their effects analyzed. GAMBIT's meshing toolkit helps to decompose geometries for structured hex meshing or perform automated hex meshing with control over clustering.

Meshing will be done, where the flow has to be studied. Here, the mesh was done around the vehicle. The model is decomposed to accommodate both the Hexahedral elements and Tetrahedral elements. Three dimensional model consists of 97,339 hexahedral elements and 1,80,794 tetrahedral elements. Two dimensional model consists of 2967 quadrilateral cells. The mesh can be examined for the skewness of a cell. Each colour in the meshed element indicates the skewness value. The range of skewness is from 0 to 1. The quality of a cell is excellent if the skewness value lies between 0 to 0.25 and it is poor if it exceeds 0.80.

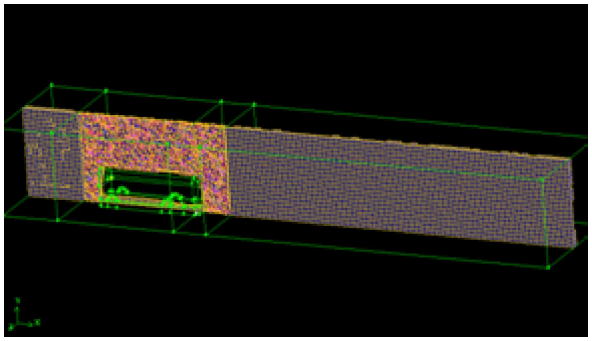

Fig.2 Meshed model

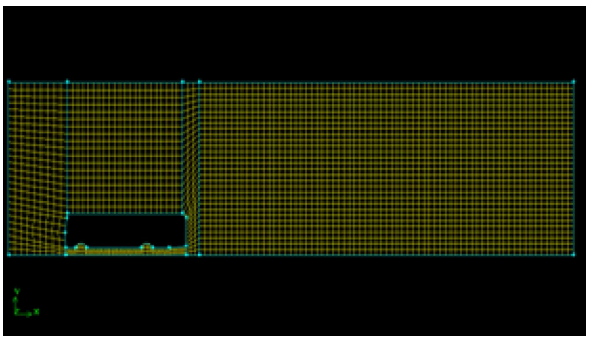

Fig.3 Surface mesh of the model

2.3 Boundary Conditions

Boundary conditions specify the flow variables on the boundaries of the physical model. They are, therefore, a critical component of FLUENT simulations and it is important that they are specified appropriately.

We have to specify the zone in GAMBIT software according to the required output. The boundary type specified for this analysis is velocity inlet and pressure outlet. GAMBIT software also allows us to specify the continuum, which indicates the fluid or solid medium inside the meshed model. The meshed model is then imported into FLUENT software and analysis is performed. We have to specify air as the material, which flows inside the model.

3. RESULTS AND DISCUSSIONS

3.1 Analysis Done on the Actual Profile

Flow analysis has been performed using the FLUENT software. CFD helps us to predict the flow simulations. Analysis were performed for both inlet velocities of 25m/s and 28m/s. Results shows that the drag force gets increased as the velocity increases. The stagnation pressure also increases as the velocity increases.

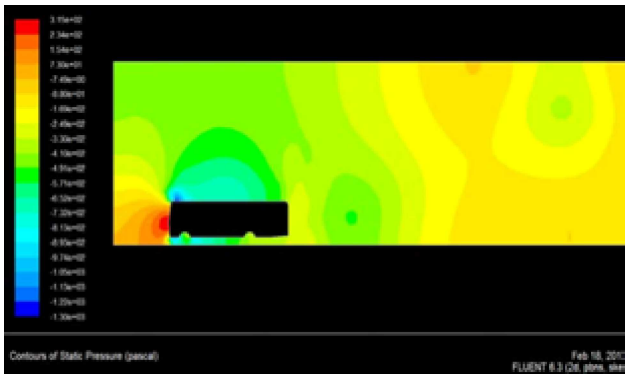

Fig.4 Pressure plot

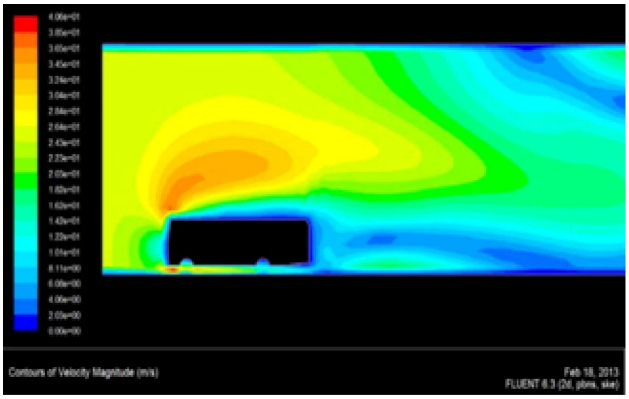

Fig.5 Velocity plot

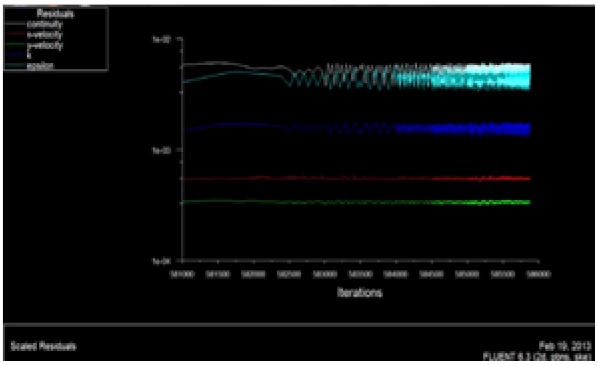

Fig.6 Residuals

3.2 Analysis done on the modified profile: Flow analysis has been performed on the modified profile of the vehicle for the inlet velocity of 25m/s.

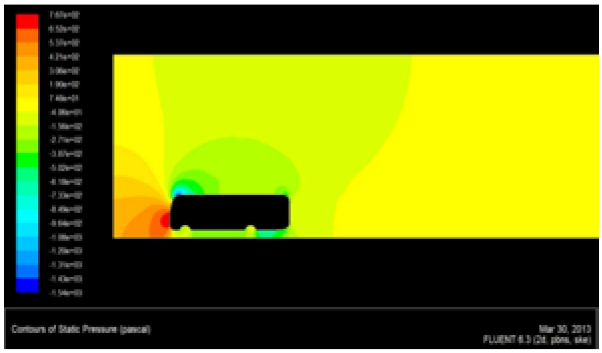

Fig.7 Pressure plot

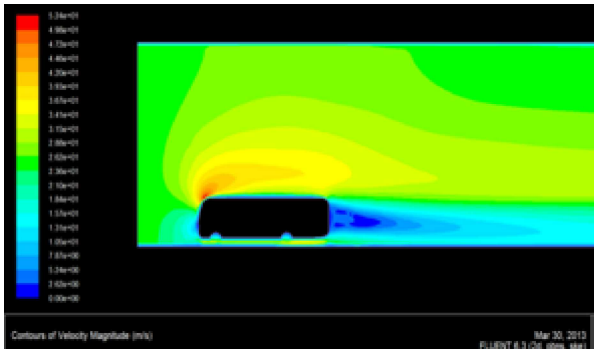

Fig.8 Velocity plot

4. CONCLUSION

Flow analysis has been done on the actual profile and modified profile of the vehicle, and their air flow characteristics were studied. By modifying the profile, boundary layer separation gets delayed which results in reduced drag. The pressure intensity level and area of the wake region gets reduced. Drag force gets reduced by 20% after modifying the profile.

REFERENCES

[1] Emmanuel Guilmineau "Computational Study of Flow around a Simplified Car Body", Wind Engineering and Industrial Aerodynamics, Vol. 96, 2008, pp.1207-1217.

[2] FreederiqueMuyl, Laurent Dumas, Vincent Herbert "Hybrid Method for Aerodynamic Shape Optimization in Automotive Industry", Computers & Fluids, Vol.33, 2004, pp.849-858.

[3] Jeonglae Kim , Seonghyeon Hahn , Jinsung Kim , Dong-kon Lee , Jin Choi , Woo- Pyung Jeon & Haecheon Choi "Active Control of Turbulent Flow Over a Model Vehicle for Drag Reduction", Turbulence, Vol. 5, 2004, pp. 19.

[4] Mathieu Roumeas, Patrick Gillieron, and Azeddine Kourta, "Drag Reduction by Flow Separation Control on a Car after Body", Numerical Methods In Fluids, Vol. 60, 2009, pp. 1222–1240.

[5] S N Singh, L Rai, P Puri and A Bhatnagar, "Effect Of Moving Surface On The Aerodynamic Drag Of Road Vehicles", Automobile Engineering, Vol. 219, 2005, pp.127-134.

[6] S.O.Kang, S.O.Jun, H.I.Park, K.S.Song, J.D.Kee, K.H.Kim and D.H.Lee, "'Actively Translating a Rear Diffuser Device For The Aerodynamic Drag Reduction of a Passenger Car", Automotive Technology, Vol. 13, No. 4, 2012, pp.583-592.

[7] Subrata Roy and pradeep Srinivasan, "External Flow Analysis of a Truck for Drag Reduction", SAE International, Vol. 01, 2000, pp.3500.

[8] H.K.Versteeg and W.Malalasekara, "An Introduction to Computational Fluid Dynamics".

[9] Dr. R.K.Bansal, "A Text book of Fluid Mechanics and Hydraulic Machines".

Synthesis of Biodiesel from Castor Oil and its Combustion Studies in Diesel Engine

A. Sundaramahalingam[1] and K. Karuppasamy[2]
[1]P.G. Scholar, [2]Assistant Professor, Department of Mechanical Engineering, Regional Centre of Anna University, Tirunelveli - 627 007, Tamil Nadu
E-mail: sundaraero.89@gmail.com , kssurabu2001@yahoo.co.in

Abstract

Increasing fuel prices and fast depletion of fossil fuels together with growing environmental concerns have led to the development of alternate fuels for internal combustion engines. Bio fuels combined with diesel can effectively substitute diesel fuels and reduce emissions from in-use diesel vehicles. Exhaust Gas Recirculation (EGR) is widely being used to reduce and control the oxides of nitrogen (NOx) emission from diesel engines. EGR controls the NOx because it lowers the oxygen concentration and flame temperature of the working fluid in the combustion chamber. In this present work, the effect of EGR on performance, emission and combustion of a Kirloskar VS1 water-cooled DI diesel engine has been experimentally investigated by using biodiesel produced from castor oil using anion exchange resin (with quaternary ammonium groups in a chloride form) as a heterogeneous catalyst in a batch method. Emissions of hydrocarbons (HC), Oxides of Nitrogen (NO_X), carbon monoxide (CO) and smoke opacity of the exhaust gas were measured. Performance parameters such as exhaust gas temperature (EGT) and specific fuel consumption (SFC) were calculated. Reductions in NOx and exhaust gas temperature were observed but emissions of CO and smoke were found to have increased with usage of EGR.

Keywords: *Biodiesel, Castor oil, Combustion, Exhaust Gas Recirculation (EGR), Performance, Emission.*

1. INTRODUCTION

Petroleum-based fuels are limited reserves concentrated in certain regions of the world. These sources are on the verge of reaching their peak production. The scarcity of known petroleum reserves will make renewable energy sources more attractive. There are many alternative (non-conventional) energy sources are available such as wind, solar, geothermal, OTEC and biomass. Bio-fuels made from biomass feed stocks have gained importance in the recent past for its ability to replace fossil fuels which are likely to run out within a century. The environmental issues concerned with the exhaust gases emission by the usage of fossil fuels also encourage the usage of biodiesel which has proved to be eco-friendly far more than fossil fuels.

2. EGR TECHNIQUE FOR NO_X REDUCTION

Exhaust gas recirculation (EGR) is an effective method for reducing NO_X emissions from internal combustion engines. Exhaust gas consists of CO_2, N_2 and water vapours mainly. Re-circulated exhaust gas displaces fresh air entering the combustion chamber with carbon dioxide and water vapour present in engine exhaust. As a consequence of this air displacement, lower amount of oxygen in the intake mixture is available for combustion. Reduced oxygen available for combustion lowers the effective air–fuel ratio. This effective reduction in air–fuel ratio affects exhaust emissions substantially. In addition, mixing of exhaust gas with intake air increases the specific heat of intake mixture, results in reduction of flame temperature. Thus combination of lower oxygen quantity in the intake air and reduced flame temperature reduces rate of NO_X formations. The EGR (%) is defined as the mass percent of the recirculated exhaust (M_{EGR}) in the total intake mixture ($M_{air}+M_{EGR}$).

$$EGR\% = \frac{M_{EGR}}{M_{air}+M_{EGR}} * 100 \quad (1)$$

3. METHODOLOGY

3.1 Materials

Castor oil was purchased in the commercial market. Potassium hydroxide and Methanol (95% pure) used in the tests were kindly supplied by Nice chemicals Pvt. Ltd. Anion-exchange resin with quaternary ammonium groups in a chloride form was purchased from Aqua Ion exchange systems, Coimbatore. To generate the catalytic

activity, the resin was first washed with deionised water to remove impurities. And then, the resin was immersed into the solution of 5.0 wt.% KOH in methanol for 12 h to transform from chloride form into hydroxyl form. Finally, the alkaline Anion exchange rein is stored in airtight condition before use.

3.2 Biodiesel Production

Transesterification was carried out in laboratory scale in a 250 mL flat bottom Erlenmeyer flask in a batch method using magnetic stirrer and hot plate apparatus. The castor oil was charged into a flat bottom conical flask and it is heated to temperature of 60 °C in the test set up. When the required transesterification reaction temperature was reached, methanol-oil molar ratio of 12:1 and catalyst of 30 gm was added into the reactor. The reaction was started by stirring at specified rpm. The transesterification reaction was stopped after reaching required time (4 h) and the catalyst was separated. The product was then allowed to settle down overnight. Then the top layer (methyl ester) was separated using a separating funnel.

3.3 Experimental Procedure

Experiments were conducted in a single cylinder 4 stroke DI diesel engine coupled with an Eddy current dynamometer. For recirculation of the exhaust gas, appropriate plumbing was done. No insulation on the pipe line was provided therefore allowing the re-circulated exhaust gases to partially cool down. The schematic diagram of the experimental setup is shown in figure 1. The quantity of EGR can be regulated by a control valve installed in the EGR loop. An orifice was installed in the EGR loop to measure the flow rate of the re-circulated exhaust gas. The specification of the test engine is shown in table 1.

Table 1 Specifications of Test Engine

Make and model	Kirloskar SV1
General details	4 stroke, water cooled, direct injection
Rated power	5.9 kW
Rated speed	1800 rpm
Loading type	Eddy current loading
Bore	87.5 mm
Stroke	110 mm
Compression ratio	17.5 : 1

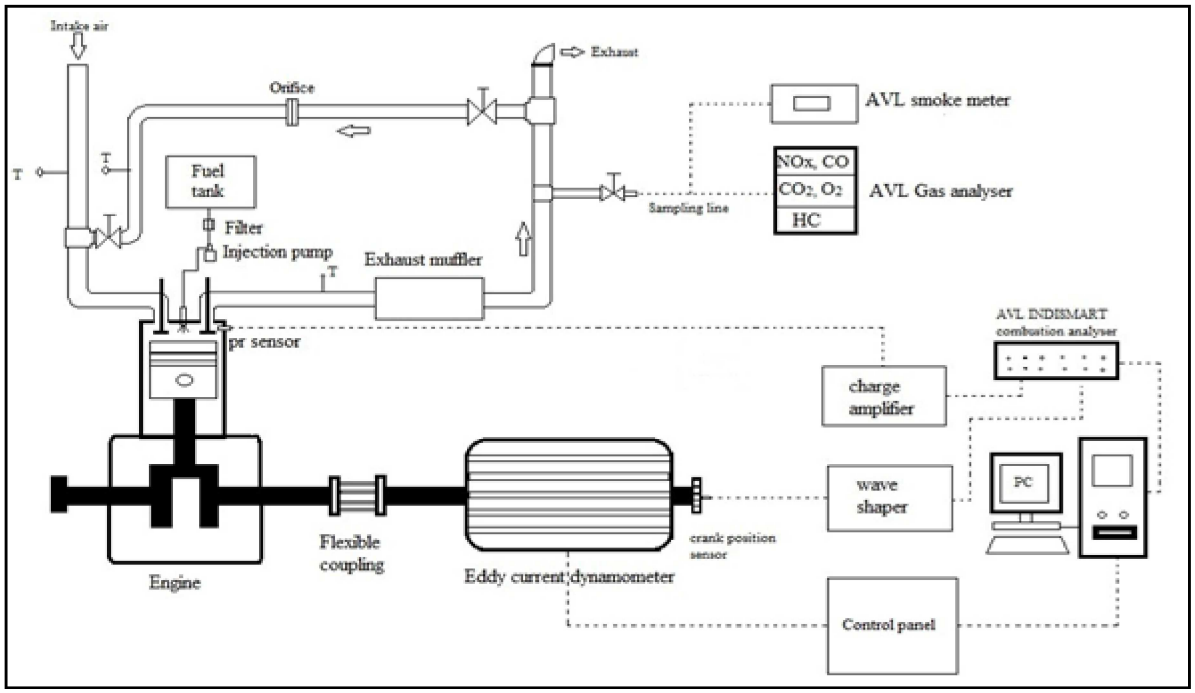

Fig.1 Schematic diagram of experimental setup

Thermocouples were installed in several locations to measure the exhaust gas temperature, EGR temperature and cooling water temperature. Fuel consumption was measured using gravimetric fuel consumption meter. Exhaust gas emissions were measured using AVL DIGAS 4000 LIGHT gas analyser and the smoke opacity was measured using smoke opacity meter (Make: AVL, Model: 407). The combustion parameters were measured by AVL indismart combustion analyser.

4. RESULTS AND DISCUSSION

To achieve the objective of the study, the engine was run at different loads at 1800 rpm without EGR and with 25% EGR to investigate the effect of EGR on engine performance, emission and combustion. Pure diesel and B40 were used as the test fuels. The data for fuel consumption, exhaust gas temperature, HC, NO_X, CO, smoke opacity, pressure versus crank angle diagram and heat release diagram were recorded. Then, engine performance, emission and combustion patterns were analysed and presented graphically.

4.1 Engine Performance Analysis

Figure 2 represents the SFC of test fuels at different loads with and without EGR. The specific fuel consumption is higher for B40 at all loading conditions compared to diesel. Because of lower calorific value of biodiesel blend, more amount of fuel is required to produce the same power output. With the implementation of EGR, SFC is reduced. However, at higher engine loads, SFC with EGR is almost similar to that of without EGR. At higher loads, amount of fuel supplied to the cylinder is increased at higher rate and oxygen available for combustion gets reduced. Thus, air fuel ratio is changed and this increases the SFC.

Figure 3 shows the variation of exhaust gas temperature with brake power. It has been observed that with increase in load, exhaust gas temperature also increases.

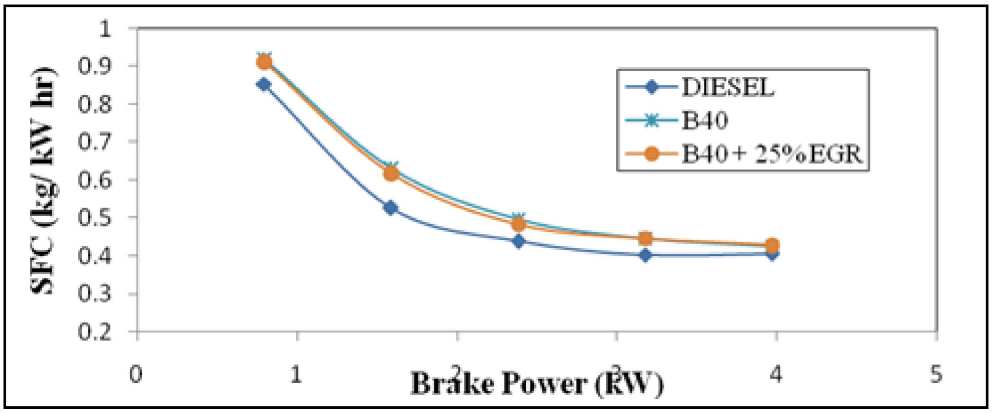

Fig.2 Variation of SFC with Brake Power

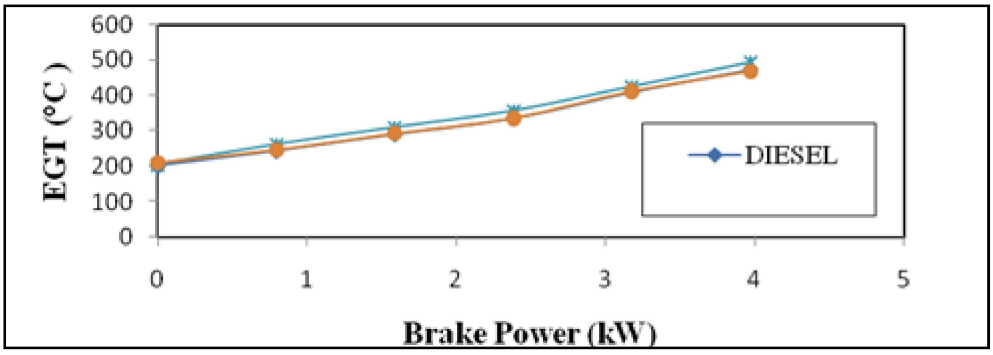

Fig.3 Variation of Exhaust Gas Temperature with Brake Power

EGT for B40 is higher than the diesel. It may be due to the presence of constituents with higher boiling points in COME than in diesel. Those constituents having higher boiling points were not adequately evaporated during the main combustion phase and continued to burn in the late combustion phase. This resulted in a slightly higher exhaust gas temperature for B40. When the engine is operated with EGR, the temperature of exhaust gas is reduced. The reasons for temperature reduction are relatively lower availability of oxygen for combustion and higher specific heat of intake air mixture.

4.2 Engine Emission Analysis

Figure 4 shows the variation of carbon monoxide emission for test fuels at different loads. CO is usually formed when there is no sufficient O_2 to oxidize the fuel. The physical properties of fuel such as density and viscosity have a greater influence on CO emissions than its chemical properties. This may lead to higher fuel spray

droplet size for castor oil methyl ester blends, compared with that of standard diesel fuel. Also the CO emission of B40 increases with the implementation of EGR. Because the recirculated exhaust gas reduces the amount of oxygen incoming into the combustion chamber results in rich mixture at different locations. This heterogeneous mixture does not combust completely and results in higher carbon monoxide emissions.

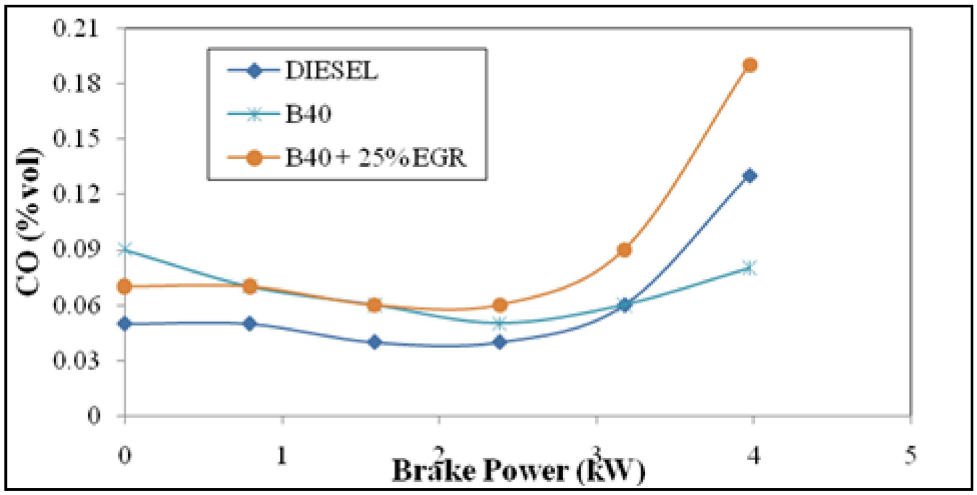

Fig.4 Variation of CO emissions with Brake Power

Figure 5 shows the variation of HC emissions with Brake power. Unburned hydrocarbon (HC) emission for B40 is higher than those of diesel fuel at lower loads due to its high viscosity and density as stated earlier. But at higher loads, the HC emission decreases.

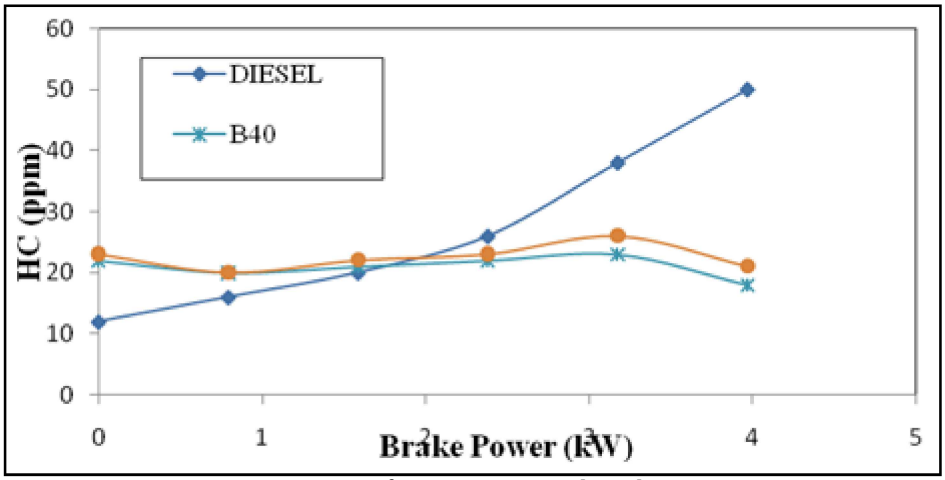

Fig.5 Variation of HC emissions with Brake Power

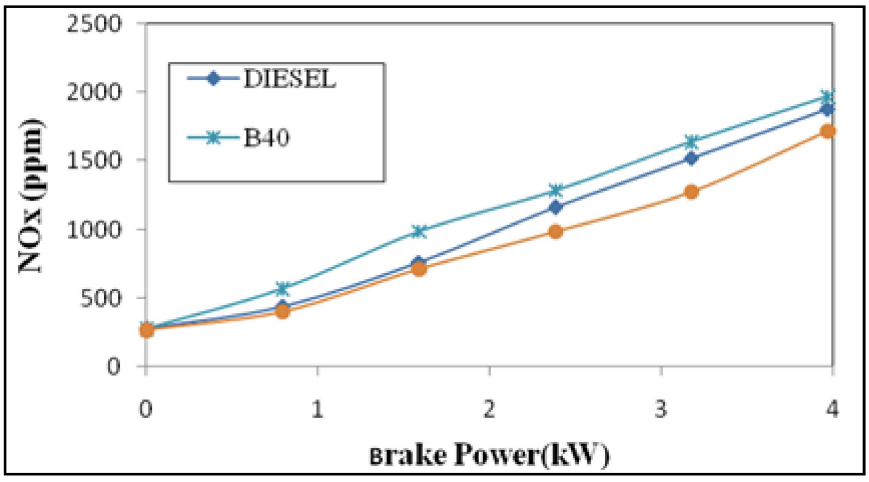

Fig.6 Variation of NO_x with Brake Power

This is because of better combustion of biodiesel inside the combustion chamber due to the availability of oxygen atom in biodiesel. By using EGR, the HC emissions increases due to decreased oxygen intake as mentioned earlier in CO emissions.

The variation of NO_x is shown in figure 6. As load increases, the NO_x emission also increases. NO_x emission of B40 is higher than diesel because of its higher exhaust gas temperature. This proves that the most important factor for the emissions of NO_x is the combustion temperature in the engine cylinder and the local stoichiometry of the mixture.

By using EGR the NO_x emission is reduced. The reasons for reduction in NO_x emission using EGR are reduced oxygen concentration and decreased flame temperatures in the combustible mixture.

The smoke opacity of the exhaust gas is measured to quantify the particulate matter present in the exhaust gas. The smoke opacity is shown in figure 7. Higher smoke opacity is observed when the engine is operated with EGR compared to without EGR.

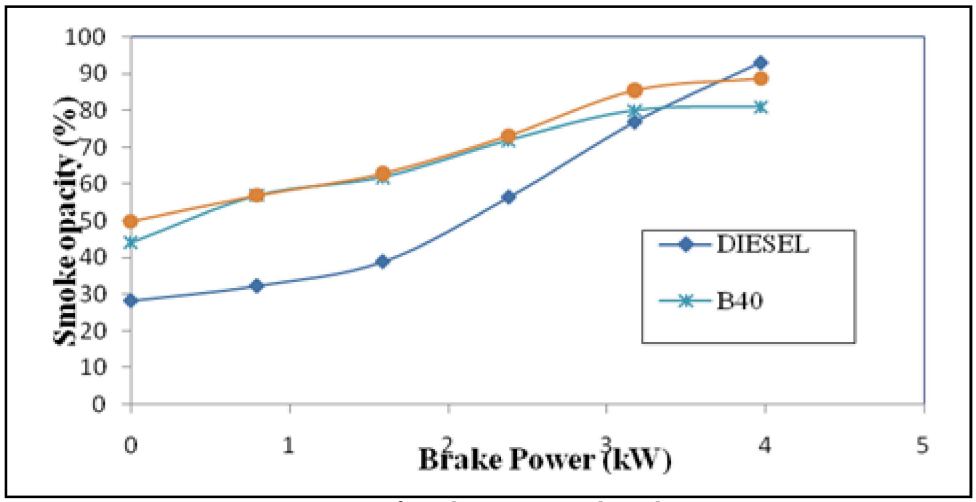

Fig.7 Variation of smoke opacity with Brake Power

EGR reduces the availability of oxygen for combustion of fuel, which results in relatively incomplete combustion and increased formation of particulate matter.

4.3 Engine Combustion Analysis

Figure 9 shows the variation of cylinder pressure with crank angle at full load. B40 gives high combustion pressure compared to that of standard diesel due to longer ignition delay and may be due to the lower cetane number. The fuel absorbs more amount of heat from the cylinder immediately after injection and resulting in longer ignition delay. And also EGR increases the peak pressure of the test fuels.

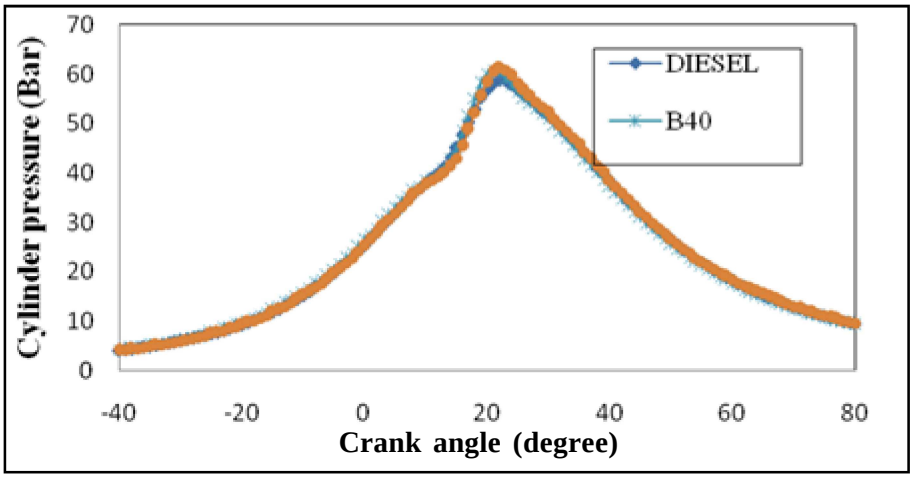

Fig.9 Variation of cylinder pressure with crank angle at full load

Figure 10 shows the variation of heat release rate at full load. B40 shows a maximum heat release rate of 179.11 kJ/m^3, which is higher than that of the diesel. As the concentration of biodiesel increases in the blend, the ignition delay increases and hence a higher heat release is produced. With the implementation of EGR the heat release rate also increases.

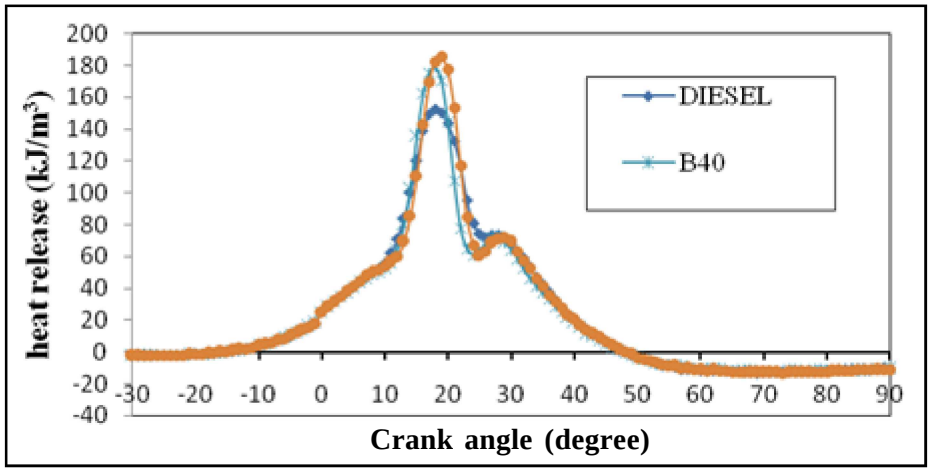

Fig.10 Variation of heat release rate at full load

5. CONCLUSION

A single cylinder diesel engine was operated successfully with diesel and B40 with and without EGR with an objective to reduce NOX emission. The following conclusions are drawn based on the investigation.

- The specific fuel consumption for B40 is 5.3 % higher than diesel when operating without EGR. When operating with EGR the SFC decreases slightly, and at higher loads it is similar to without EGR.
- There is a 4.8 % increase in NOX for B40 without EGR and it decreases by 12 % than diesel when operated with EGR at full load.
- At all loads, exhaust gas temperature decreases marginally with EGR.
- The smoke density for B40 is 78 % higher than diesel with the implementation of 25% EGR at no load and the percentage decreases with increase in load.
- The CO emission for B40 with EGR is 46% higher than diesel at full load.

It can be concluded that castor oil methyl ester blend (B40) could be used in a conventional diesel engine with EGR to reduce the NO_X emissions with slight increase in CO and smoke.

REFERENCES

[1] M.M. Abdelaal and A.H. Hegab, "Combustion and Emission Characteristics of A Natural Gas-Fueled Diesel Engine with EGR", Energy Conversion and Management, Vol.64, 2012, pp.301-312.

[2] D.Agarwal, S.K. Singh and A.K. Agarwal, "Effect of Exhaust Gas Recirculation (EGR) on Performance, Emissions, Deposits and Durability of a Constant Speed Compression Ignition Engine", Applied Energy, Vol.88, 2011, pp.2900–2907.

[3] Bahattin Эюcan and Ньseyin Aydэn, "Improving The Usability of Vegetable Oils as A Fuel in A Low Heat Rejection Diesel Engine", Fuel Processing Technology, Vol.98, 2012, pp.59-64.

[4] Bello, E.I. and Makanju, A. "Production, Characterization and Evaluation of Castor Oil Biodiesel as Alternative Fuel for Diesel Engines", Journal of Emerging Trends in Engineering and Applied Sciences, Vol.2, 2011, pp.525-530.

[5] P.K. Devan and N.V. Mahalakshmi, "Performance, Emission and Combustion Characteris-Tics of Poon Oil and its Diesel Blends in a DI Diesel Engine", Fuel, Vol.88, 2009, pp.861–67.

[6] Jaьar Hussain, K.Palaniradja, N. Alagumurthi and R. Manimaran, "Eьect of Exhaust Gas Recirculation (EGR) on Performance and Emission Characteristics of a Three Cylinder Direct Injection Compression Ignition Engine", Alexandria Engineering Journal, Vol.51, 2012, pp.241–247.

[7] T. Lakshmanan and G. Nagarajan, "Study on Using Acetylene in Dual Fuel Mode with Exhaust Gas Recirculation", Energy, Vol.36, 2011, pp.3547-3553.
[8] M. Mani, G.Nagarajan and S. Sampath, "An Experimental Investigation on a Di Diesel Engine Using Waste Plastic Oil with Exhaust Gas Recirculation", Fuel, Vol.89, 2010, pp.1826–1832.
[9] K. Muralidharan and D. Vasudevan, "Performance, Emission and Combustion Character-Ristics of a Variable Compression Ratio Engine Using Methyl Esters of Waste Cooking Oil and Diesel Blends", Applied Energy, Vol.88, 2011, pp.3959–3968.
[10] Y. Ren, B.He, F.Yan, H.Wang, Y. Cheng, L.Lin, Y. Feng and J. Li, "Continuous Biodiesel Production in A Fixed Bed Reactor Packed With Anion-Exchange Resin As Heterogeneous Catalyst", Bioresource Technology, 2011.
[11] O. S.Valente, Mбrcio Josй da Silva, Vanya Mбrcia Duarte Pasa, C. R. Pereira Belchiorc and Josй Ricardo Sodrй, "Fuel Consumption and Emissions from a Diesel Power.

An Advanced Wearable Personal Health System, Which Monitors Vital Human Parameters, Based On an 8-Bit Atmel Microcontroller

GauravGautamRoy[1], AkshaySugathan[2], G.J. KirthyVijay [3] and Jeffrey Thomson[4]

[1]3/302 Garden estate, GladyAlwarisroad, Thane, Maharashtra - 400 610, India

[2]QRT NO T1/27,NCL Colony, Singrauli, Madhya Pradesh - 486 889, India

[3]Vasundhara Heights, Flat no-1903, Plot no-5, Sectro-11, Sanpada, Navi, Mumbai, Maharashtra - 400 705, India

[4]Department of Electronics and Instrumentation, SRM University, Chennai - 603 203, Tamil Nadu.

Abstract

World's ageing population and predominance of obstinate diseases have led to a high demand of ambulatory healthcare system, which can monitor vital- signs. Our aim is to develop a generic clothing technology which successfully integrates biosensors woven into a shirt.

We have therefore developed an ambulatory device which enables the measurement of heart rate, electro dermal activity, and skin temperature with non-invasive sensors. Since we are combining parameters such as body temperature, blood pressure, galvanic skin resistance, and oxygen saturation, we get to know about the patient's integral condition. One of the key features of our system is fall detection, which mainly arises from the complication of heart attack during which body's vitals-sign changes and patient tends to collapse. This system gives warning to prevent such complications.

Our research is mainly orientated towards two complementary directions: Improving the relevancy of each sensor and increasing the number of sensors for having a more synthetic and robust information.

Keywords: *Ambulatory device, On-invasive sensors, Wearable electronics.*

1. INTRODUCTION

New information technologies offer today the possibility of a commendable care for the isolated people, people at risk or with reduced mobility. These naturally include equipment's which are heavy and/or intrusive, and these kind of ethical problems limit the development in the field of discrete monitoring.[1] Studies have shown that in prevention of the patients at risk, the system must be discrete and reliable. Health monitoring already takes place in various settings: at home for prevention and in hospital for continuous assessment, hence it has become a pressing need for patients, to provide better quality of care. Due to this, non- invasive measurements are very suitable as they are painless; chances of skin infection are less, user friendly, ease of use while reading results and more. And when these methods are equipped with clothes the possibilities increases. This is mainly due to the reason that clothes provide an endless possibility for the location of sensors, as they are in continuous contact with surface of the skin.

In order to know about the patient's integral condition, we are measuring vital parameters which help us decide the health condition of a patient. [2] Smart wearable systems act as a human interface for the ever increasing knowledge about health and translate this knowledge into personalized feedback for the user in any situation and with any disease status:

1.1 For Elderly Population

Smart biomedical clothes helps us in detection of any complications at an early state which is very helpful as information gathered can be used for a better understanding of the disease state. This results in limiting of acute events that may lead to hospitalization. Elderly people face a problem of attending checkups; hence the smart clothes can continuously monitor the body parameters for better diagnosis.

1.2 For Military

For soldiers to carry out a smart battle they should be both mentally and physically fit. Smart clothes can be used for analyzing on hard and/on risky tasks, works:

at low or high temperatures, or with high metabolism activity but also for detection if a subject is in a good state (mentally and physically) for carrying out a task correctly. The shirt will provide a constant feedback of the physiological states of the soldiers in the battlefield, and immediate assistance will be provided, in case of injury.

1.3 For Chronic Patient

With adequate information from the system chronic patients can be given advice on how to improve risks like hypertension, overweight, diabetes, high/low blood pressures, stress through personalized training plans and changes in diets and behavior. Early detection through long-term analysis will reduce the damage to serve events dramatically.

1.4 For Athlete's

Interactive gaming and other self-motivated programs will help the athlete's to enjoy a healthier lifestyle. The real time monitoring of vital parameters by the system will not only help the athlete's to adapt a healthier lifestyle but will also effectively improve personal performance due to better fitness and more effective way of scoping with stress.

2. ARDUINO PLATFORM

The e-textile should be cost effective and easy configurable for the patients. Hence, we opted for arduino based lilypad. It's an open-source physical computing platform based on a simple microcontroller board, and a development environment for writing software for the board. There are many other microcontrollers and microcontroller platforms available for physical computing. Parallax Basic Stamp, Net media's BX-24, Phidgets, MIT's Handyboard, and many others offer similar functionality. All of these tools take the messy details of microcontroller programming and wrap it up in an easy-to-use package. [4]

Lilypad is one of the processors by Arduino, which is textile based. It consists of an ATmega328 with the Arduino bootloader and a minimum number of external components to keep it as compact. Board will run from 2V to 5V. The latest version of the LilyPad supports automatic reset for even easier programming. The back side of the LilyPad is completely flat and we can use a surface mount programming connector to keep the header from poking.

Through. The Lilypad328 has a clock speed of 8Mhz. [5] LilyPad is a wearable e-textile technology developed Each LilyPad was creatively designed to have large connecting pads to allow them to be sewn into clothing. It has a special provision for analog input and digital output.

Power and sensor boards are specially designed for the lilypad. The lilypad has the advantage that it is washable as well.

The Arduino has the following Advantages:

Cross-platform: The arduino software runs on Windows, Machintosh OSX and Linux operating systems, although most microcontroller systems are limited to Windows.

Open source and extensible software: The arduino programming environment is easy- to-use for beginners, yet enough for advanced users to take advantage as well..

Simple and programming environment: The arduino is easy-to-use with in-built examples and sample programmes on the forum.

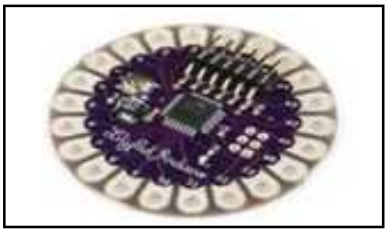

Fig .1The arduino lilypad is a processor which can be sewn to the shirt.

2.1. VITAL PARAMETERS

The vital parameters, which we have successfully implemented using arduino Lilypad are

Human body temperature
Galvanic Skin resistance

The main purpose for measuring the parameters is for continuous monitoring of patients and notifying the doctor, if any complication is encountered by the patient.

2.1.1.Temperature Measurement

The commonly accepted average core body temperature (taken internally) is 37.0°C (98.6°F).

In healthy adults, body temperature fluctuates about 0.5°C (0.9°F) throughout the day, with lower temperatures in the morning and higher temperatures in the late afternoon and evening, as the body's needs and activities change. The time of day and other circumstances also affect the body's temperature. The temperature change above and below the critical level lead to phenomenon of fever, hyperthermia, hypothermia.

The measurement of body temperature is carried out using temperature sensor (such as SHT15 by Sensirion.). This temperature sensor gives out voltage which is proportional to the temperature in °C. The output of temperature sensor (SHT15) is given to the Arduino- Atmega 2560.We are choosing the following sensor because it has maximum accuracy from 20°C-40°C version of body temperature to digital input is carried by regression analysis. Generally the manufactures provide data sheet of the product, which consists of voltage values for different temperatures.

Using the given data we make a scattered graph showing the relation between the voltage and the temperature, by seeing trend of the graph we were able to formulate a relationship between the voltage reading from the pin and the temperature. Formula for temperature measurement-Temperature=(5.0*analog Read (temping)*100.0)/1024.

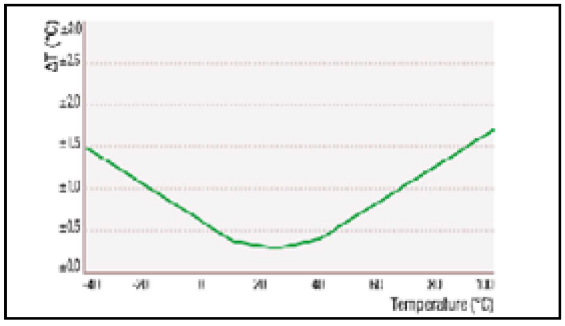

Fig 2.The characteristic graph of SHT 15, which has maximum accuracy from 20ÚC-40ÚC

2.1.1. a. Signal Conditioning Circuit for Body Temperature

The sensor SHT15 has a maximum output current of 4 -mA.which cannot be processed by the arduino. Hence we had to develop the following signal conditioning circuit to match the in- built analog –to-digital converter (ADC), to increase the resolution and sensitivity of the sensor. It helps to increase the voltage level before it is affected by noise.

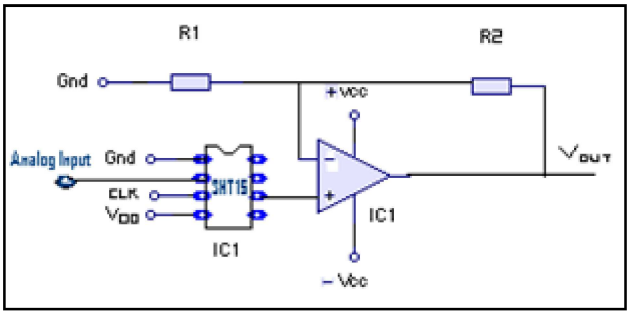

Fig 3.Circuit diagram for the conditioning circuit for temperature

2.1.2. Galvanic Skin Resistance

Electro dermal Response EDR is actually the medically preferred term for changing of electrical skin resistance due to psychological condition.[6] GSR reflects sweat gland activity and changes in the sympathetic nervous system and measurement variables. Measured from the palm or fingertips, there are changes in the relative conductance of a small electrical current between the electrodes. The activity of the sweat glands in response to sympathetic nervous stimulation (Increased sympathetic activation) results in an increase in the level of conductance. There is a relationship between sympathetic activity and emotional arousal, although one cannot identify the specific emotion being elicited. Fear, anger, startle response and orienting response are all among the emotions which may produce similar GSR responses [7].

2.1.2. a. Measurement of Galvanic Skin Resistance

The Skin conductance is the reciprocal of that resistance easement of human body sweat. We obtain a weak signal/noise ratio, when the analog reading is directly taken from the sensor. A circuit is required which produces an output voltage proportional to the change in skin resistance. GSR is a measurement of the electrical conductance of the skin.Sweating causes changes in the conductance, which offers an indication of nervous state, because the sweat glands are controlled by the sympathetic nervous system.

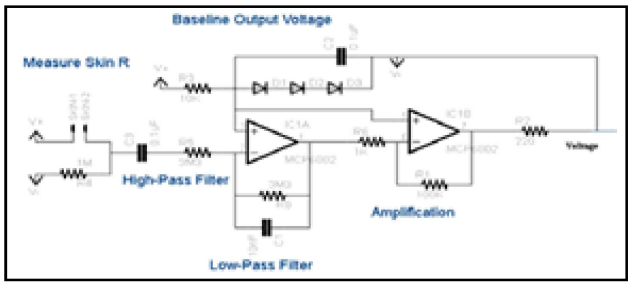

Fig 4 the conditioning circuit for galvanic skin resistance

The circuit needs to filter out noise and amplify the GSR signal. It employs both a low & high pass filter to create a 0.5 Hz to 5 Hz band pass which works well for GSR since it is a slow 1 to 2 Hz signal. The low-pass filter cuts off high frequency noise above 5 Hz such as 60 Hz noise from AC Power. The high-pass filter cuts off frequencies below 0.5 Hz. Arduinoscope, a processing sketch, is running and graphing the output of the Arduino, via serial link over USB.

The high-pass filtering subtracts the baseline average skin resistance leaving the only change in skin resistance within the 1-2 second range of GSR. The result is that the GSR sensor is able to auto-calibrate for each user regardless of the baseline skin resistance. The arduino will notify the user, in presence of a sudden spike in Galvanic skin resistance, along with the increase in other physiological parameters.

Although not accurate, as it varies from person to person, it is a methodology which can only determine if the patient is in the state of emergency.

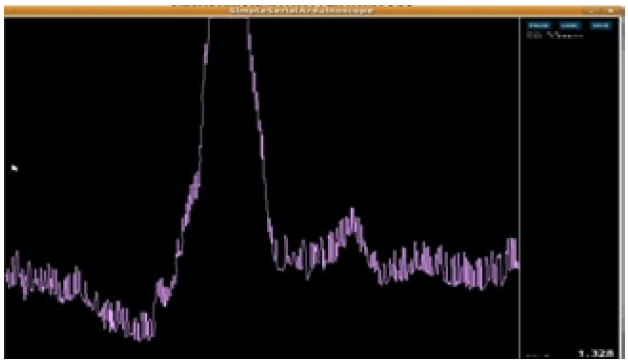

Fig 5.An example of externally simulated spike in Arduinoscope.

3. CONCLUSION

Health monitoring system can be implemented using arduino platform, as it can be easily programmed and open-source software, hence the easy availability of programs. The sensors for various parameters can be designed and easily integrated according to the requirements of the patient. The two parameters measured by monitoring system can continuously tabulate the medical condition of the patient.

REFERENCES

[1] André Dittmer, Richard Meffre, Wearable Medical Devices Using Textile and Flexible Technologies for Ambulatory Monitoring ANDREAS LYMBERIS, Ph.D., and SILAS OLSSON, M.Sc.] Intelligent Biomedical Clothing for Personal Health And Disease Management: State of the Art and Future Vision

[2] Sannino, Giovanna Developments in E-systems engineering (DeSE), 2011 Date of Conference: 6-8 Dec. 2011Inst. of High Performance Comput. & Networking, [3] Guide/Introduction to arduino http://arduino.cc/en/

[4] Introduction to lilypad http://lilypadarduino.org/

[5] Galvanic skin resistance http:// www.extremenxt.com/gsr.html GSR History, & Physiology taken from BIOFEEDBACK Methods and Procedures in clinical practice (1977) written by George D Fuller, Ph.D. Sensing Galvanic Skin Resistance(GSR) posted by Drew Fustini.

Development of Flexible Bearing

K.S. Mohanraj, Dr. K. Ravichandran and G. Swetha
Department of Rubber and Plastic Technology, Anna University (MIT), Chennai - 600 044, Tamil Nadu
E mail : ksmohanmit@gmail.com[1], ravi@mitindia.edu[2].

Abstract

Elastomeric base isolation systems are proven to be effective in reducing seismic forces transmitted to buildings. However, due to their cost, the use of these devices is currently limited to large and expensive buildings. A fibre reinforced elastomeric isolator utilizes fibre fabric, such as carbon fibre, glass fibre, and etc. as the reinforcement material instead of solid steel plates. The fibre fabric reinforcement is extensible in tension and has no flexural rigidity. Elastomers normally used in the isolator are natural rubber, neoprene, butyl rubber and nit rile rubber etc.These devices were fabricated by binding alternating layers of rubber and fibre mesh. The fibre mesh is used to increase the vertical stiffness of the bearings while maintaining low lateral stiffness. Characterizing the behaviour of a fibrereinforced bearing "shape factor" of the bearing, Poisson's ratio of the elastomeric material and flexibility of the reinforcing sheets and investigate the effect of reinforcement flexibility on compressive behaviour of elastomeric bearings with different geometrical and material properties. Bonding with fibre reinforcements can increase the stiffness of elastic layers only when the elastic layer is compressed.

Keywords: Compression stiffness, Elastomer, Steel/fibre, bonding, Shear stiffness.

1. INTRODUCTION

Elastomeric bearings are finding ever increasing application in today's construction industry. Although used extensively in Bridges, bearing pads are being specified in a wide variety of applications where flexible structural support and/ or vibration isolation is required. The typical application range is from concrete buildings and parking garages to heavy industrial equipment, storage tanks and pipe supports. Their popularity is understandable in view of the following advantages Performs required functions efficiently Totally maintenance free No moving parts and therefore no wear & tear No corrosion Absorbs shocks &vibrations Cheaper than mechanical bearings Simple to install Capable to accommodate small irregularities in the loading surface.

2. FUNCTION OF A BASE ISOLATER

A base isolated bearing must perform the following basic functions Support vertical loads with a minimum of deflection. Allow horizontal movement with minimal resistance thereby reducing detrimental Effects of creep, shrinkage and temperature change. Allow rotational movement with minimum resistance. Obtain uniform distribution of loads.

3. ELASTOMERS

Elastomeric Bearings have no moving parts to perform their required functions. Instead, they achieve this through deformation of the Elastomers. Obviously then, the properties of the Elastomers largely determine the behaviour of the bearing. Although a wide variety of Elastomers are available, only two types are allowed in base isolated bearings (I) Natural Rubber (ii) Neoprene.

3.1 Natural Rubber

Natural rubber is an elastomeric material which is used as Low frequency anti vibration mountings Structural bearings. So that it should have the following properties Very high resilience , low damping for maximum vibration isolation efficiency , very low creep and low chemical and oil resistance.

4. REINFORCEMENTS

Enforcing a material into another material will produce new kind of structure with enhanced properties of primary material. In flexible bearings steel and fibber used as the reinforcements which will stiffen the its structure when it is subjected loading

4.1 Steel

Bonding of sheets of rubber to thin steel reinforcing plates to produce a composite with very high vertical and low in-plane stiffness. Present applications of these isolators, which are in general expensive and heavy, are often restricted to the protection of critical facilities, such as command centres, computer facilities, hospitals, landmark and historic structures.

4.2 Fibre

For the effective use of fibres in Elastomers Fibres should be significantly stiffer than the matrix,i.e. have a higher modulus of elasticity than the matrix Fibre content by volume must be adequate. There must be a good fibre-matrix bond.Fibre length must be sufficient. Fibres must have a high aspect ratio, i.e. they must be long relative to their diameter. Fibre fabrics used in the bearings are bi-directional carbon fibre fabric and twisted bi-directional glass fibre fabric

4.2.1 Glass Fibre

Unlike glass fibber used for insulation, for the final structure to be strong, the fibber's surfaces must be almost entirely free of defects, as this permit the fibber to reach gigapascal tensile strengths. If a bulk piece of glass were to be defect free, then it would be equally as strong as glass fibber; however, it is generally impractical to produce bulk material in a defect-free state outside of laboratory conditions.[3]The manufacturing process for glass fibber suitable for reinforcement uses large furnaces to gradually melt the silica sand, limestone, kaolin clay, fluorspar, colemanite, dolomite and other minerals to liquid form. Then it is extruded through bushings, which are bundles of very small orifices (typically 5–25 micrometres in diameter for E-Glass, 9 micrometres for S-Glass).

5. METAL AND FIBBER REINFORCED ISOLATOR

The reinforcing elements of multi-layer elastomeric isolation bearings, which are normally steel plates, are replaced by a fibre reinforcement. The fibber-reinforced isolator is significantly lighter and could lead to a much less labour-intensive manufacturing process. In contrast to the steel reinforcement, which is assumed to be rigid, the fibber reinforcement is flexible in extension.The primary weight in isolators due to the reinforcing steel plates, which are used to provide vertical stiffness to the rubber-steel composite element. The high cost of producing the isolator's results from the labour involved in preparing the steel plates and assembly of the rubber sheets and steel plates for vulcanization bonding in a mold.Both the weight and the cost of isolators can be significantly reduced by eliminating the steel reinforcing plates and replacing them with a fibrereinforcement. The reduction in weight is possible because fibber materials are now available with an elastic stiffness that is of the same order as steel. The reinforcement needed to provide the vertical stiffness may be obtained by using a similar volume of a very much lighter material. Manufacturing cost may be reduced if the use of fibber allows a simpler, less labour-intensive process.

6. FUNDAMENTAL CONCEPTS OF BASE ISOLATION

The term base isolation uses the word a) isolation in its meaning of the state of being separated and b) base as a part that supports from beneath or serves as a foundation for an object or structure. The structure (a building, bridge or piece of equipment) is separated from its foundation. The original terminology of base isolation is more commonly replaced with seismic isolation nowadays, reflecting that in some cases the separation is somewhere above the base – for example, in a building the superstructure may be separated from substructure columns. In another sense, the term seismic isolation is more accurate anyway in that the structure is separated from the effects of the seismic, or earthquake.

7. EXPERIMENTAL SECTION

The steps involved in the experimental work is carried out in following orderMixing,Making RC & sizing fibre to the required shape, Applying bonding agent, Molding, testing & results.

Table 1 Specification of Base Isolator

Bearing Type	SRBI	FRBI
Elastomer Used	Natural rubber	Natural rubber
Reinforcements	Steel	Glass fibre
Shape	Circular	Circular
Size	150mm dia	150mm dia
Thickness of Rubber Layer	1-2mm	1-2mm
Thickness of Reinforcement	1-1.5mm	0.5-1mm
No. of. Rubber Layers	25	22
No. of. Reinforcement Layer	23	20

7.1 Preparation of Rubber Compound

With 40 or 50phr of filler (HAF), rubber compound will be prepared, other all ingredients will be taken to the required amount, Mixing can be done by a 2 roll mill or a kneader in 25minutes, each and every ingredient are to be taken constant intervals to mix thoroughly.

7.2 Making Rubber Compound & Fibre

Sheeting out the rubber compound from 2 roll mill in the thickness of 1or 2mm and then cut it to the circular shape with the diameter of 70mm. Fibre also has to cut at the same shape and size.

Fig.1(a)bidirectional oriented glass fibre

Fig.1(b)adhesive coated steel plate

7.3 Making & Applying Adhesives on Steel/Fibre

If steel is the reinforcement, the adhesive slurry has toluene and chemlockand then apply it on the steel plates and dry it for one hour.If reinforcement is glassfibre, adhesive has to be prepared separately. For that, take equal amount of ingredients such as tetra methylthiuramdisulphide (TMTD), zinc oxide & tetraethyl orthosilicate (TEOS) and then mix it all thoroughly after that add 0.1% of potassium permanganate (KMNO4) with it, finally add methyl ethyl ketone (MEK) as it required to make slurry and then apply it on the cutted fibre layers, keep it all in an oven at 80 C for 1 to 3hours.

7.4 Molding

Arrange equal number of steel/fibre and rubber layers in the mold. An isolator has maximum of 22 rubber layers and 20 fibre layers.After that keep it in compression molding machine at 150 C for 15 minutes.Finally take the product out from the moldand send it for testing.

Fig.2 Model of a base isolator

8. TESTING

Compression and shear test is done in universal testing machine (UTM) by subjecting compression and shear loads. Deflections were measured by using deflectometer which is attached in the UTM. Results obtained by a graph which is load vs. deflection and calculation of the stiffness for both compression & shear by using the formula which is given below:

Stiffness = load/deflection-

Or

$$K = P/\delta \qquad (1)$$

9. RESULTS & DISCUSSION

It is proved that stiffness is increased in fibre reinforced isolator while comparing with steel reinforced isolator. Minimum deflection was exerted in FRP isolator so that stiffness has been increased in it the reason why the fibre has no flexural rigidity.

REFERENCES

[1] A. Seval Pinarbasi , B. Yalcin Mengi, "Layers Bonded to Flexible Reinforcements", International Journal of Solids and Structures, Vol.45, 2008, pp.794-820.

[2] Hsiang-Chuan Tsai , "Compression Stiffness of Circular Bearings of Laminated Elastic Material Interleaving With Flexible Reinforcements", International Journal of Solids and Structures, Vol.43, 2006, pp.3484-3497.

[3] Hsiang-Chuan Tsai, "Deformation Analysis Of Infinite-Strip Bearings Of Laminated Elastic Material Interleaving With Tension-Only Reinforcements", International Journal of Solids and Structures, Vol.45, 2008, pp.2836–2849.

[4] Sarvesh K Jain and Shashi K Thakkar, "Seismic Response of Building Base Isolated With Filled Rubber Bearings under Earthquakes of Different Characteristics", 12wcee 2000.

[5] A. B. M. Saiful Islam, Mohammed Jameel and Mohd Zamin Jumaat, "Seismic Isolation in Buildings to be A Practical Reality: Behavior of Structure and Installation Technique", Journal of Engineering and Technology Research Vol.3, No.4, 2011, pp. 99-117.

[6] S. Pinarbasi, U. Akyuz and Y. Mengi, "Effect of Reinforcement Flexibility on Compressive Behavior of Strip-Shaped Elastomeric Bearings", 8th International Congress on Advances in Civil Engineering, 15-17 September 2008.

[7] Michael G.P. de Raaf, Michael J. Tait and Hamid Toopchi-Nezhad, "Stability Of Fiber-Reinforced Elastomeric Bearings In An Unbounded Application", Journal of Composite Materials published online 22 February 2011.

[8] Habib Sadid, Bridger D. Morrison "Low-cost Base Isolation Devices for Residential Buildings".

[9] M. J. Tait, H. Toopchi-Nezhad and R. G. Drysdale, "Influence Of End Geometry On Fiber Reinforced Elastomeric Isolator Bearings", The 14thworld Conference On Earthquake Engineering 2008.

[10] Concetta Onorii, Mariacristina Spizzuoco, Andrea Calabrese, Giorgio Serino "Applicability and reliability of innovative low-cost rubber isolators" the Conference of Rectors of Italian Universities (project No. 141 – year 2008 call).

Investigation on Interaction of Local and Distortional Buckling of Cold Formed Steel Columns

M. Anbarasu[1] and D. Aktharnawas[2]
[1&2]Department of Civil Engineering, Government College of Engineering, Salem - 636 011, Tamil Nadu
Email: aktharnawas@gmail.com

Abstract

This paper deals with the investigation on interaction of local and distortional buckling of cold formed steel lipped channel columns under axial compression. The cross sectional dimensions are fixed based upon the limitations given in the draft IS801 code. The sections were chosen in order to have nearly coincidental local and distortional buckling failure load by performing elastic buckling analysis using CUFSM software. Six sections were chosen for this study with Pinned-Pinned end condition. The finite element package ANSYS was used to carry out the numerical analysis for the columns. The finite element model was validated with the Experimental results available in the literature. The verified model was used for the parametric study for 3 yield stress values. The parametric results were compared with the Direct Strength Method (North American Specification), and a new design equation was proposed.

Keywords: *Cold formed Steel, Column, Local buckling and Distortional buckling.*

1. INTRODUCTION

The cold formed steel sections are subjected to various modes of failure based on the length of the column under axial compression. The short wave length columns subjected to local buckling failure, the intermediate half-wavelength columns subjected to both local and distortional buckling where the long half wavelength columns failure by flexural/flexural-torsional buckling. The various modes of buckling are shown in the figure1.

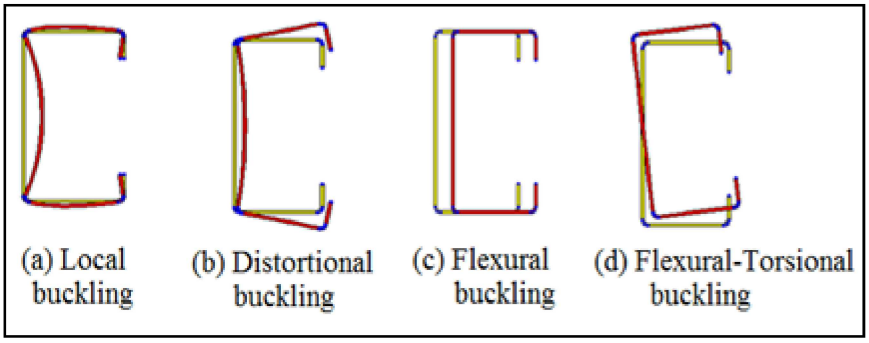

Fig.1 Various modes of buckling

The local buckling was a mode of failure where rotation only occurs at the plate elements as shown in Figure 1(a). This type of buckling occurs nearer to the end of the columns. Distortional buckling was combination of both the rotation and transition in the section as shown in Figure 2(b). In flexural buckling the section was subjected to bending about principle axis as shown in Figure 3(c) where in flexural- torsional buckling, the section was subjected to twisting about longitudinal axis as shown in Figure 3(d).

Kwon, Y.B., and Hancock (1992) conducted Tests on cold formed channel with local and distortional buckling where the elaborate study on local and distortional buckling by experimental study was made. Ben Young, Jintang Yan (2002) conducted Finite element analysis on the fixed-ended plain channel columns by comparing various experimental results with numerical results.

Derrick C Y Yap , Gregory J. Hancock (2008) describes the design and testing of web-stiffened high strength steel cold-formed lipped channel columns. A design method is proposed to improve the prediction of the local buckling DSM strength curve and at the same time, design methods are proposed to improve the distortional buckling DSM strength curve by accounting for the interaction of local and distortional and overall buckling modes.

Kwon, Y.B., and Hancock (2009) conducted Compression tests on high strength cold-formed steel channels with buckling interaction. Simple design strength formulas in the Direct Strength Method for the thin-walled cold-formed steel sections failing in the mixed mode of local and distortional buckling have been studied. The strengths predicted by the strength formulas proposed are compared with the test results for verification.

Dinar Camotim also discussed in his paper (2010) about the interaction mode failures, Numerical, experimental results and DSM design considerations on the fixed end lipped channel columns.

V. Marimuthu, M. Saravanan (2012) conducted numerical studies on the behaviour of intermediate length cold formed steel lipped channel compression members about the prequalified sections based upon the limitations given in the draft IS 801 code.

From the review of literature it was found that the study on Local/Distortional buckling interaction is limited. This papers aims to study the Local/Distortional buckling interaction effect on ultimate strength of lipped channel columns. Six sections were chosen based on the limitations given in the draft IS801 code using CUFSM software to have L/D interaction. The finite element model was developed using ANSYS. The finite element model includes geometric and material non linearity. It was validated with the Experimental results available in the literature (2002). The validated model was used for the parametric study for 3 yield stress values. The parametric results were compared with the Direct Strength Method (North American Specification), and a new design equation was proposed.

2. SECTION GEOMETRIES

2.1 General

Sections were selected on basis of the prequalified section conditions which was given in the Draft IS-801. The sections were selected by trial and error procedure using CUFSM software. From the buckling plot it is ensured to have the interaction of local and distortional buckling. The lengths of the specimens were obtained from the buckling plot as shown in Figure 2. The interaction failure was considered based on that the ratio of the local to distortional buckling load factor which should be among 0.9 to 1.1. Figure 2 shows the interaction of local/distortional buckling mode of the selected specimen.

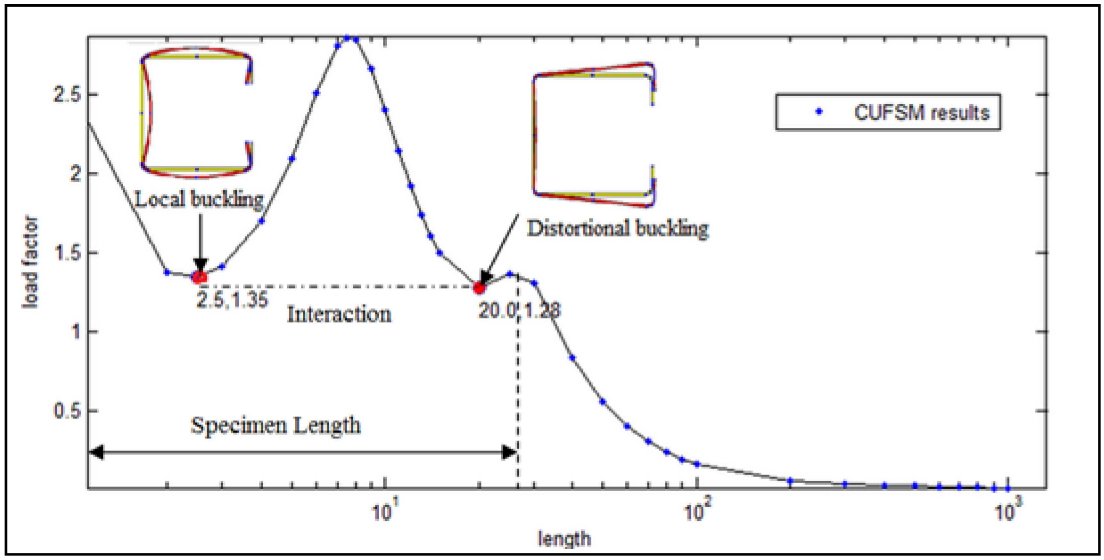

Fig.2 Buckling plot showing Interaction of Local and Distortional Buckling

Section Dimensions (mm)				Length (mm)
h	b	d	t	
60	60	10	1.2	762
75	75	15	1.2	1016
80	80	20	1.2	1016
80	50	10	1.6	940
60	35	12	1.6	508
80	60	16	1.6	915

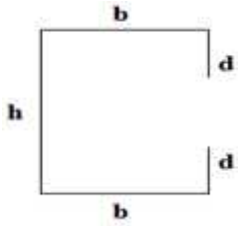

Fig. 3 Geometry of Section

2.2 Labeling of Specimen

Labeling of Specimen was done as depicted below.

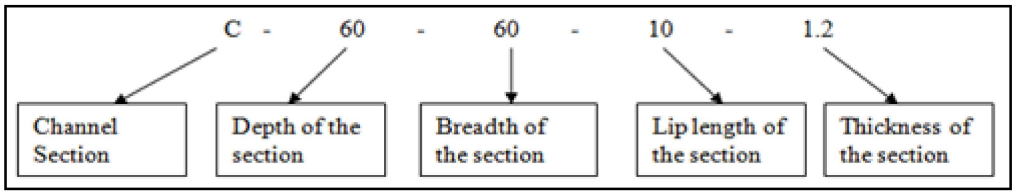

3. FINITE ELEMENT ANALYSIS

3.1 General

The finite element program ANSYS 13 was used to simulate the behavior of pin-ended cold-formed lipped channel columns. The numerical simulation consisted of two stages. In the first stage, an Eigen buckling analysis was performed on a "perfect" geometry to establish probable buckling modes of a column. In the second stage, a non-linear analysis by incorporating both geometric and material non- linearity's was then performed using the Arc length method to obtain the ultimate load and failure modes of columns.

3.2 Element Type and Mesh

The Shell 181 thin elements were used in the FEM. SHELL181 is suitable for analyzing thin to moderately-thick shell structures. It is a four-node element with six degrees of freedom at each node: translations in the x, y, and z directions, and rotations about the x, y, and z-axes. (If the membrane option is used, the element has translational degrees of freedom only). The degenerate triangular option should only be used as filler elements in mesh generation. The meshing size of the specimen was kept approximately as 10mmx10mm.

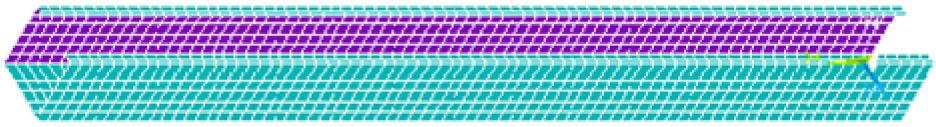

Figure 4 Modeling of Specimen C-80-80-20

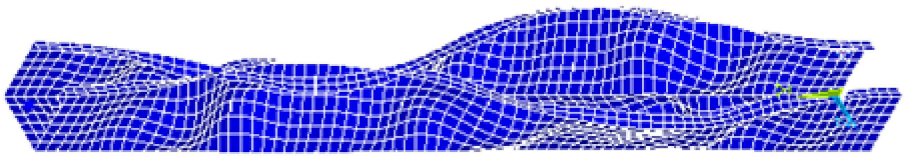

Fig 5 Buckling mode shows L/D interaction of Specimen C-80-80-20

3.3 Boundary Condition

The FEM simulated the channel columns compressed between simply supported ends. The rigid region was created at both the ends as shown in Figure6.

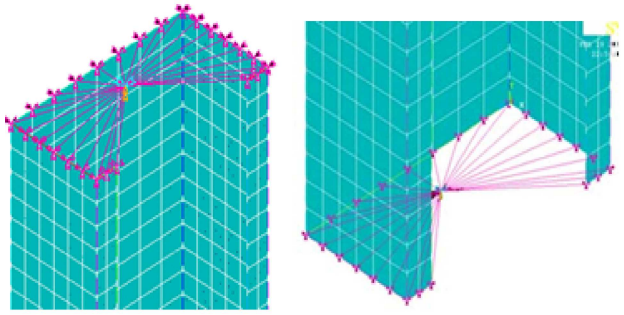

Fig.6 Model showing rigid region at top and bottom

3.4 Method of Loading

Axial compressive load was applied to the master node at the top end and the corresponding reaction was recorded at the bottom end master node.

3.5 Material properties

The poisons ratio was taken as 0.3 and the yield stresses were varies as 250, 350, 450 Mpa and corresponding strains were considered. The material property was considered to be multi linear.

3.6 Geometric Imperfections

The geometric imperfection was included as 0.25 times the thickness of the specimen and the specimen was being updated. Before testing the specimen the sections were subjected to geometric imperfections due to handling and transportation. Hence the geometric imperfections were approximately taken as 0.25 times the thickness of the specimen.

3.7 Validating ANSYS Procedure

To validate the FEA Procedure experimental result available in the Literature (Ben young, 2002) was used. The test result and the numerical analysis result were compared in the Table 3.

Table 3 Comparison of Experimental Result with the Numerical Result

Specimen ID	Experimental Result, kN	Numerical Result, kN
P-36-F-1000	89.2	87.8

4. PARAMETRIC STUDY

The verified model was used in the parametric study. Parametric study was carried out for 3 yield stress values (250 Mpa, 350 Mpa, 450 Mpa) with two thicknesses of 1.2 and 1.6 mm. From the buckling plot it was observed that the change in yield stress value doesn't affect the buckling interaction. The interaction was also ensured for the all three yield stress values. In the parametric study a total of 18 analysis cases were carried out by using the verified model.

4.1 Parametric Study Results

The parametric study results were shown in table 4. The sample axial load vs. axial displacement curve obtained from the nonlinear analysis program ANSYS for C-80-80-1.2 was shown in Figure 7(a) and 7(b) for the yield stresses 250 and 450Mpa.

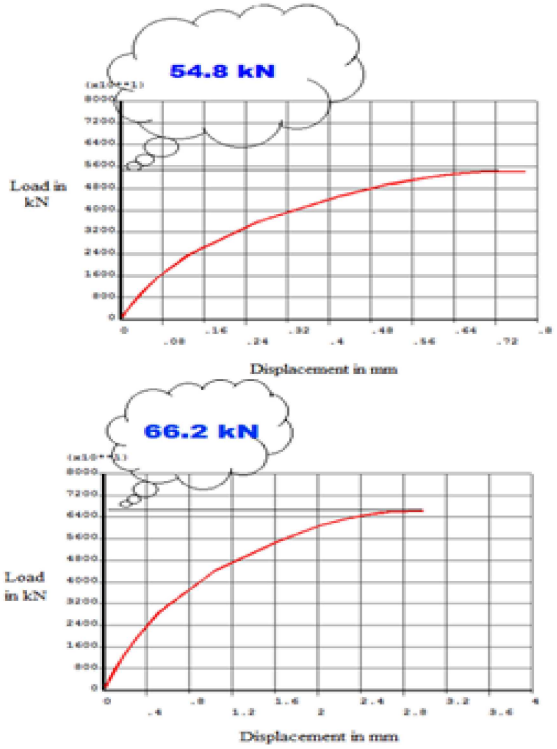

Figure 7 Load vs. Displacement curve((a) 250Mpa, (b) 350Mpa) for C-80-80-20

5. THEORETICAL ANALYSIS

In this paper Direct Strength Method (North American Specifications (AISI S100-2007) was used for the theoretical analysis. The results getting from this code were tabulated in table 4.

6. RESULTS AND DISCUSSION

From the parametric study results it was observed that Ultimate load obtained from the Finite element analysis were lesser than the Direct strength method. The ratio between the ultimate loads from FEM to DSM was in the mean and standard deviation of 0.92 and 0.05 respectively.

Table 4 Comparison of Finite Element Results with Theoretical Results

Sl.No.	Specimen ID	Thickness 't' in mm	Length in mm	L/D	Yield stress in Mpa	P_{FEM}	P_{DSM}	P_{FEM}/P_{DSM}
1	C-60-60-10	1.2	762	1.07	250	48.50	49.30	0.98
2		1.2	762	1.08	350	57.80	60.50	0.96
3		1.2	762	1.07	450	62.72	69.89	0.90
4	C-75-75-15	1.2	1016	0.95	250	51.37	52.37	0.98
5		1.2	1016	0.95	350	53.39	56.78	0.94
6		1.2	1016	0.96	450	57.33	58.80	0.97
7	C-80-80-20	1.2	1016	0.90	250	54.80	58.17	0.94
8		1.2	1016	0.92	350	66.22	70.81	0.94
9		1.2	1016	0.98	450	76.75	81.14	0.95
10	C-80-60-16	1.6	915	1.03	250	70.25	81.46	0.86
11		1.6	915	1.03	350	89.12	101.50	0.88
12		1.6	915	1.03	450	119.68	131.56	0.91
13	C-80-50-10	1.6	940	1.01	250	58.36	69.31	0.84
14		1.6	940	1.01	350	78.42	85.75	0.91
15		1.6	940	1.02	450	101.36	110.82	0.91
16	C-60-35-12	1.6	510	1.00	250	44.36	54.24	0.82
17		1.6	510	1.00	350	67.98	73.64	0.92
18		1.6	510	1.00	450	93.69	108.11	0.87
							Mean	0.92
							S.D	0.05

The interaction of local/distortional buckling reduces the ultimate load carrying capacity of the lipped channel columns with pinned end conditions. The buckling interaction leads to premature failure of the column. Based on the linear regression analysis a equation was proposed to design the lipped channel columns undergoing local/distortional buckling interaction.

The residual square value for the proposed equation was 0.979 which indicates the regression line best fits with the data.

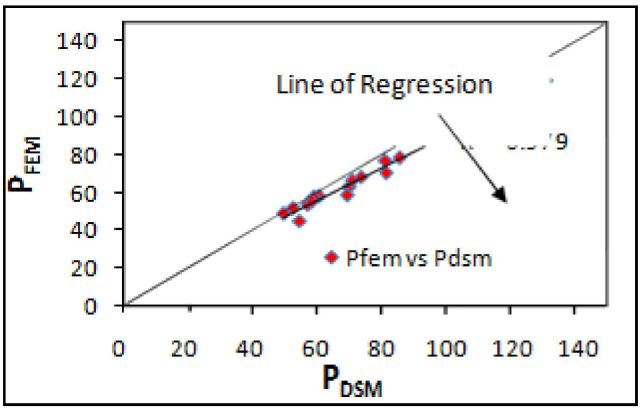

Fig.8 P_{DSM} vs. P_{FEM} curve

$$P_{FEM} = (0.861 * P_{DSM}) + 3.784 \quad (1)$$

7. CONCLUSION

This paper presents a finite element analysis and design of cold-formed channel columns compressed between simply supported ends. A finite element model including geometric and material non-linearity has been developed and verified against experimental results available in the literature. The failure modes predicted by the finite element analysis was Local/Distortional interaction, but the DSM predict as either local or distortional buckling. This shows that DSM didn't consider the local/distortional buckling interaction. Therefore DSM unconservatively predicted the ultimate strength of simply supported lipped channel columns. The interaction of the local and distortional buckling was the main reason for premature failure of the sections. This failure tends to reduction in ultimate capacity of the specimen. Hence, a column strength equation was proposed to calculate the ultimate capacity of the simply supported lipped channel columns. This equation was simple and reliable; it can be easily applicable for the practical design.

REFERENCES

[1] Ben Young, Jintang Yan, " Finite Element Analysis And Design Of Fixed-Ended Plain Channel Columns", Elsevier Science, Vol.38, 2002, pp.549-566.

[2] Derrick C Y Yap , Gregory J. Hancock, "Experimental Study of High Strength Cold-Formed Stiffened Web Steel Sections", Centre for Advanced Civil Engineering, 2008.

[3] Al.Kwon et., "Compression Tests Of High Strength Cold-Formed Steel Channels With Buckling Interaction", Journal of Constructional Steel Research, Vol.65, 2009, pp.278-289.

[4] Y.B. Kwon and G.J. Hancock, "Tests of Cold Formed Channel with Local and Distortional Buckling", Journal of Structural Engineering ASCE, Vol.117, 1992, pp.1786-1803.

[5] North American Specification (NAS), (2001), Specification for the design of cold–formed steel members. North American cold-formed steel specification, American Iron and steel Institute, Washington, D.C.

[6] P. Borges Dinis, Dinar Camotim, "Local/distortional mode Interaction in Cold- formed Steel Lipped Channel Beams", Thin walled Structures, Vol.48, 2010, pp.771-785.

[7] V. Marimuthu, M. Saravanan and P. Prabha, "Numerical Studies On The Behaviour Of Intermediate Length Cold Formed Steel Lipped Channel Compression Members", Journal of Structural Engineering, Vol.39, 2012, pp.15-19.

A Road Mishap Positioning System and Identification of Injured Person Details Using E-Card

R.T.Paari[1] and J.Subhashini[2]
Department of Electronics and Communication Engineering, SRM University Kattankulathur -603 203, Chennai.
E-mail:pradeeppaari@gmail.com. subhasivaj@gmail.com.

Abstract

RFID(Radio Frequency Identification) technology is used for designing a Real-time Hospital Patient Management System(HPMS). Automatic Crash Notification is a system designed to be used in a crash situation. When a crash occurs, the intelligent system is activated and automatically sends crash details to the appropriate Emergency Medical Service Center. The position of the vehicle can be send to the rescue team using GPS technology. So the rescue team can easily find out the place of accident and they can hurry to the accident spot. In a health care context, the use of RFID technology can be employed to facilitate for automating and streamlining patient identification processes in hospitals and use of mobile devices like PDA, smart phones for designing the health care management systems.

Keywords: *Crash Notification Sensor, Global positioning system(GPS), Global System For Mobile Communication(GSM), Hospital Patient Management System(HPMS), Radio Frequency Identification(RFID).*

1. INTRODUCTION

Tracking living beings and devices using the Global Positioning System (GPS) has become prevalent and indispensable over the last few years. Applications range from military and national security to personal safety and comfort. This paper reviews the recent application areas and discusses the benefits and issues of GPS tracking. The use of GPS tracking and monitoring in our day to day lives can be broadly classified into the following categories: security (e.g., securing assets, tracking the potentially dangerous individuals such as parolees), navigation (e.g., in-car navigation systems), care (e.g., assisted living for the elderly), environment (e.g., wildlife monitoring), and resource optimization(traffic monitoring, fleet management).Equipping people with GPS is quite sensitive with respect to their privacy, and one should justify the use ethically. To ensure that private data is not revealed to unauthorized parties, collected private data is often anonymized. Such anonymization can be achieved by inserting fake data into the source data or by removing potentially identity revealing data selectively. Another technique to restrict drilling into private data is to block data queries that may result in identifying individuals.

Radio Frequency Identification technology (RFID) technolgy is used to improve the Crash Notification System with First-Aid Profile (FAP). First-Aid active RFID tag is pre-coded with a unique serial number (FAP-ID) that can be used to gain access to the First-Aid Profile of that tagged person. Compatible reader detects the presence of First-Aid tags and reports their FAP-IDs to the control unit, so that in crash situation all passengers FAP-IDs will be messaged to emergency medical service center. .In this paper, the possibilities and constraints of using RFID technology for identifying passengers in vehicle is investigated, based on the given hardware technological solution. Several tests are designed and carried out to investigate communication between the active RFID tag and the reader.

This system is designed in a move to reduce the death by intimating the crash details to the emergency medical service center for providing first-aid as early as possible. In recent years, with the miniaturization of biomedical sensors the fast development and popularization of information processing and wireless data transmission technology the research of wireless medical monitoring system has became a hot topic. By utilizing the wireless technique to transmit information between medical sensor and monitoring control center, the free space of patients is enlarged, and the efficiency of the modern management of hospitals is improved. Besides, the problem of lack of unremitted real-time care for every patient, which is caused by the shortage of health care members is also solved. Therefore, the portable wireless medical monitoring products will become popular in the future market. Thus by using the wireless

technology one can easily find out the person's details which is stored in the database and by making use of those details, doctor can easily find out the person's existing body conditions and blood group. Hence all the facilities for treatment are made before the person reaches the hospital. This reduces the treatment time and reduces the number of death rates.

2. BLOCK DIAGRAM AND DESCRIPTION

2.1. Vehicle Section

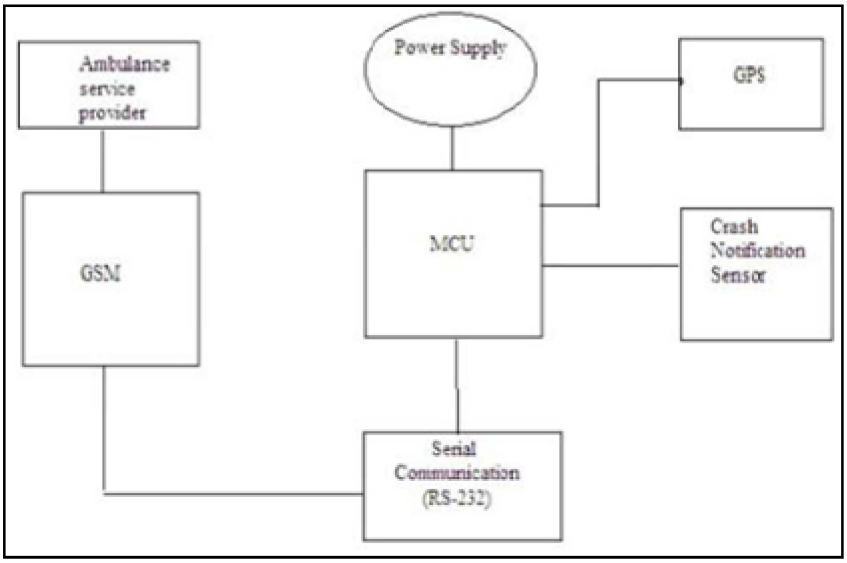

Fig.1 Vehicle section architecture

A microcontroller is a functional computer system on a-chip. It contains a processor core, memory, and programmable I/O peripherals.It has inbuilt memory and timer. Amplified signals from the sensors are fed to the Micro Controller Unit (MCU). If system enters a precarious mode, the unlock unit is enabled by the MCU.MCU gets the location values from GPS. Crash message will be transferred to the GSM device through RS232 protocol.GSM will send the message to ambulance service provider.

GPS uses the satellite details and continuously generates the current location of the vehicle and represent it in the form of latitude and longitude values. The sensor used here is the crash sensor i.e. vibrating sensor. This sensor indicates the higher vibration produced during the collision and indicate the vibration through producing an equivalent voltage signal. A threshold voltage level can be fixed and the sensor produces signal provided the produced voltage exceeds the threshold value.

2.2. Person Section

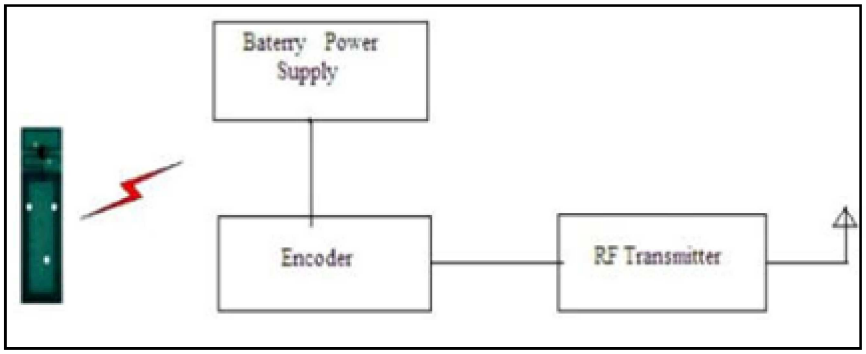

Fig.2 Person Section Architecture

In person section each person has a RFID tag. Each person's unique ID is encoded using a encoder.

Each RFID tag has a transmitter which transmits a unique ID and it is placed near the receiver.

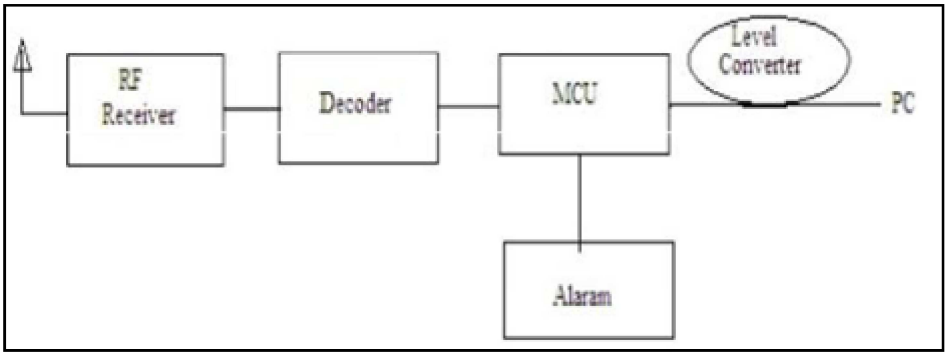

Fig.3 Receiver section architecture

In receiver section, a receiver unit receives the person ID and decoded it, and fed to the microcontroller. If any data is received in the pc section the alarm to be active. At this time ID is shown in the display unit. And also ID transfer to pc occur through serial communication, which display the person's information that get from the data base.

3. LOCATION VISUALISATION

Once a location is known, then one may wish to mark it on a map to visualize the location. Marking the location on a map when the coordinates of the location are known is quite straightforward. Google maps, for example, provide simple interfaces to mark locations. A GPS device normally provides locations in the NMEA (National Marine Electronics Association) format.

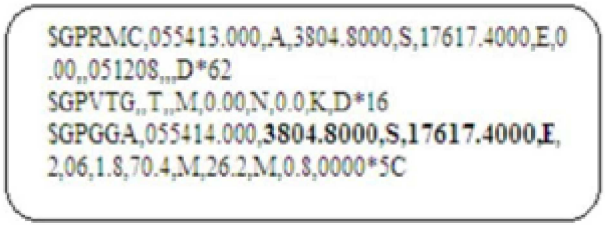

Fig.4 NMEA Format

The GGA message(commencing with the key $GPGGA) contains detailed GPS position information, and is the most frequently used data message for location. The latitude is the second field of the message which is marked as N (north) or S (south) in the third field. The longitude is the fourth field of the message which is marked as E (east) or W (west) in the fifth field. Both GPS-enabled devices and RFID-tagged items have the potential to reveal to unauthorized parties sensitive location information To be able to report its location, the device should have communication capabilities. We therefore assume a mobile device that is able to send and receive SMS text messages.

4. RESULT AND DISCUSSIONS

4.1 Vehicle Section

Fig.5 Location data marked on google map

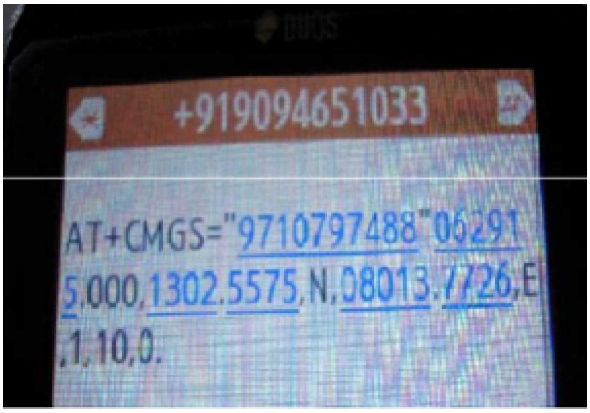

Fig.6 Output for vehicle section

Output consists of the sender number, receiver number, longitudinal and latitudinal values. +919094651033 represents the sender number i.e. sim number which is inserted in the GSM modem of the vehicle section. 9710797488 represents the receiver number i.e. the number which is programmed in the MCU to which the message has to be sent. 062915,000,1302.5575, N, 08013.7726, E, 1,110,0, represents the longitudinal and latitudinal values of the location.

4.2 Receiver Section

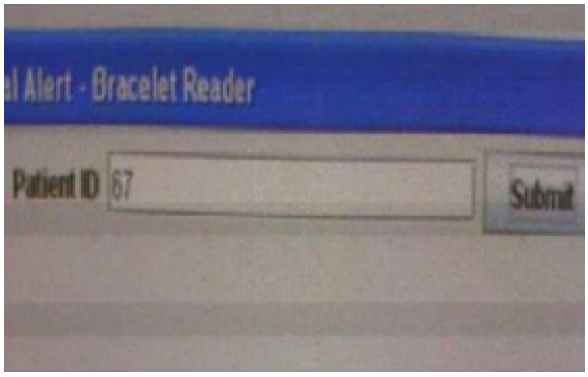

Fig.7 Displaying person's ID

PC section has one receiver unit. It receives the person ID and decode it.ID is fed to the microcontroller. If any data received in the PC section the alarm will be active.ID transfer to the PC through serial communication. At this time this ID is shown in display section. This display section displays the person information got from database stored in server. In receiver section there are two parts of output**.** The computer first receives the person's unique RFID and displays on the monitor**.** . In this section the number 67 represents the person's unique ID which is encoded into the chip of the particular person**.** Clicking the "Submit" button will navigate to the person's details page which is stored in database. This helps the doctor to know about patient details quickly without checking his/her condition this reduces treatment time.

4.3 Person's Details

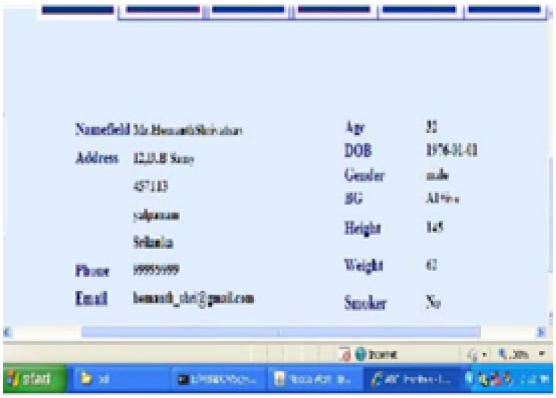

Figure. 8. Displaying person's details

In the second part, the monitor displays the person's details. It is illustrated in Fig. 11. It displays the person's name, address, phone number, E-mail ID , age ,date of birth, gender ,blood group, height, weight etc. It also includes emergency contact details, Person's medical history and also date of the treatment, hospital details, prescription etc. Thus these details helps doctors to know all the details of patients before carrying out of various tests thus it reduces the treatment time and helps to save the patients from critical.

4.4 Person's Physician Details

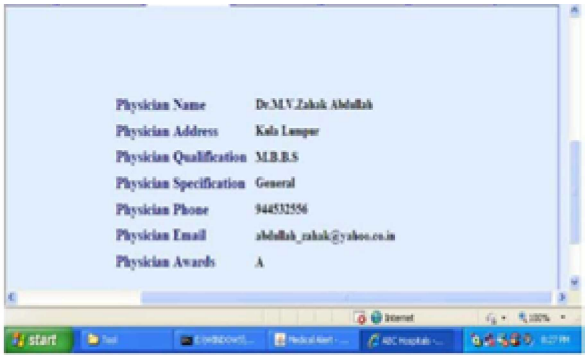

Fig.9 Displaying person's physician details

In the second window, which is illustrated in Fig. 12 displays the person's physician details which can be used for reference. This reference details can be used for further proceedings in the treatment.

5. CONCLUSION

This system is designed in a move to reduce the deaths which occur due to delays. The first aspect of this paper is to reduce the deaths which occur due to delay in intimating the accident details to ambulance service and the second one is to identify the details of person using a RFID tag. Person's photo identity can be included in the database. With this enhancements system can be more efficient. technologies is used for information transferring System is low cost and compact. Effective alert system. stores every information of patients in data base. Treatment time is reduced. There is no lack of intelligence in the detection systems. It does not fails to track the collision. Automatic collision inform is possible. Way of monitoring people is not manual. Easiest way of monitoring and collecting patients information. Accesible through world-wide .Need not necessary to hold the patients documents.

REFERENCES

[1] J. A. A´ lvarez *et al.*, "Where do We Go? OnTheWay: A Prediction System for Spatial Locations", in ICUC '06: Proceedings of the 1st International conference on Ubiquitous Computing, 2006, pp.46–53.

[2] N. Chadil, A. Russameesawang and P. Keeratiwintakorn, "Realtime Tracking Management System Using GPS, GPRS and Google earth", in Proceedings of the 5th International Conference on ElectricalEngineerin/ Electronics,Computer, Telecommunications/and Information Technology, Vol.1, 2008, pp. 14-17.

[3] J. Voelcker, "Stalked by Satellite-An Alarming Rise in GPS Enabled Harassment", IEEE Spectrum, Vol.43, No.7, July 2006, pp. 15–16.

[4] B. Hoh et al., "Preserving Privacy in GPS Traces Via Uncertainty aware Path Cloaking", in CCS '07: Proceedings of the 14th ACM Conference on Computer and Communications Security. ACM 2007, pp. 161–171.

[5] K. Michael, A. McNamee and M. Michael, "The Emerging Ethics of Human Centric GPS Tracking and Monitoring", in Proceedings of the International Conference on Mobile Business June 2006, pp. 34–43.

[6] Peter Jones, Colin Clarke-Hill, Peter Shears, Daphne Comfort, and David Hillier, "Radio Frequency Identification in the UK: Opportunities and Challenges", in proceedings of the International journal of Retail and Distribution Management vol.32, no.2/3, 2004, pp.164- 171.

[7] P. Juang *et al.*, "Energy-efficient Computing for Wildlife Tracking: Design Tradeoffs and Early Experiences with Zebranet", SIGOPS Oper. Syst. Rev., Vol.36, No.5, 2002, pp. 96–107.

[8] M. Spirito, "On the Accuracy of Cellular Mobile Station Location Estimation", IEEE Transactions on Vehicular Technology, Vol.50, No.3, 2001, pp. 674-685.

[9] Korhonen, J. Parkka and M. Van, "Health Monitoring in the Home of the Future", IEEE Engineering in Medicine and Biology , Vol.5, 2003, pp.66-73.

[10] I F.Akyildiz, "Wireless Sensor Networks: A Survey Computer Networks", Vol.38, No.9, 2002, pp.393-422.

Implementation and Analysis of USB Device Drive for Atmel Processors

V. Saratha and C. Sherine Nivya Nayagam
Department of Electronics and Communication, Mepco Schlenk Engineering College, Sivakasi -626 005.
E-mail: sarajan.v@gmail.com and sherinenivya@gmail.com

Abstract

A Universal Serial Bus (USB) device drive is designed for Atmel processors. At present the device drives are unique for distinct families. Here, the proposed device drive can be used for accessing the hardware services connected to the peripheral modules which uses processors of different Atmel families. The initial step includes the establishment of the serial communication between the PC and the drive. This is done by using the Visual Basic. Also we focus for enabling the transmission and reception of data from applications that uses various Atmel processors. The process also includes the performance analysis of the designed device drive.

Keywords: Atmel processors, Device drive, USB.

1. INTRODUCTION

The device driver sets the ports to enable communicate to a Specific device. It then passes on the Operating System's (OS) identification requests and help the OS allocate the device's resource settings within the OS. USB devices are relatively complicated. For example, typically USB devices have their own microcontroller to handle the USB communications. These microcontrollers are programmed with "firmware".

This is software that provides the USB device with its functionality. Usually the device will send data in the form of Hex codes. The driver decodes this HEX(Hexadecimal) packet, does any necessary filtering of data, and maps the coordinates for use by the OS. Because of the device driver, the OS can communicate with many different devices. The driver translates between specific devices and a general operating system. The OS only speaks in terms of higher level code and data structures. The device just streams data.

2. NEED FOR USB DEVICE DRIVE

The device drives available are unique for every processor. Hence there is need for installation of driver software every time when a new processor has been used in the peripheral modules that belong to various applications. The proposed design overcomes this problem by the usage of firmware which enables the use of common device drive for various processors belonging to Atmel. In addition, it has the facility of changing the baud rate according to the requirement of the application.

3. SYSTEM DESIGN AND DEVELOPMENT

The block diagram of the proposed design is as in figure 1. The Personal Computer (PC) host is installed with Visual Basic for the purpose of interfacing and enabling the serial communication using Serial Interface Engine (SIE) with the USB device drive. This is done by using Microsoft Comm (MSComm) control in Visual Basic. The application module also communicates serially with the device drive. The USB device drive is designed and made to be detected by the PC by installing the driver software in the PC. When the application is connected, the interrupt is enabled and the required event task is commenced as per the application.

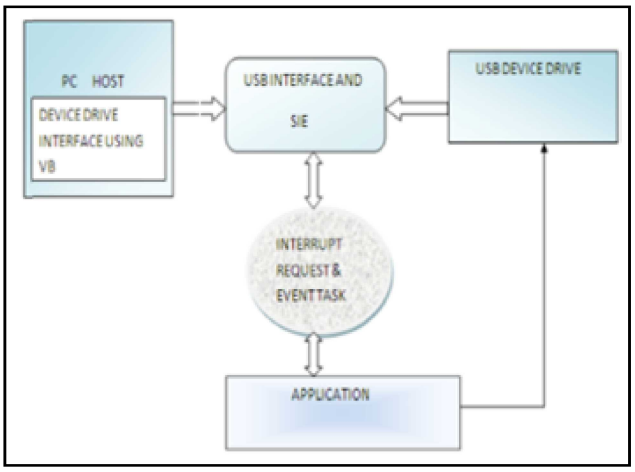

Fig.1 Overall block diagram

4. BLOCK DIAGRAM OF USB DEVICE DRIVE

The Block Diagram of the proposed USB Device Drive is given in Figure.2. MAX 232 is used for the

purpose of serial communication. The applications are connected to the input ports of the microcontroller and the output ports are used for the communication with the PC. For accessing more than a application, more MSComm control is used.

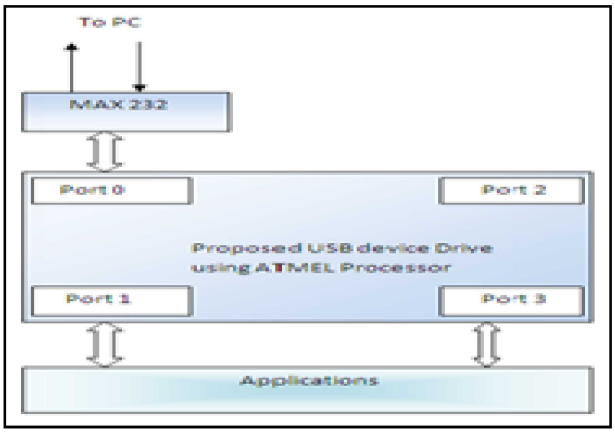

Fig.2 Block diagram of USB device drive

5. DESIGNED HARDWARE USB DEVICE DRIVE

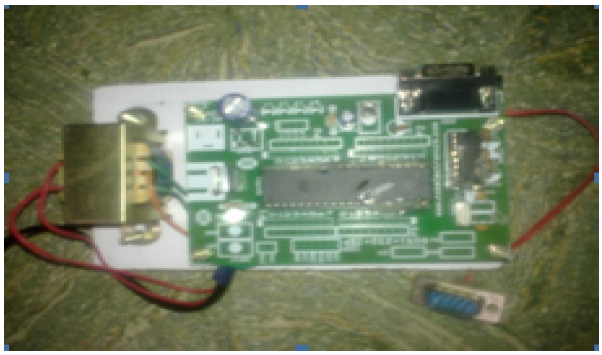

Fig.3 Designed Hardware USB device drive

6. COMPONENTS REQUIRED

The hardware components required for this proposed design includes the processors AT89C51, AT89S52, AT90S2313. MAX232 for purpose of serial communication. The software required includes Visual Basic and Keil Micro Vision. Visual Basic Software is used for the purpose of establishing serial communication.

7. EXAMPLE APPLICATION DESIGN

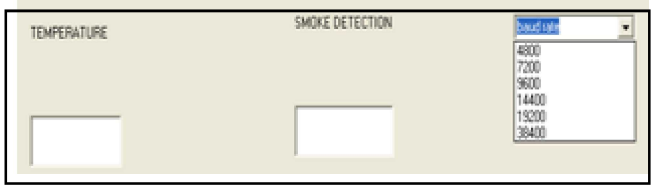

Fig.4 Example application design

The design includes example application such as temperature sensing and smoke detection. For temperature sensing application the sensed data is transmitted via the USB device drive to the Visual Basic application in the PC. The facility to change the Baud rate is also provided.

8. WINDOWS DRIVER ARCHITECTURE

There are two types of Windows drivers, legacy and Plug and Play (PnP) drivers. The focus here is only on PnP drivers, as all drivers should be PnP drivers where possible. PnP drivers are user friendly since very little effort is required from users to install them. Another benefit of making drivers PnP is that they get loaded by the operating system only when needed, thus they do not use up system resources needlessly. Legacy drivers were implemented for Microsoft's earlier operating systems and their architecture is outdated.

9. OBTAINING DRIVER USAGE INFORMATION

The device manager found in the control panel system applet provides driver information for users. It lists all currently loaded drivers and information on the providers of each driver and their resource usage. It also displays drivers that failed to load and their error codes. In the proposed design, once the designed device drive is connected to the PC, the port number is viewed in the device manager. The user needs to enter this port number as input to enable the application.

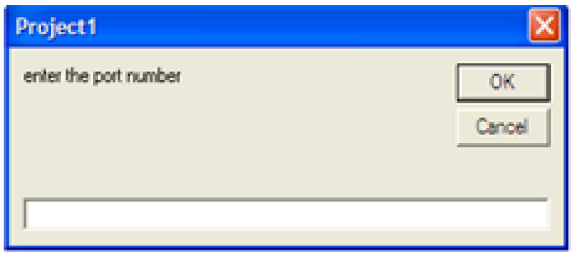

Fig.5 Obtaining driver information

10. SERIAL COMMUNICATION

The MSComm control is used for providing serial communication for our applications by allowing the transmission and reception of data through the serial port.

10.1 MSComm: MSComm control provides 2 ways of handling communication. Event-driven communications is a very powerful method for handling serial port interactions. Another method is polling for events and

errors by checking the value of communication event (comm event) property. In many situations we want to be notified the moment an event takes place, such as when a character arrives or a change occurs in the Carrier Detect (CD) or Request To Send (RTS) lines. In such cases, the MSComm control's ONComm event is used to trap and handle these communication events. The ONComm event also detects and handles communication errors.

10.2 ONComm

When the ONComm() event is fired the value of the CommEvent property is checked to see what exactly had happened. The CommEvent property will contain a different value for each different kind of communication errors that occurs.

11. INTERRUPT HANDLING

An interrupt service routine (ISR) is responsible for reacting quickly and efficiently to device events. It is invoked almost directly via a hardware-defined exception mechanism that interrupts the current flow of processor execution and enables the potential return to that flow after completion of the ISR. In general, the length of the ISR should be minimized so as to maximize the burst rate of device events that can be achieved, to reduce ISR invocation latency of all ISRs, and to minimize the overall CPU processing required for a given number of device events. Any additional per-interrupt processing can have a negative impact on all three aspects of interrupt processing.

12. PROCESSORS

12.1 AT89c51

The AT89c51 is a low power, high performance CMOS 8-bit microcomputer with 4K bytes of Flash programmable and erasable read only memory (PEROM). The on-chip Flash allows the program memory to be reprogrammed in- system or by a conventional non volatile memory programmer. By combining a versatile 8-bit CPU with flash on a monolithic chip, the Atmel AT89C51 is a powerful microcomputer which provides a highly – flexible and cost effective solution to many embedded control applications.

12.2 AT89s52

The AT89s52 is a low power, high performance CMOS 8-bit microcontroller with 8K bytes of in-system programmable Flash memory. The on- chip Flash allows the program memory to be reprogrammed in-system or by a conventional nonvolatile memory programmer. By combining a versatile 8-bit CPU with in-system programmable Flash on a monolithic chip, the Atmel AT89S52 is a powerful microcontroller which provides a highly-flexible and cost effective solution to many embedded control applications.

12.3 AT90s2313

The AT90s2313 is a low power CMOS 8-bit microcontroller based on the AVR RISC architecture. By executing powerful instructions in a single clock cycle, the AT90s2313 achieves throughputs approaching1 MIPS per MHZ allowing the system designed to optimize power consumption versus processing speed. The AVR core combines a rich instruction set with 32 general purpose working registers. All the 32 registers are directly connected to the Arithmetic Logic Unit (ALU) allowing two independent registers to be accessed in one single instruction executed in one clock cycle. The resulting architecture is more code efficient while achieving throughputs up to ten times faster than conventional CISC microcontrollers.

13. IMPACT

The proposed USB device drive overcomes the problem of using separate drivers for different Atmel processors, thus reducing the complexity. This also has the provision to change the baud rate according to the requirement of the application.

REFERENCES

[1] Ms. Disha Juriasinghani, Mr. Tanay Krishna Dev, "Embedded System for USB WiFi Bridge", International Journal of Engineering Research and Applications (IJERA) Vol. 2, No.1, Jan- Feb 2012.

[2] William Buchanan , "PC interfacing: Communications and Windows Programming", Addison Wesley, 1998.

[3] Asim Kadav and Michael M. Swift, "Understanding Modern Device Drivers", in ASPLOS '12: Proceedings of the 17th International Conference on Architectural Support for Programming Languages and Operating Systems, March 2012.

[4] Gong Yun, Sun Li-hua, "Analysis and Implementation of USB Driver Based on VxWorks, Electrical and Control Engineering (ICECE)", 2010 International Conference.

[5] Guo Li; Mingli Li; Gensen Zhao; Jinmei Zang, "Research on USB Driver for Data Acquisition", Future Computer and Communication (ICFCC), 2010 2nd International Conference.

Adaptive Wavelet Thresholding Method for MRI Medical Image Denoising

Dr. M.G.Sumithra[1] and B.Deepa[2]
[1]Bannari Amman Institute of Technology, Sathyamangalam - 638 401, Erode District, TamilNadu
[2]V.S.B Engineering college,Karur - 639 111, TamilNadu
E-mail: mgsumithra@rediffmail.com, cool.deeps.143@gmail.com[2]

Abstract

Image denoising has become an essential exercise in medical imaging especially the Magnetic Resonance Imaging (MRI).In recent years, technological development has significantly improved in analyzing medical imaging. This paper proposes an adaptive threshold estimation method for denoising medical images in the wavelet domain using Daubechies wavelet. The proposed method called NormalShrink is computationally more efficient and adaptive because the parameters required for estimating the threshold depend on subband data. The threshold is computed by σy2/yy where y and yy are the standard deviation of the noise and the subband data of noisy image respectively. σ is the scale parameter, which depends upon the subband size and number of decompositions. Experimental results on several test images are compared with various denoising techniques like Wiener Filtering , BayesShrink and SureShrink . To benchmark against the best possible performance of a threshold estimate, the comparison also include Oracleshrink. Experimental results show that the proposed threshold removes noise significantly and remain within 4% of OracleShrink and outperforms SureShrink, BayesShrink and Wiener filtering most of the time. Further the results are evaluated using objective and subjective measures.

Keywords: *Discrete Wavelet Transform, Image Denoising,Wavelet Thresholding.*

1. INTRODUCTION

An image is often corrupted by noise in it's acquit ion and transmission. Image denoising is used to remove the additive noise while retaining as much as possible the important signal features. In the recent years there has been a fair amount of research on wavelet thresholding and threshold selection for image de-noising [1], [3]-[10], [12], because wavelet provides an appropriate basis for separating noisy signal from the image signal. The motivation is that as the wavelet transform is good at energy compaction, the small coefficient is more likely due to noise and large coefficient due to important signal features [8]. These small coefficients can be threshold without affecting the significant features of the image. Thresholding is a simple non-linear technique, which operates on one wavelet coefficient at a time. In its most basic form, each coefficient is threshold by comparing against threshold, if the coefficient is smaller than threshold, set to zero; otherwise it is kept or modified. Replacing the small noisy coefficients by zero and inverse wavelet transform on the result may lead to reconstruction with the essential image characteristics and with less noise. Since the work of Donoho and Johnstone [1], [4], [9],[10], there has been much research on finding thresholds, however few are specifically designed for images. In this paper, a near optimal threshold estimation technique for image denoising is proposed which is subband dependent i.e. the parameters for computing the threshold are estimated from the observed data, one set for each subband.

1.1 INTRODUCTION TO WAVELET TRANSFORM

In most of the applications of image processing, it is essential to analyse a digital signal. If the data will be transformed into any other domain then the structure and features of the signal may be better understood. There are several transforms available like Fourier transform, Hilbert transform, Wavelet transform, etc. The wavelet transform is better than Fourier transform because it gives frequency representation of raw signal at any given interval of time, but Fourier transform gives only the frequency- amplitude representation of the raw signal, but the time information is lost. So we cannot use the Fourier transform where we need time as well as frequency information at the same time. Daubechies wavelet is the first wavelet family which has set of scaling function which are orthogonal. This wavelet has

finite vanishing moments. Daubechies wavelets have balanced frequency responses but non-linear phase responses. Daubechies wavelets are useful in compression and noise removal of audio signal processing because of its property of overlapping windows and the high frequency coefficient spectrum reflect all high frequency changes.

2. TYPES OF NOISES

2.1 Salt and Pepper Noise

Salt and pepper noise is a form of noise typicallyseen on images. It represents itself as randomly occurring white and black pixels. A "spike" or impulse noise drives the intensity values of random pixels to either their maximum or minimum values. The resulting black and white flecks in the image resemble salt and pepper. This type of noise is also caused by errors in data transmission.

2.2 Speckle Noise

In medical literature, speckle noise is referred to as 'texture' and may possibly contain useful diagnostic information. Physicians generally have a preference for the original noisy images, more willingly, than the smoothed versions because the filter, even if they are more sophisticated, can destroy some relevant image details. In our work, we recommend hybrid filtering techniques for removing speckle noise in ultrasound images. The speckle noise model has the following form (* denotes multiplication). For each image pixel with intensity value f_{ij} ($1< i < m, 1 < j < n$ for an m x n image), the corresponding pixel of the noisy image g_{ij} is given by,

$$g_{i,j} = f_{i,j} + f_{i,j} * n_{i,j} \quad (1)$$

where, each noise value n is drawn from uniform distribution with mean 0 and variance σ^2.

2.3 Gaussian Noise

Gaussian noise is statistical noise that has a probability density function of the normal distribution (also known as Gaussian distribution). Noise is modeled as additive white Gaussian noise (AWGN), where all the image pixels deviate from their original values following the Gaussian curve. That is, for each image pixel with intensity value fij ($1< i <m, 1<j < n$ for an m x n image), the corresponding pixel of the noisy image gij is given by,

$$g_{i,j} = f_{i,j} + n_{i,j} \quad (2)$$

where, each noise value n is drawn from a zero -mean Gaussian distribution.

2.4 Poisson noise:

J = imnoise (I,'poisson') generates Poisson noise from the data instead of adding artificial noise to the data. If I is double precision, then input pixel values are interpreted as means of Poisson distributions scaled up by 1e12. For example, if an input pixel has the value 5.5e-12, then the corresponding output pixel will be generated from a Poisson distribution with mean of 5.5 and then scaled back down by 1e12. If I is single precision, the scale factor used is 1e6. If I is uint8 or uint16, then input pixel values are used directly without scaling.

3. WAVELET THRESHOLDING

Let $f = \{f_{ij}, i, j = 1,2\ldots M\}$ denote the MxM matrix of the original image to be recovered and M is some integer power of 2. During transmission the image f is corrupted by independent and identically distributed (i.i.d) zero mean, white Gaussian Noise n_{ij} with standard deviation σ i.e. $n_{ij} \sim N(0, \sigma^2)$ and at the receiver end, the noisy observations $g_{ij} = f_{ij} + \sigma n_{ij}$ is obtained. The goal is to estimate the image f from noisy observations g_{ij} such that Mean Squared error (MSE) [11] is minimum. Let W and W^{-1} denote the two dimensional orthogonal discrete wavelet transform (DWT) matrix and its inverse respectively. Then $Y = W_g$ represents the matrix of wavelet coefficients of g having four subbands (LL, LH, HL and HH) [7], [11]. The sub-bands HH_k, HL_k, LH_k are called details, where k is the scale varying from 1, 2 …… J and J is the total number of decompositions. The size of the subband at scale k is $N/2^k$ x $N/2^k$ .The subband LL_J is the low-resolution residue. The wavelet thresholding denoising method processes each coefficient of Y from the detail subbands with a soft threshold function to obtain X. The denoised estimate is inverse transformed to $f = W^{-1}X$.In the experiments, soft thresholding has been used over hard thresholding because it gives more visually pleasant images as compared to hard thresholding; reason being the latter is discontinuous and yields abrupt artifacts in the recovered images especially when the noise energy is significant.

4. ESTIMATION OF PARAMETERS FOR NORMALSHRINK

This section describes the method for computing the various parameters used to calculate the threshold

value (T_N), which is adaptive to different subband characteristics.

$$T_N = \frac{\beta \hat{\sigma}^2}{\hat{\sigma}_y} \quad (3)$$

Where, the scale parameter в is computed once for each scale using the following equation:

$$\beta = \sqrt{\log\left(\frac{L_k}{J}\right)} \quad (4)$$

L_k is the length of the subband at k^{th} scale. $\hat{\pm}^2$ is the noise variance, which is estimated from the subband HH_1, using the formula [7][13]:

$$\hat{\pm}^2 = \left[\frac{median(|Y_{ij}|)}{0.6745}\right]^2 , Y_{ij} € \text{ Sub band } HH_1 \quad (5)$$

and $\hat{\pm}_y$ is the standard deviation of the subband under consideration computed by using the standard MATLAB command. To summarize, the proposed method is named as *NormalShrink* which performs soft thresholding with the data driven subband dependent threshold T_N .

5. IMAGE DENOISING ALGORITHM

This section describes the image denoising algorithm, which achieves near optimal soft thresholding in the wavelet domain for recovering original image from the noisy one. The algorithm is very simple to implement and computationally more efficient. It has following steps:

1 Perform multiscale decomposition [11] of the image corrupted by various noises using wavelet transform.
2 Estimate the noise variance σ^2 using equation (5).
3 For each level, compute the scale parameter β using equation (4).
4 For each subband (except the lowpass residual)
  a) Compute the standard deviation σ_y.
  b) Compute threshold T_N using equation (3).
  c) Apply soft thresholding to the noisy coefficients.
5 Invert the multiscale decomposition to reconstruct the denoised image *f*.

6. EXPERIMENTAL RESULTS AND DISCUSSIONS

The proposed wavelet transform method has been implemented using MATLAB 10.0. The wavelet transform employs Daubechies' least asymmetric compactly supported wavelet with eight vanishing moments [14] at four scales of decomposition. To assess the performance of NormalShrink, it is compared with SureShrink, BayesShrink, OracleThresh and Wiener. The measurement of medical image enhancement is difficult and there is no unique algorithm available to measure enhancement of medical image. We use statistical tool to measure the enhancement of medical images. The Root Mean Square Error (RMSE) , Peak Signal-to-Noise Ratio (PSNR) and Image Enhancement Factor (IEF) are used to evaluate the enhancement of medical images.

$$RMSE = \sqrt{\frac{\sum (f(i,j) - g(i,j))^2}{mn}} \quad (6)$$

$$PSNR = 20 \log_{10}\left(\frac{255}{RMSE}\right) \quad (7)$$

Here f (i,j) is the original medical image with impulse noise, g(i,j) is an enhanced image and m and n are the total number of pixels in the horizontal and the vertical dimensions of the image.

$$IEF = \frac{\left(\sum_i \sum_j (n_{ij} - r_{ij})^2\right)}{\left(\sum_i \sum_j (x_{ij} - r_{ij})^2\right)} \quad (8)$$

Where r refers to original image, n gives the corrupted image x denotes the restored image. If the value of RMSE is low and value of PSNR is high then the enhancement approach is better. The original noisy image and enhanced image of MRI brain cancer image, MRI Knee image, and the MRI brain image obtained by wavelet transform with adaptive threshold are shown in the following figures.

The performance analysis of wavelet transform for various thresholding techniques for MRI Brain image corrupted by salt and pepper noise is shown in fig 1. Oracle Shrink removes the noises present at the edge of image, while Sure Shrink performs better than oracle Shrink. Comparative results are seen for Normal Shrink, thereby proposed method performs in a better manner than other.

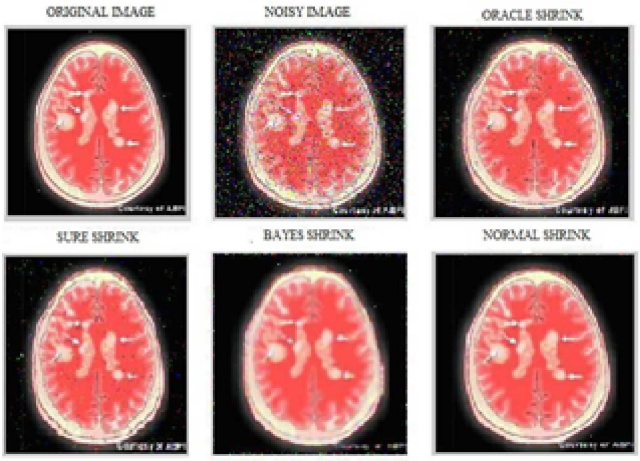

Fig.1.Wavelet Transform analysis for MRI Brain image

Figure 2 indicates the performance of wavelet transform for various thresholding techniques for the image corrupted by Gaussian noise. It is observed from the results that the proposed method is showing enhanced performance than the other thresholding techniques even for higher decibel(dB) of noise level.

The performance of PSNR estimation using different thresholding methods for MRI Brain image affected by various noises is shown in figure 3. It is observed that for all types of noises, the proposed Normal Shrink is performing in an enhanced manner than the others. In case of speckle noise PSNR value increases in linear manner for the filtering methods as considered in this paper.

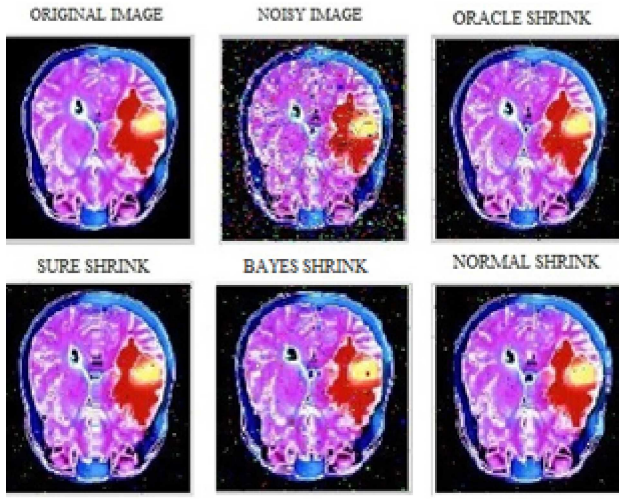

Fig.2.Wavelet Transform analysis for MRI Brain cancer image

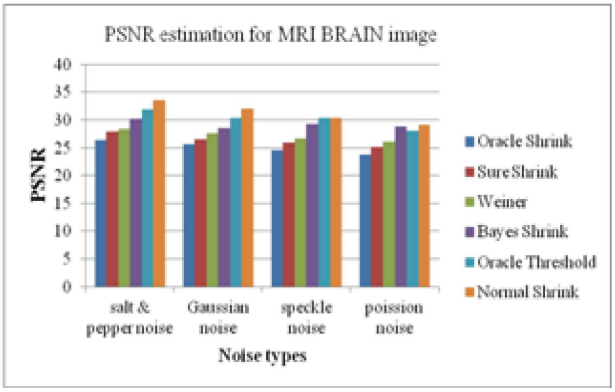

Fig.3. Performance of PSNR estimation for MRI Brain image

It is seen from the figure 4 that, better image quality is obtained after denoising, while using Normal Shrink for all type of noises and in case of Gaussian both Sure Shrink and Weiner method performs in an equal manner.

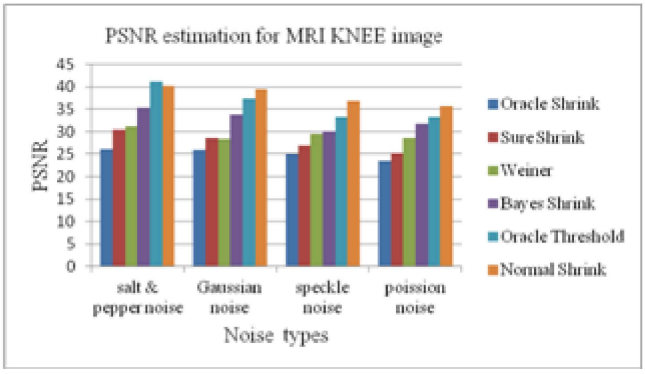

Fig.4. Performance of PSNR estimation for MRI Knee image

It is inferred from the figure 5 that the mean square error for enhanced and noisy image is seen low in proposed method for all types of noises. The maximum error value is seen for Weiner filter for the poisson noise and for the Oracle Shrink corrupted by the Gaussian noise.

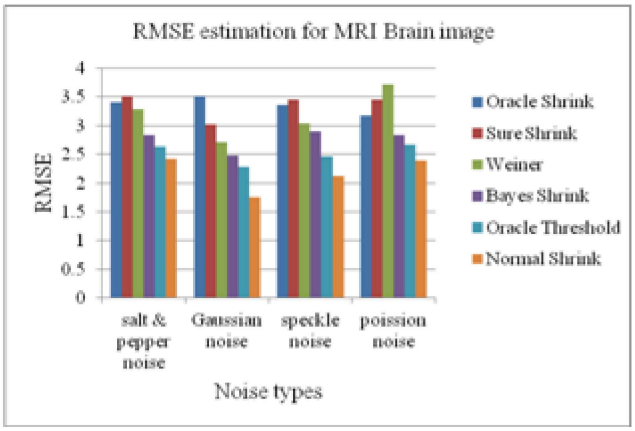

Fig.5. Performance of RMSE estimation for MRI BRAIN image

It is seen from the figure 6 that, better image quality is obtained after denoising, while using Normal Shrink for all type of noises where more error measurements is seen in Oracle Shrink and Sure Shrink method.

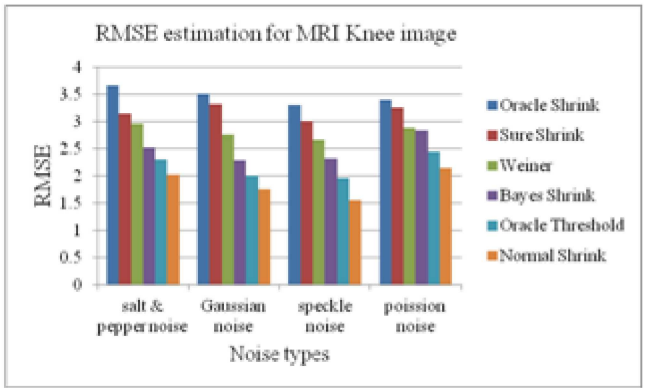

Fig.6. Performance of RMSE estimation for MRI Knee image

Table1.1.IMF for the MRI Brain Cancer Image

Noise Types	Methods				
	Oracle Shrink	Sure Shrink	Weiner Filter	Bayes Shrink	Normal Shrink
Salt & Pepper	12.94	17.32	23.45	27.53	28.66
Gaussian	15.22	16.72	22.59	24.29	26.33
Poission	11.83	14.72	18.93	22.64	26.83
Speckle	13.63	15.61	25.66	28.31	29.31

Table1.2.IMF for the MRI Knee image

Noise Types	Methods				
	Oracle Shrink	Sure Shrink	Weiner filter	Bayes Shrink	Normal Shrink
Salt & Pepper	10.43	13.72	16.52	20.513	22.364
Gaussian	12.212	14.712	18.179	19.91	20.233
Poission	13.43	15.32	16.162	18.42	19.53
Speckle	15.73	18.42	19.76	23.11	24.261

To benchmark against the best possible performance of a threshold estimate, the comparison include Oracle Shrink, the best soft thresholding estimate obtainable assuming the original image known. Normal Shrink outperforms Sure-Shrink and BayesShrink most of the time in terms of PSNR as well as in terms of visual quality. Moreover Normal-Shrink is 4% faster than Bayes Shrink.The choice of soft thresholding over hard thresholding is justified from the results of best possible performance of a hard threshold estimator, OracleThresh. Comparisons are also made with the best possible linear filtering technique i.e. Wiener filter (from the MATLAB image processing toolbox, using 3× 3 local window).

7. CONCLUSION

In this paper, a simple and subband adaptive threshold is proposed to address the issue of image recovery from its noisy counterpart. The image denoising algorithm uses soft thresholding [1] to provide smoothness and better edge preservation at the same time.Experiments are conducted to assess the performance of Normal Shrink in comparison with the Oracle Shrink, Sure Shrink, Bayes Shrink, OracleThresh and Wiener. The results show that Normal Shrink removes noise significantly, remain within 4% of OracleShrink, and outperforms SureShrink, BayesShrink and Wiener filtering most of the time. Moreover Normal-Shrink is 4% faster than BayesShrink. It is further suggested that the proposed threshold may be extended to the compression framework, which may further improve the denoising performance.

REFERENCES

[1] D.L.Donoho, "De-noising by soft-thresholding", IEEE Trans. on Inf.Theory, Vol.41, No.3, 1993, pp.613-627.

[2] Javier Portilla, Vasily Strela, Martin J Wainwright, Eero P. Simoncelli, October 2001, Adaptive Wiener Denoising using a Gaussian Scale Mixture Model in the wavelet Domain, Proceedings of the 8th International Conference of Image Processing Thessaloniki, Greece.

[3] S. Grace Chang, Bin Yu and M. Vattereli, Sept 2000, Adaptive Wavelet Thresholding for Image Denoising and Compression, IEEE Trans Image Processing, vol. 9, pp. 1532-1546.

[4] D.L. Donoho and I.M. Johnstone, "Adapting to unknown Smoothness via Wavelet Shrinkage", Journal of American Statistical Assoc., Vol.90, No.432, Dec 1995, pp.1200-1224.

[5] S. Grace Chang, Bin Yu and M. Vattereli, "Wavelet Thresholding for Multiple Noisy Image Copies", IEEE Trans. Image Processing, Vol.9, Sept 2000, pp.1631- 1635.

[6] S. Grace Chang, Bin Yu and M. Vattereli, "Spatially Adaptive Wavelet Thresholding with Context Modeling for Image Denoising", IEEE Trans. Image Processing, Vol.9, Sept. 2000, pp.1522-1530.

[7] M. Vattereli and J. Kovacevic, "Wavelets and Subband Coding", Englewood Cliffs, NJ, Prentice Hall, 1995,

[8] Maarten Jansen, Noise Reduction by Wavelet Thresholding, Springer –Verlag New York Inc.-2001.

[9] D.L. Donoho and I.M. Johnstone, "Ideal Spatial Adaptation via Wavelet Shrinkage Biometrica", Vol.81, 1994, pp. 425-455.

[10] D.L. Donoho and I.M. Johnstone, "Wavelet Shrinkage: Asymptopia?", J.R. Stat. Soc. B, ser. B, Vol. 57, No.2, 1995, pp.301-369.

[11] Savita Gupta and Lakhwinder kaur,NCC-2002, Wavelet Based Image Compression using Daubechies Filters, In proc. 8th National conference on communications, I.I.T. Bombay.

[12] M. Lang, H. Guo and J.E. Odegard, "Noise Reduction Using Undecimated Discrete wavelet transform", 1995, IEEE Signal Processing Letters.

[13] P.H. Westrink, J. Biemond and D.E. Boekee, "An Optimal Bit Allocation Algorithm for Sub Band Coding", in Proc. IEEE Int. Conf. Acoustics, Speech, Signal Processing, Dallas, TX, , 1987, pp. 1378-1381.

[14] Daubechies, "Ten Lectures on Wavelets", 1992, Vol. 61, of Proc. CBMS-NSF Regional Conference Series in Applied Mathematics. Philadelphia, PA: SIAM.

[15] Salem Saleh Al-amri, N.V. Kalyankar and S.D. Khamitkar, 2010, "A Comparative Study of Removal Noise from Remote Sensing Image", International Journal of Comp. Science, Vol.7, No.1, pp.32-36.

Design and Implementation of Security Based ATM System

R.Viswabharathi[1] and A.Suvarnamma[2]

[1&2]Department of Electronics and Communication Engineering, SRM University,Kattankulathur.

E-mail:sarvangen90@gmail.com and suvarnahudson@gmail.com

Abstract

The project deals with prevention of ATM Machine from robbery based on RF Transmitter and Receiver technique. Vibration sensor is used here which senses vibration produced from ATM machine when robbery occurs. This system uses ARM controller based embedded system to process real time data collected using the vibration sensor. Once the vibration is sensed the beep sound will occur from the buzzer and at the same time alert message will send to the nearby police station and corresponding bank through the LCD display board. Then the door will get automatically closed and the gas gets leaked to make the robbery person into unconscious state. This will prevent the robbery and the person involving in robbery can be easily caught.

Keywords: *Automatic Teller Machine, Multimedia message service, Radio frequency module, Security system.*

1. INTRODUCTION

As the social computerization and automation has been increased and the ATM and credit card has been installed and spread out to simplify the activity for financial activity, the banking activity has been simplified, however the crime related with financial organization has been increased in proportion to the ratio of spread out of automation and devices. Those crimes for the financial organization have been increased gradually from year 2000 to 2003, little bit decreased in 2004, and then increased again from year 2005. In the year of 2007, 212,530 of theft and 4,439 of robber cases are happened, and 269,410 of theft and 4,409 of robber cases are happened in year 2010, so that the cases of theft and robber have been increased gradually during past 10 years. Among the crime for financial organization, the cases of theft and robber have very high proportion of over 90% and the crime for the ATM has been increased because the external ATM in the gas station and convenience store has been increased and it is always exposed to the crime. Therefore, this study is going to suggest the method of rapid reaction and minimization of loss by detecting the location of the machine at real-time when it has been stolen can be found through RF Transmitter and receiver.

So by using the RF modules theft of external ATM machine can be predicted, which is installed in the convenience store and gas station. In this project we are using buzzer to give signal for corresponding bank and police station. Camera is used to take image frame and send MMS message to the nearby police station. Here stepper motor is used to close the door of the ATM and relay pump is used for emit gas and bring the theft to unconscious stage.The proposed method is used to overcome the drawback found in the existing method. Here we are using RF transmitter to send the location of ATM system to the nearby police station and is received RF receiver. If the robbery is occurred the information is send to the police station and bank. The buzzer is used for alerts. Stepper motor is used for closing the door of ATM. Once the door get closed automatically camera get initialize and tends to capture the image. The captured image is saved in hard disk, and image is send to the police station through MMS modem. Relay pump is used to leaked the gas inside the ATM to bring the thief into unconscious stage.

Here, the MATLAB and Keil tools are used to implement the idea and results are obtained. The MATLAB is used for image capture and keil tools is used run the stepper motor for automatic door lock and also to initialize the camera to capture. The simulated output will be shown in the results.

Figure 1 depicts the functional block diagram of the proposed system in which how the ARM7 is interfaced with vibration sensor, stepper motor, RF transmitter, hard disk, alarm, camera and relay pump.In this block diagram of design the ATM security system by real time embedded module of ARM 7 is a developmental platform.

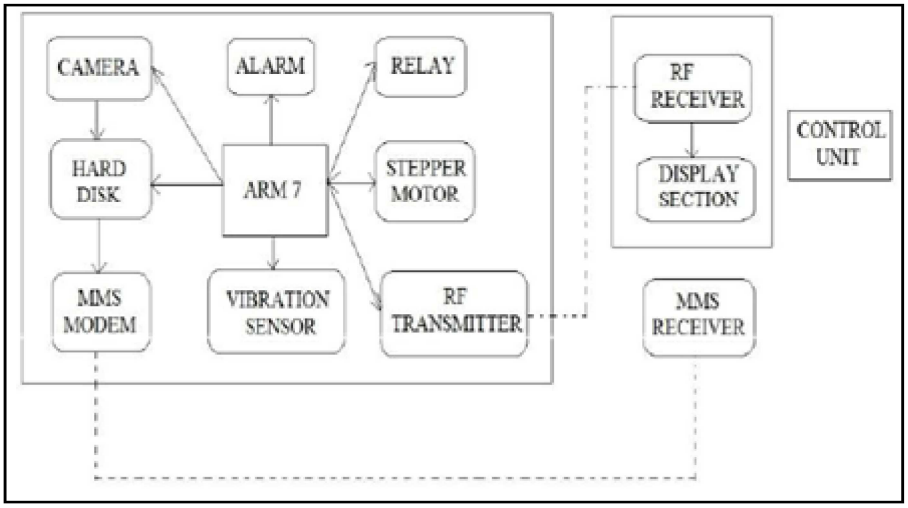

Fig.1 Functional block diagram

It have a fuction of controlling all the device and vibration sensor will sense only if the given voltage will exceeds. After sensing the voltage value the vibration sensor will send command to the controller units. The voltage may be given as a digital format either 0 or 5.The controller unit will send the function to RF transmitter and receiver. Then RF will tends to function. Normally RF values Ranges from 10KHz to 300GHz. we are using as 433.92MHz as ULTRA HIGH FREQUENCY.The RF receiver will get the frequency and send the information to LCD display.This LCD consists of two glass panels, with the liquid crystal material sand witched in between them.The lcd display will give the information about the location of the ATM The LCD's don't generate light and so light is needed to read the display. By using backlighting, reading is possible in the dark. The LCD's have long life and a wide operating temperature range.In the receiver section it has Display,RF Receiver and mobile phone.

The controller will give the function to the stepper motor to activate.The stepper motor will having the normal general working function.we are using single phase stepper motor,with 4 poles.The stepper motor is used to lock to the door automatically by rotating. The controller immediately send the alert activate the camera for taking the image.Normally the camera will take video.After receiving the alert from the controller it tends to take the flash to take the image.That image is stored in hard disk.Here hard disk is used as a memory storage element.This will be act as a permanent storage.It will be helpful during the power cut,it can store the image permanently.The image is taken and stored in the hard disk and send to a modem.The MMS message will be send to a receiver section. there is a cell phone it will receive the MMS message on both the bank and police station.At last,Relay will active,the relay will leakout the gas to bring the person to unconscious stage.

3. HARDWARE CONFIGURATION OF THE SYSTEM

The hardware configuration of the security based ATM system of a shown as a figure 2. consists of he following parts are:camera,Arm 7 microcontoller, stepper motor ,RF frequency module, vibration sensor,data transmission,control units.

3.1.Camera

Interesting visual information is composed of silent and dynamic features, such as the color and shape of landmarks, and motions of vehicles. A color video camera is selected as the onboard visual sensor in our system, which has a compact size and a weight less than 30 g, as well as 380 TV line resolution and 40æ% field of view.

3.2 Embedded Module

Figure 2 design as a proposed scheme of ATM security system by the real time embedded module has development platform, ARM 7 we employed the security based system. Arm 7 TDMI-S is the 32 bit microprocessor. In this processor uses a pipeline to increase the speed of the flow of the instructions to the processor and opration take place simultaneously and the processing ,memory system to opearte continuously.in this ARM 7 TDMI-S processor has the 32-bit ARM instruction set and 16-bit thumb instruction set.

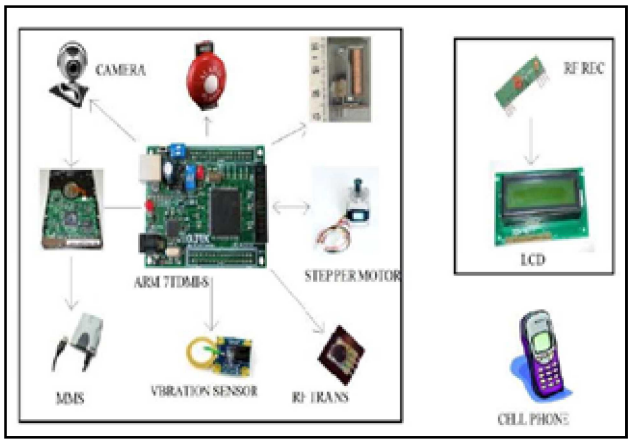

Fig.2 Hardware diagram

In this we choose the 16 bit thumb instruction of ARM7 TDMI-S,reason is on On execution, 16-bit Thumb instructions are transparently decompressed to full 32-bit ARM instructions in real time, without performance loss and it offers a long branch range, powerful arithmetic operations, and a large address space.

3.3 Vibration Sensor

The piezoelectric sensor as we choose the vibration sensor of security based ATM system, its performs an operation of the converts as a physical quantity of mechanical strain to electrical energy and it also sense the two physical quantitys are pressure and acceleration. The piezoelectric sensor has strain sensitivity of 5.0 V/u and threshold value has 0.000001to5 u.

3.4 Stepper Motor

The stepper motor is used for to lock the door of the ATM security system. In the stepper motor we choose the unipolar motor. The motor's position can then be commanded to move at 900 and hold at one of these steps without any feedback sensor (an open-loop controller), as long as the motor is carefully sized to the application.

3.5 RF Transceiver Module

Radio Frequency, any frequency within the electromagnetic spectrum associated with radio wave propagation. When an RF current is supplied to an antenna, an electromagnetic field is created that then is able to propagate through space. Many wireless technologies are based on RF field propagation. The 10 kHz to 300 GHz frequency range that can be used for wireless communication. The TWS- 434 extremely small, and are excellent for applications requiring short-range RF remote controls. The transmitter module is only 1/3 the size of a standard postage stamp, and can easily be placed inside a small plastic enclosure. TWS-434-The transmitter output is up to 8mW at 433.92MHz with a range of approximately 400 foot (open area) outdoors. Indoors, the range is approximately 200 foot, and will go through most walls. The TWS-434 transmitter accepts both linear and digital inputs, can operate from 1.5 to 12 Volts-DC, and makes building a miniature hand-held RF transmitter very easy. The TWS-434 is approximately 1/3 the size of a standard postage stamp RWS-434- The receiver also operates at 433.92MHz, and has a sensitivity of 3uV. The WS-434 receiver operates from 4.5 to 5.5 volts-DC, and has both linear and digital outputs.

3.6 Communication Links

For the data transmission to control unit ,we use the multimedia messaging service is standard way to send messages that include multimedia content to and from mobile phones.

3.7 V Control Unit

In the control unit ,we have RF receiver to receive data at 433.92Mhz about
,which location of the ATM centre and displayed in 2x16 LCD Board.and mms data can received by cell phone.

4. RESULT

Enable the 13th bit to run the stepper motor and camera tends to capture the image is displayed as L in serial windows

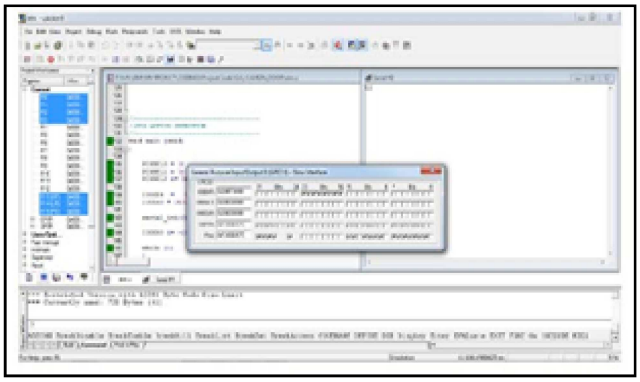

Fig.3 Stepper motor simulated output

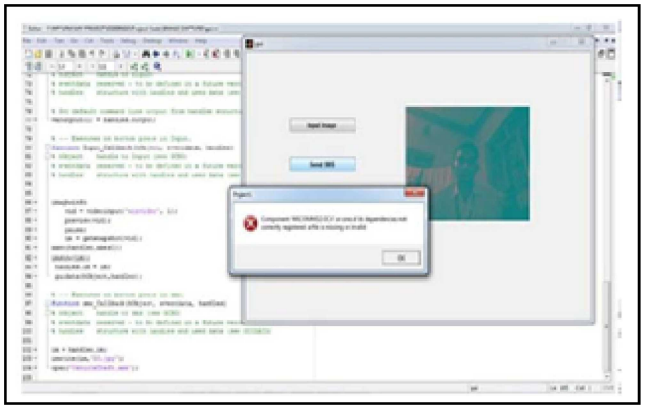

Fig. 4 Matlab simulated output

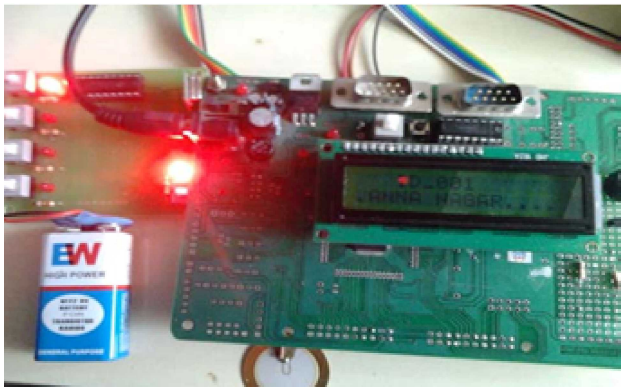

Fig.5 Working model of security based ATM displays the output

5. CONCLUSION

In this project, the vibration sensor will sense the signal and send it to the ARM7 is tends to activate the stepper motor to run, this is done using Keil. Similarly image is capture using web cam and displayed. This is done in MATLAB simulator. Thus simulation part of the project is completed. Software level simulation is done in MATLAB Simulator for image capturing and in KEIL simulator for running the stepper motor operation.

REFERENCES

[1] Faune Hughes, Daniel Lichter,Richard Oswald, and Michael Whitfield, "Face Biometrics:A Longitudinal Study", Seidenberg School of CSIS,Pace University, White Plains,NY 10606,USA.

[2] GaryG.Yen, Nethrie Nithianandan, Facial Feature Extraction Using Genetic Algorithm, Intelligent Systems and Control Laboratory School of Electrical and Computer Engineering. Oklahoma State University, Stillwater, OK 74074-5032, USA.

[3] D.L. Jiang, Y.X. Hu, S.C. Yan, H.J. Zhang, "Efficient 3D Reconstruction for Face Recognition", 0031_3203/2004Patternrecognition society :doi:10.1016/j. patcog.2004.11.004.

[4] Animetrics offers FaceR™ CredentialME Service on Sprint 3G and 4G networks August 12th, 2010.

[5] G. Zigelman, R., Kimmel, N. Kiryati, "Texture Mapping Using Surface Flatten-ing via Multi-dimensional Scaling", IEEE Trans. Visualization and CompGraphics, Vol.8, 2002, pp.198-207.

[6] T. F. Cootes, C. J. Taylor, D. Cooper and J. Graham, "Ac-Tive Shape Models Their Training and Application", CVIU, Vol.61, No.1, Jan. 1995, pp.38–59.

[7] C. Vogler, Z. Li, A. Kanaujia, S. Goldenstein and D. Metaxas, "The Best of Both Worlds: Combining 3d De-Formable Models with Active Shape Models", ICCV 2007.

[8] Kim, Bo-Ra, "Domestic ATM Status and Meanings", Payment and Settlement, and IT, Vol. 44, 2011, pp.76.

[9] Shin, Young-Seok, "Design of Zigbee Location Tracing Monitoring System", IT publication, Vol.17, 2009, pp. 20.

[10] Choi, Sang-Min, "Location Detection Monitoring System Using Zigbee Technology", Master Degree Paper of Information Communication Engineering, Honam Univ. 2009.

[11] Jong Min Kim, DongHwi Lee and Kuinam J Kim, "The Study for Application of ZigBee Location Tracing Monitoring System for ATM device Theft", 2010.

Effect of Carbon Black Loading On the Swelling and Wear Characteristics of Nr/Br Rubber Compounds

M.Ramar [1] and K.Sridharan [2]
Department of Rubber & Plastics Technology, Anna University (MIT Campus), Chennai-44, Tamil Nadu
E-mail: ramar9987@gmail.com, sridharank_cad@yahoo.co.in

Abstract

The main purpose of this work is to study the effect of carbon black loading on the swelling and wear characteristics of NR/BR rubber compounds. The wear characteristics of the samples which are in normal atmospheric condition will differ from the samples which are exposed to fuels such as Aromatic oil, Toluene. The wear or abrasion involves removal of small particles leaving behind pits in the surface and then followed by removal of large particles. The detachment of such small particles plays an important role in initiating the abrasion and this is related to either a structural unit or localized stresses in the rubber. Periodical swelling tests have been performed by immersing four cylindrical rubber blocks in liquids such as aromatic oil, toluene for 48,144,240 hours respectively. At last the swelling ratio, mass loss of various samples has been compared in this work. The images of wear pattern, particle size of the worn out samples are given in this work. Wear co-efficient of various samples are to be compared based on Archard wear theory in my future work.

Keywords: Abrasion, Particle size, swelling test, Wear pattern.

1. INTRODUCTION

Rubber materials are used in wide range of engineering applications. This work deals with the swelling and wear behavior of NR/BR rubber compounds. Blending of elastomers is widely practiced to improve the processing characteristics and physico-mechanical properties and to reduce the cost of individual rubbers. Poly- butadiene rubber (BR) has better abrasion resistance than natural rubber (NR) and hence the blends of NR/BR are extensively used in the manufacture of tires [9].There is no distinction between wear and abrasion[7], although other researcher (schallamach.A) defined abrasion as that produced by laboratory machine on a rubber piece and wear as something that happens to tires or other rubber products.

Abrasion process involves removal of small particles (1-5 μm) leaving behind pits in the surface and then followed by removal of large particles (> 5 μm) [4].The detachment of such small particles plays an important role in initiating the abrasion and this is related to either a structural unit or localized stresses in the rubber[6]. This present work deals with the wear characteristics of tire tread portion which is made of NR/BR rubber compounds. Dr.B.N.J.Persson found out a fact [8] that the detached rubber particles are usually very small, e.g., tire tread wear on road surfaces produces particles with sizes D 1–100 μm. He said that most of the particles are in the micrometer range but the largest particles give the largest wear volume.

Abrasion behavior is a complex phenomenon, which depends on a combination of processes, including mechanical, mechano-chemical and thermo-chemical degradation [5]. In order to study a system of such complexity, it is first necessary to understand the individual processes in detail and then relate these results to the general picture of wear phenomena. The mechanical loading process, in the form of frictional work, has been long recognized as the principle cause of mechanical wear in elastomeric materials [10].

This work deals with the swelling behavior of NR/BR rubber compounds (tire tread portion) exposed to liquids such as aromatic oil, toluene. It is well known that when a rubber comes in contact with the liquid hydrocarbon, generally a mass transfer takes place. The liquid enters the rubbery state material by following a process controlled by Fickian diffusion [3]. This diffusion of such liquids will affect the wear characteristics of tire tread portion. The wear pattern, particle size of rubber block in normal atmospheric condition will be different from other atmospheric conditions like oil, toluene due to such diffusion.

2. EXPERIMENTAL

2.1 Sample for Swelling Test

The samples investigated in this study, were composed of NR/BR blend compounded with (HAF-N330) carbon black according to the recipe shown in the above table. Ingredients of the rubber compound were mixed on a Two-roll laboratory mill. The ingredients were added according to ASTM D15 [1].For this formulation, the vulcanization process was performed at 150^0C for 25 minutes from an electrical resistance heating press. The Specimens for swelling test have cylindrical shape button of size 16 mm diameter and 10 mm height.

The swelling test was conducted by taking two different atmospheric conditions such as aromatic oil (Mahathol AR) and toluene. In my future work, four different compositions of carbon black (0,22.5,45,90 parts) shall have to be taken to investigate the effect of carbon black loading on swelling and wear characteristics of NR/BR rubber compounds.

This present work deals with the swelling and wear behavior of NR/BR rubber compounds by taking 67.5 parts of carbon black (HAF).

Table 1. Composition of NR/ BR Blend

Ingredients	Phr
Natural rubber (NR)	120
Poly-butadiene Rubber (BR)	30
6PPD	3
ZnO	7.5
Stearic acid	3
Carbon black (HAF-N330)	67.5
Process oil	7.5
Wax	1.5
TBBS	2.25
Sulphur	2.25

3. MEASUREMENTS

3.1 Swelling Study

Periodical swelling tests were performed in two different atmospheric conditions such as fuels like aromatic oil, toluene. Four cylindrical rubber buttons of size 16 mm diameter, 10 mm height, mass around 2.20 grams were taken in a beaker of size 250 ml. The fuels such as aromatic oil, toluene were filled with more care in the beaker. Since toluene is a volatile liquid, the beaker which possesses toluene was covered firmly without any leakage.

First Swelling test was performed as per ASTM D 471 [2] by taking four(16 mm diameter and 10 mm height) cylindrical buttons which were cured with the help of hydraulic press, by the immersion method in aromatic oil at room temperature for 48,144,240 hours respectively. Second Swelling test was performed by taking four(16 mm diameter and 10 mm height) cylindrical buttons which were cured with the help of hydraulic press, by the immersion method in toluene at room temperature for 48,144,240 hours respectively. The swelling ratio is defined as:

$$Q\% = \frac{M_t - M_0}{M_0} * 100 \qquad (1)$$

Where M_0 and M_t are the mass of the test piece before swelling and after time "t" of immersion, respectively. The samples (four cylindrical shape buttons of size 16 mm diameter, 10 mm height) were taken out from the beaker were cleaned thoroughly with the help of tissue paper without squeezing it. The mass of the samples was measured by electronic digital balance with 0.001 gram accuracy. Then the samples were dried for two days in room temperature for doing abrasion test which will provide wear characteristics of rubber block. The hardness (Shore A) of normal cylindrical buttons (buttons which were not subjected to Swelling test) and the hardness of cylindrical buttons which were undergone Swelling in fuels like aromatic oil, toluene were measured periodically with the help of Durometer (hardness tester).The drying procedure (at room temperature for two days) shall have to be extended in my further work by keeping the swollen samples in an hot air oven at a temperature of 70^0Cetc. for 24 hours respectively.

3.2 Abrasion Process

The particle size of the samples at normal (room temperature) atmospheric condition will differ from the particle size of the samples which were exposed to liquids like aromatic oil, toluene.

The images obtained by ahigh accuracy microscope will show the wear pattern of the samples kept in normal condition, exposed in aromatic oil, toluene. The value of wear Coefficient (K) is to be determined based on Archard wear theory in my future work.

$$\frac{\Delta m}{\varrho} = K \frac{F_N}{H} L \qquad (2)$$

$$K = \frac{\Delta m \times H}{F_N \times \varrho \times L}$$

V = wear volume K = wear Coefficient

F_N = normal load ϱ = density

Δm = Mass loss H = Hardness

L= Sliding Distance

4. RESULT AND DISCUSSION

4.1 Swelling Test Results

The results of swelling test gave the following information.

(i) The diffusion of Aromatic oil into the rubber network increased gradually with respect to the increment in exposure time. This behavior gave a slight linear increment in the swelling ratio (Qt). The maximum value of swelling ratio (Qt) (240 hours exposure time) is lesser than 25% for oil swollen samples.

(ii) The diffusion of Toluene into the rubber network increased vigorously when there was an increment in exposure time. This behavior gave a wide linear increment in the swelling ratio (Qt). The minimum value of swelling ratio (Qt) (240 hours exposure time) is greater than 200% for toluene swollen samples.

The following figure shows the changes in swelling ratio for different exposure time.

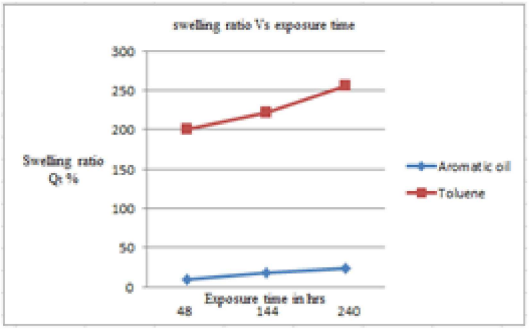

Fig.1 Swelling ratio Vs exposure time

4.2 Abrasion Test Results

The results of abrasion test gave the following information.

(i) There was a slight increment in mass loss when there was an increment in exposure time for all oil swollen samples. However, the mass loss of normal condition samples was slightly greater than the mass loss of oil swollen samples.

(ii) There was no variation in mass loss when there was an increment in exposure time for all toluene swollen samples. However, the mass loss of toluene swollen samples was approximately doubled as compared to the mass loss of oil swollen samples.

The following figure shows the comparison of mass loss of different samples.

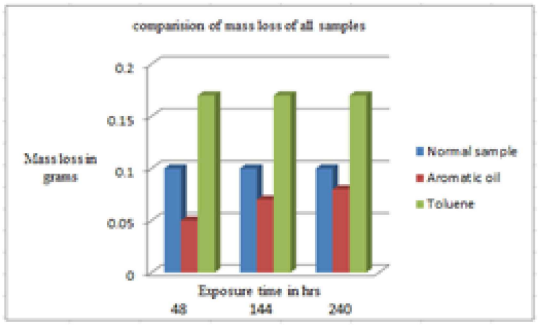

Fig.2 Comparison of mass loss of different samples

During abrasion, the normal condition samples gave dry debris as compared oil swollen samples. The worn out particles of normal condition samples was so small as compared to other swollen samples. But, the worn out debris did not stick on the worn surface. The following figure shows the images of wear pattern and particle size of normal condition sample taken by a high resolution optical microscope.

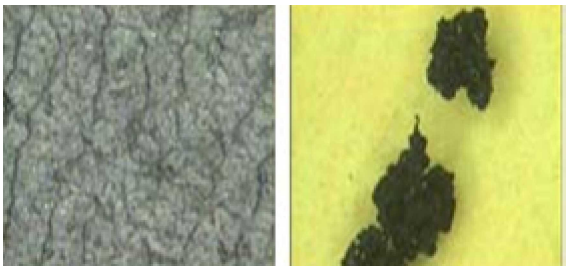

Fig.3 Wear pattern and particle size of normal sample

In the wear process of oily abrasion, no dry debris but only a less smooth and shiny particulate debris were produced and clogged on the worn surface. In the worn surface a sticky layer was also formed in the shape of ridge pattern. The appearance and arrangement of ridges were very uniform. This result was similar to the experimental work of S.W.Zhang which was done in 1984. The shiny particulate debris formed a cluster of particles during abrasion. The following figure shows the images of wear pattern and particle size of oil swollen samples taken by a high resolution optical microscope.

Fig.4 Wear Pattern and particle size of oil swollen samples

The following figure shows the images of wear pattern, particle size of toluene swollen samples taken by using high resolution optical microscope.

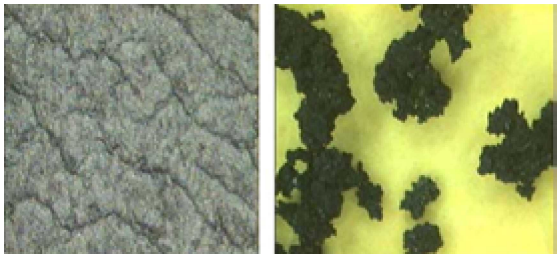

Fig.5 Wear pattern and particle size of toluene samples

5. CONCLUSION

As the diffusion of toluene into the rubber network was much better than the diffusion of oil into the rubber network, the value of swelling ratio (Q_t) of toluene swollen sample was nearly 10 times the value of swelling ratio of oil swollen samples. If there was an increment in exposure time, the value of mass loss of toluene swollen samples was nearly 2 times the value of mass loss of oil swollen samples.

REFERENCES

[1] ASTM D 15, "Standard Test Method for Rubber Property-sample Preparation for Physical Testing of Rubber Products", Annual Book of ASTM Standards,Philadelphia, 1958.

[2] ASTM D 471, "Standard Test Method For Rubber Property-Change in Properties of Elastomeric Vulcanizates Resulting From Immersion In Liquids", Annual Book of ASTM Standards, Philadelphia, 1957.

[3] J. Crank, "Mathematics of Diffusion", Oxford; Clarendon Press, 1975.

[4] N. S. M. El-Tayeb & R. Nasir, "Effect of Soft Carbon Black on Tribology of Deproteinised And Polyisoprene Rubbers", Wear, 262, 350-361, (2007).

[5] D. F. Moore, "The Friction and Lubrication of Elastomers", Pergamon, Oxford; 1972.

[6] A. H. Muhr & A. D. Roberts, "Rubber Abrasion and Wear", Wear, Vol.158, 1992, pp.213-228.

[7] K. N. Pandey, D. K. Setua & G. N. Mathur, ", Material Behaviour Fracture Topography of Rubber Surfaces, An SEM Study", Polymer Testing, Vol. 22, 2003, pp.353-359.

[8] B.N.J. Persson, "Theory of Powdery Rubber Wear", Journal of Physics. Condensed Matters, Vol.21, No.8, 2009, pp.485.

[9] Rani Joseph, K.E.George, D.Josepf Francis & K.T.Thomas, "Studies On The Cure Characteristics And Vulcanizate Properties of 50/ 50 NR/BR blend", International Journal of Polymeric matter, Vol.12, 1987, pp.53-64.

[10] A. Schallamach, "Recent Advances in Knowledge of Rubber Friction and Tire Wear", wear, Vol.41, 1968, pp.209-244.

SVM and PWM Technique Based Diode-Clamped Multi-Level Inverter for Renewable Energy Systems

S. Angulakshmi, G. Divya and C. Anustiya
Panimalar Engineering College, Poonamallee, Chennai - 600 123, Tamil Nadu
E-mail:[1]angu.october2@gmail.com,[2]divya.ash92@gmail.com and [3]geminics91@gmail.com

Abstract

This paper describes a SVM and PWM technique based diode-clamped multi-level inverter for renewable energy systems. The study is carried out for three different cases. In the first case, one of the two dc-link capacitors of the inverter is replaced by a battery bank and the other by a super capacitor bank. In the second case, dc-link capacitors are replaced by two battery banks. In the third case, ordinary dc-link capacitors are replaced by two super capacitor banks. Long term and short tern power fluctuations are mitigated by the former system whereas smoothing is done by the two later systems. These topologies eliminate the need for interfacing dc-dc converters and thereby improve overall system efficiency. The idea of using Space Vector Modulation technique can produce undistorted current even in the presence of imbalance in dc-link voltages. Further, small vector selection-based sharing and state of charge balancing techniques are also proposed in this paper.

Keywords: Diode-clamped three-level inverter, Direct integration of battery energy storage systems, Space vector modulation, Unbalanced operation of diode- clamped three-level inverter.

1. INTRODUCTION

The system stability issues are the major drawback of renewable energy sources [1]-[5]. A promising solution to this problem is the use of energy storage devices. Recently emerged devices are batteries and super capacitors. As a result, power quality is enhanced using batteries and super capacitors [3]-[5].

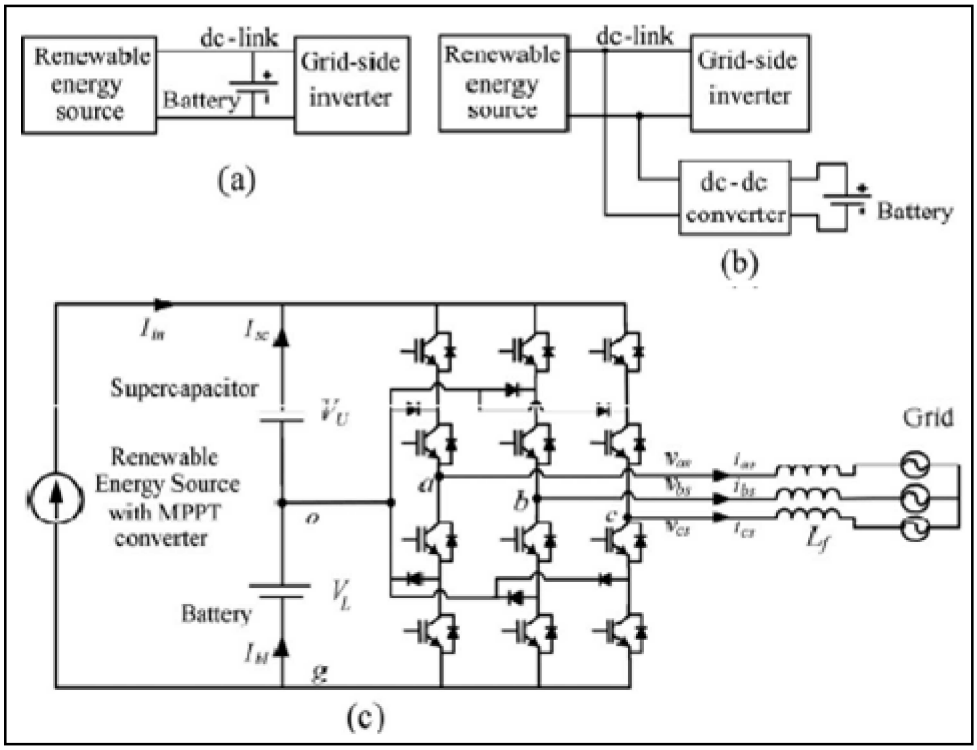

Figure 1 Interfaces for Battery Energy Storage Scheme. (a) Direct connection to the dc link. (b) Connection to the dc link through a dc–dc converter. (c) Proposed super capacitor direct integration scheme.

When it comes to the system integration, the simplest way of adding a battery (or) Super capacitor bank is the direct connection to the dc link of the grid side inverter as shown in Figure 1(a). But it suffers from several drawbacks such as large internal resistance, fixed current distribution governed by internal resistors and lack of control over the power flow.

Therefore, to overcome the above drawbacks a simple configuration is shown in Figure 1(c). In the figure, the dc-link capacitors of a standard diode-clamped 3 level inverter are replaced by a two super capacitor banks. Latter part of this paper discusses two more cases, one with two super capacitor banks and the other with two battery banks. The primary source can be wind, solar, fuel cell or some other sources of renewable energy. If a change in the source or load happens, the power imbalance will be compensated by the battery bank and/ or super capacitor bank.

A simple topology has been proposed in [6] for photovoltaic systems. This proposed solution is based on Sinusoidal Pulse Width Modulation with Carrier Amplitude Modulation that is proved in section 2. The major drawback here is it is effective only for small and slow changes in the dc-link voltages and its control flexibility over the small vector is limited. Taking these faults into account, a new Space Vector Modulation method has been developed for diode-clamped multi-level inverter with variable dc-link voltages because full controllability over small vector solution is available in the proposed SVM method. Relevant equations and diagrams are given in section 3.

2. EFFECTS OF UNBALANCED DC-LINK VOLTAGE

For the diode-clamped three-level inverter, shown in Figure 1(c), line-to-ground voltages can be derived from switching states *Sa*, *Sb* , and *Sc* , and the results are given in Table 1.

If the inverter is connected to a balanced three-phase load, corresponding phase voltages can be derived from line-to-ground voltages, these phase voltages are transformed into the *dq* reference frame by and the resultant coordinates for the vectors in sector 1 are given in Table 2.

Table 1 Switching States and Line-To-Ground Voltages

Switching States Sa, Sb, Sc	IGBT Switching Sequence of the leg (Top to Bottom)	Line to Ground Voltages Vag, Abg, Vcg
0	0011	0
1	0110	V_L
2	1100	$V_L + V_U$

Table 2 *dq* Axis Coordinates of Vectors in Sector 1

Vector	Vector Type	d axis Coordinate, xn	q axis Coordinate, yn
000	Zero	0	0
100	Negative small	$2V_L/3$	0
110	Negative small	$V_L/3$	$V_L/\sqrt{3}$
211	Positive small	$2V_U/3$	0
221	Positive small	$V_U/3$	$V_U/\sqrt{3}$
200	Large	$2(V_L+V_U)/3$	0
220	Large	$(V_L+V_U)/3$	$(V_L/V_U)/\sqrt{3}$
210	Medium	$(V_L+2V_U)/3$	$V_L/\sqrt{3}$

According to the values in Table II, locations of small and medium vectors vary with dc-link voltages as shown in Figure 2. However, locations of large vectors (200,220,020,022,002 and 202) depend only on the total dc-link voltage and would remain unchanged if the total voltage is constant. When capacitor voltages are balanced, positive and negative small vectors (211,221,121,122,112,212,100,110,010,011,001 and 101) coincide and only one inner hexagon is formed as shown in Figure 2(b). Furthermore, medium vectors (2 1 0, 1 2 0, 0 2 1, 0 1 2, 1 0 2, and 2 0 1) reach midpoints of the outer hexagon. If an unbalance is present, small vectors split and two separate inner hexagons appear as shown in Figure 2(a) and (c). In addition to that, medium vectors

move toward large vectors. the size of the inner hexagon formed with positive small vectors varies with the super capacitor voltage.

Figure 2 Space vector diagram for (a) *VU* < *VL*, Figure 3 Effects of dc-link voltage imbalance. (a) Changes applied to capacitor voltages. (b) Symmetric carriers for normal SPWM. (c) Inverter output voltage of the *a*-phase *v*as with equal carriers. (d) Fundamental components with dc offset. (e) Modified carriers. (f) Inverter output voltage of the *a*-phase *v*as with modified carriers. (g) Fundamental components without dc offset. (g) Inverter output voltage of the *a*-phase *v*as with the proposed SVM technique. (b) *VU* = *VL*, *VU* = *VL*, and (c) *VU* > *VL*.

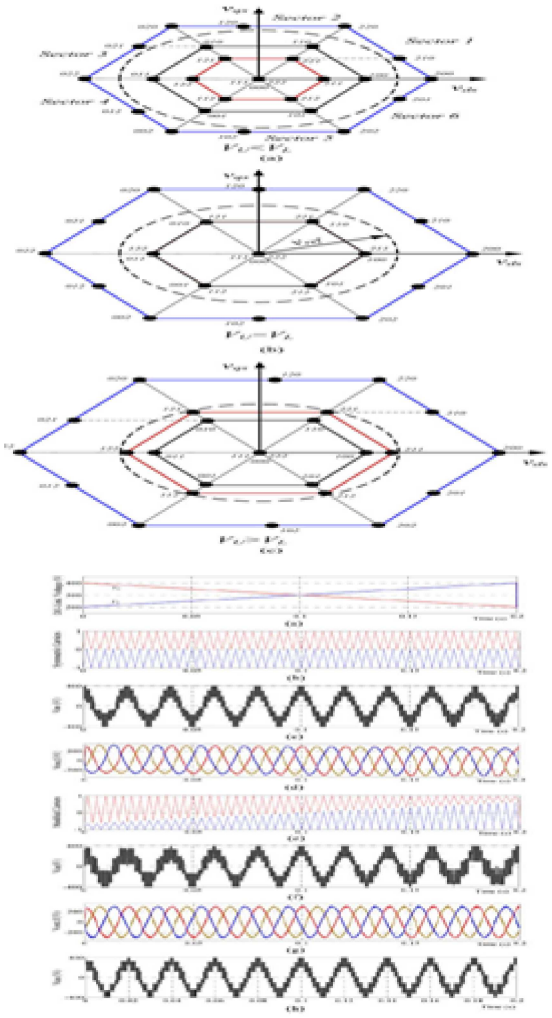

Modulation and voltage balancing control of diode-clamped three-level inverters are well documented in the literature [8], [9]–[13]. However, conventional modulation methods such as space vector pulse width modulation, SPWM, and third harmonic injection pulse width modulation are supposed to work under balanced conditions. If an unavoidable imbalance occurs, these modulation methods fail to produce desired waveforms. This effect is illustrated in Figure 3(c) and (d) where the capacitor voltages are purposely changed according to Figure 3(a). If the normal SPWM with two equal carriers, as shown in Figure 3(b) is used, a dc offset will be present in the inverter output voltage. This effect is clearly visible in the fundamental component shown in Figure 3(c). As a solution to this problem, a feed forward SPWM method is proposed in [7] where the carriers are modified according to the voltage imbalance as shown in Figure. 3(e).

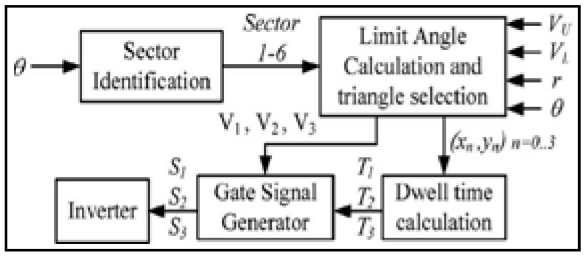

Fig.4 Simplified block diagram of the proposed SVM technique

3. PROPOSED SVM TECHNIQUE

A simplified block diagram of the proposed SVM technique is shown in Figure 4. The amplitude *r* and the angle ¯ of the reference voltage vector are generated by the grid side inverter controller. The suitable triangle is selected out of the two possible triangles. However, due to the presence of two triangles, four different limit angles, ¯1, ¯2, ¯3 and ¯4 need to be calculated for a given sector. First two limit angles (¯1 and ¯2) are related to the triangles formed with lower small vectors as shown in Figure 5(a) whereas the other two limit angles (¯3 and ¯4) are associated with the triangles formed with positive small vectors as shown in Figure 5(b).

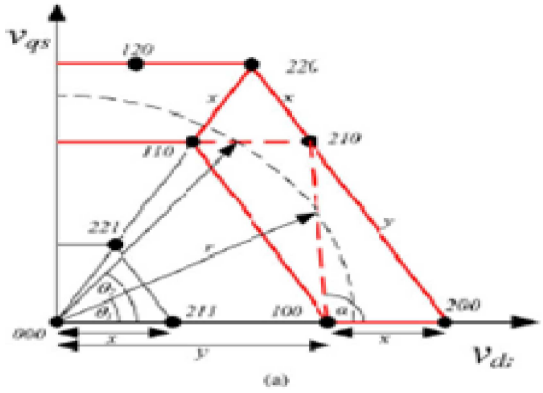

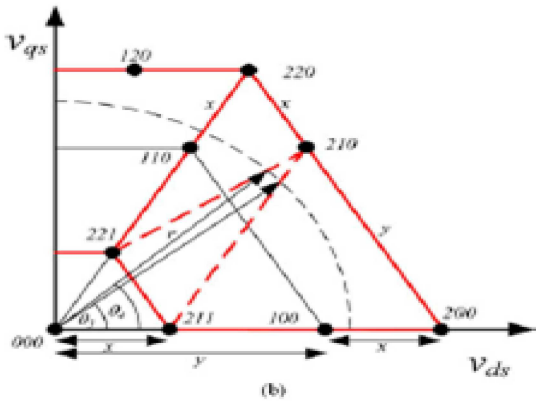

Fig. 5 Limit angles for sector 1. (a) Limit angles for triangles formed with Lower small vectors. (b) Limit angles for triangles formed with upper small vectors.

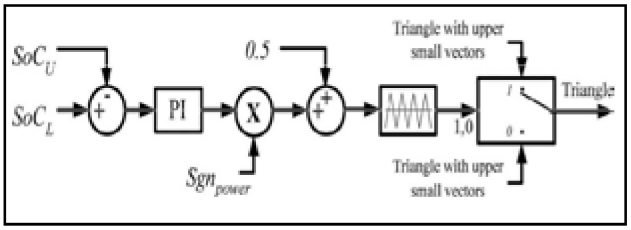

Fig.6 SOC balancing controller block diagram

4. DC-LINK CAPACITORS ARE REPLACED BY TWO SUPER CAPACITOR BANKS

The same SOC balancing controller, shown in Figure 6, is valid even when dc-link capacitors are replaced by two super capacitor banks. If the SOC of the super capacitor bank is above 80%, a gradual increase is introduced to the output power reference. This in turn reduces the charging rate. On the other hand, if the SOC of the super capacitor bank is below 20%, a gradual decrease is introduced to the output power reference. This will slow down the discharging process. In all other possible situations, the original power reference, calculated using the exponential moving average formula [7], is used. This particular power reference adjustment ensures that the super capacitor bank remains in operation at all times and a sufficient amount of energy to smoothen power fluctuations is securely maintained. Moreover, it protects the super capacitor bank from overcharging and over discharging. If there is a long-term fluctuation, that can be suppressed by changing the battery current reference to a suitable positive value or a negative value.

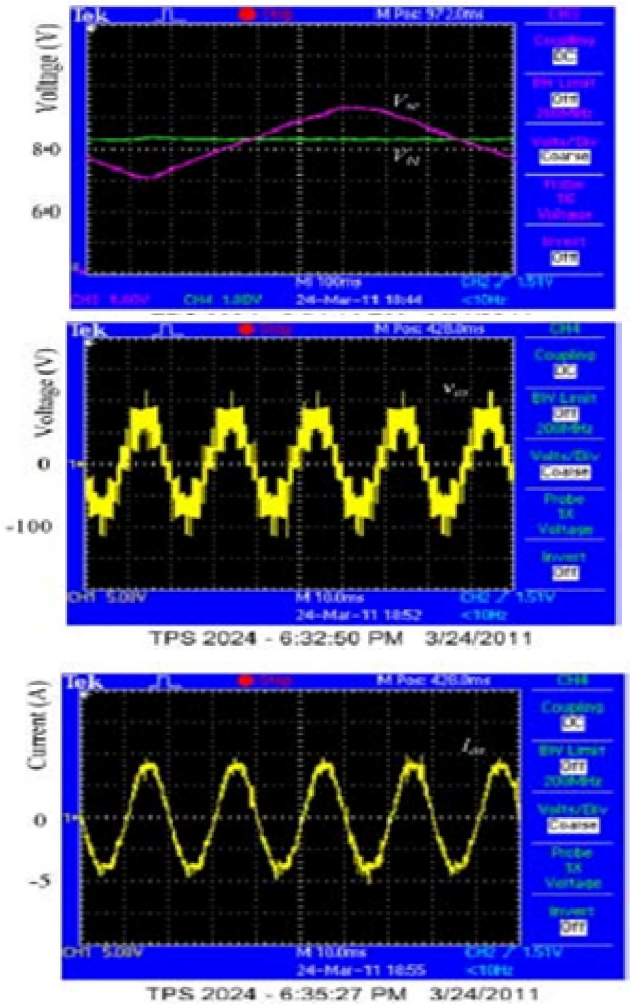

Fig.7 (a) Battery and super capacitor voltages, (b) Inverter output voltage. (c) Inverter output current

5. EXPERIMENTAL RESULTS

Experimental validations of the proposed power sharing technique for the super capacitor–super capacitor hybrid energy storage system are shown in Figure 7. Output power level is maintained at a constant level, marked as *P*out, as shown in the same graph. Battery and super capacitor voltages are shown in Figure 7(a). It is evident from the aforementioned power and current waveforms that the super capacitor bank absorbs fluctuations making the battery current small and smooth. The inverter output voltage waveform is shown in Figure 7(b). This waveform, together with the inverter output current waveform shown in Figure 7(c), proves the efficacy of the proposed SVM method to handle dc-link voltage imbalances. Even though fluctuations are present in the input power, output voltage and current waveforms are not affected.

6. CONCLUSION

A power sharing and SOC balancing controllers for directly connected super capacitor energy storage systems are presented. Proposed topologies eliminate the need for additional dc–dc converters by connecting two battery banks, two super capacitor banks or a battery bank, and a super capacitor bank directly across dc links of a diode-clamped three-level grid connecting inverter. Unavoidable dc-link voltage imbalance is the major issue with these topologies. This problem is handled by a novel space vector modulation technique. It is proved in this paper that power sharing and SOC balancing between batteries and super capacitors can be achieved by altering the small vector composition. Experimental and simulation results are presented to prove the efficacy of the proposed topology, modulation, and control techniques.

REFERENCES

[1] P. Thounthong and S. Rael, "The Benefits of Hybridization", IEEE Ind. Electron. Mag., Vol.3, No.3, Sep. 2009, pp. 25–37.

[2] P. F. Ribeiro, B. K. Johnson, M. L. Crow, A. Arsoy, and Y. Liu, "The Benefits of Hybridization", in Proc. IEEE, Dec., 2001, Vol. 89, No.12, pp.1744–1756.

[3] W. Li and G. Joos, "A Power Electronic Interface for a Battery Super Capacitor Hybrid Energy Storage System for Wind Applications", in Proc. IEEE Power Electron. Spec. Conf., Jun. 15–19, 2008, pp.1762–1768.

[4] A. M. van Voorden, L. M. R. Elizondo, G. C. Paap, J. Verboomen, and L. van der Sluis, "The Application Of Super Capacitors To Relieve Battery Storage Systems In Autonomous Renewable Energy Systems" in Proc. IEEE Power Tech Conf., Jul. 1–5,2007, pp. 479–484.

[5] S. M. Muyeen, R. Takahashi, T. Murata and J. Tamura, "Integration Of An Energy Capacitor System With A Variable-Speed Wind Generator", IEEE Trans. Energy Converters., Vol.24, No.3, pp. 740–749, Sep. 2009.

[6] M. Galvez, E. Bueno, F. J. Rodriguez, F. J. Meca, and F. J.Rodriguez, "New MPPT Algorithm For Photovoltaic Systems Connected To NPC Converters And Optimized For Large Variations Of Solar Radiation", in Proc. IEEE Energy Convers. Congr. Expo., Sep. 20–24, 2009, pp. 48–53.

[7] N. Celanovic, I. Celanovic, and D. Boroyevich, "The Feed Forward Method Of Controlling Three-Level Diode Clamped Converters With Small Dc-Link Capacitors", in Proc. IEEE Power Electron. Spec. Conf., Vol. 3, Jun. 2001, pp. 1357–1362.

[8] M. Saeedifard, H. Nikkhajoei, and R. Iravani, "A Space Vector Modulated STATCOM Based On A Three-Level Neutral Point Clamped Converter", IEEE Trans. Power Del., Vol.22, No.2, Apr. 2007, pp. 1029–1039.

[9] W.-D. Jiang, S.-W. Du, L.-C. Chang, Y. Zhang, and Q. Zhao, "Hybrid PWM Strategy of SVPWM and VSVPWM for NPC Three-Level Voltage Source Inverter", IEEE Trans. Power Electron., Vol. 25, No.10, Oct. 2010, pp. 2607– 2619.

[10] H. Akagi and R. Kondo, "A Transformer Less Hybrid Active Filter Using A Three- Level Pulse Width Modulation (PWM) Converter For A Medium-Voltage Motor Drive", IEEE Trans. Power Electron., Vol. 25, No.6, Jun. 2010, pp. 1365–1374.

[11] O. Vodyakho and C. C.Mi, "Three-Level Inverter-Based Shunt Active Power Filter in Three-Phase Three-Wire and Four-Wire Systems", IEEE Trans. Power Electron., Vol.24, No.5, May 2009, pp.1350–1363.

[12] S. Busquets-Monge, S. Alepuz, J. Rocabert, and J. Bordonau, "Pulse Width Modulations for the Comprehensive Capacitor Voltage Balance Of N-Level Three-Leg Diode-Clamped Converters", IEEE Trans. Power Electron., Vol.24, No.5, May 2009, pp.1364–1375.

[13] H. Akagi and T. Hatada, "Voltage Balancing Control For A Three-Level Diode- Clamped Converter In A Medium-Voltage Transformer Less Hybrid Active Filter", IEEE Trans. Power Electron., Vol.24, No.3, Mar. 2009, pp.571–579.

Cloud Computing Easy way of Logical Design Pattern Conversion to Program

R.Revathi[1], K.Alamelu[1], and C.Karthika[2]
[1]Information Technology, Velammal College of Engineering and Technology, Madurai, Tamil Nadu
[2]Computer Science Engineering, Velammal College of Engineering and Technology, Madurai, Tamilnadu

Abstract

Cloud computing is a new method to add capabilities to a computer without licensing new software, investing in new hardware or infrastructure or training new personnel. Raw ideas are available for free everywhere but they do not have the value they deserve. This is because, though the implementation is becoming automated day by day, proper designing of the ideas demands much of focus, effort and time. So, we propose a system wherein problems are open to the network of people connected via internet. For this we make use of the cloud facility to provide infrastructure for the databases used, plug-ins to be installed, and secured networking facility. Now, they can formulate not only ideas or provide source codes but can also design solutions based on the design standard very much similar to a flow chart. It also facilitates to design in multiple paradigms like imperative, object oriented, functional and logical. User can use their own design pattern provided; they map their design with the specified standard. The important aspect is that the designs posted will be evaluated based on empirical testing and apriority analysis. The validated solution will be made open for all to see. The solution thus provided can be viewed depending on the rank of a solution which will be allotted based on the user's rating. Hence, this application is expected to act as a supplement for the existing era of open source and open idea.

Keywords: Apriority analysis, Automatic implementer, Cloud computing, Knowledge based systems, Service oriented style, Posteriori testing.

1. INTRODUCTION

Cloud computing promises to cut operational and capital costs and, more importantly, IT departments focus on strategic projects instead of keeping the datacenter running.Cloud computing is a construct that allows one to access applications that actually reside at a location other than the person's computer or other Internet-connected device; most often this will be a distant data center. The beauty of cloud computing, as shown in figure1, is that another company holds one's application (or suite of applications). This means that they handle the cost of servers, they manage the software updates, and – depending on how one crafts his contract – one pays less for the service.

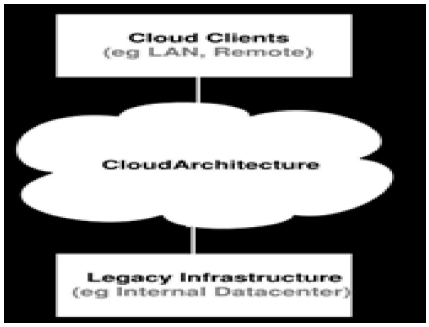

Fig.1 Cloud computing

If one has an e-mail account with a Web-based e-mail service like Hotmail, Yahoo! Mail or G-mail, then one would have had some experience with cloud computing. Instead of running an e-mail program on one's computer, one log in to a Web e-mail account remotely. The software and storage for one's account doesn't exist on his/her computer — it's on the service's computer cloud.

1.1 Cloud Computing Architechture

It is helpful to divide cloud computing system into two sections: the front end and the back end. They connect to each other through a network, usually the Internet. The front end is what the client sees. The back end is the "cloud" section of the system.The front end includes services like Web-based e-mail programs leverage existing Web browsers like Internet Explorer or Fire fox. On the back end of the system are the various computers, servers and data storage systems that create the "cloud" of computing services. A central server administers the system, monitoring traffic and client demands to ensure everything runs smoothly. It follows a set of rules called protocols and uses middleware. Middleware allows networked computers to communicate with each other.

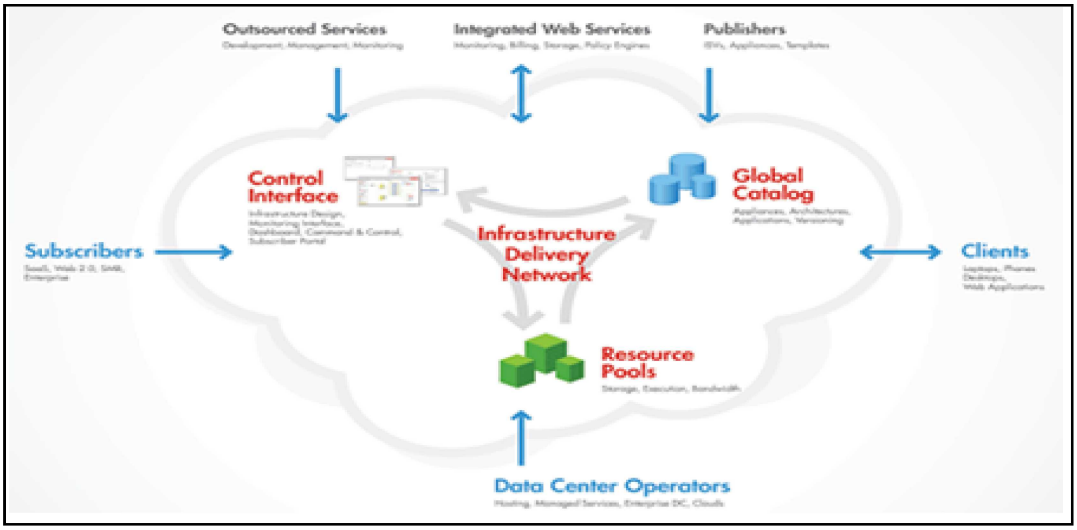

Fig.2 Cloud computing architechture

1.2 Exploitation of Cloud Computing

Why would anyone want to rely on another computer system to run programs and store data?

Here are some of the reasons:

i Clients would be able to access their applications and data from anywhere at any time.
ii It could bring hardware costs down.
iii Cloud computing systems give organizations company-wide access to computer applications.
iv Servers and digital storage devices take up space. Cloud computing give the companies an option of storing data on someone else's hardware, removing the need for physical space on the front end.
v If the cloud computing system's back end is a grid computing system, then the client could take advantage of the entire network's processing power.

Fig.3 Exploitation of cloud computing

CLOUD COMPUTING APPREHENSIONS

The two major concerns of cloud computing that are to be taken care of, are, *security* and *privacy*. To achieve the same, authentication or authorization format can be employed.

2. EXISTING SYSTEM FOLLOWING CLOUD COMPUTING

The concept of open everything and cloud computing, which has been a buzz word for quite some time, has its own limitations which has been brought into light.

2.1 Idea Presentation

Open access journals, papers, etc; provide a way for people to express their ideas so that any one may be benefited from that. Cloud offers a way to publish the ideas online in a professional manner. Of course it paves way for n-number of researches but the problem is that a voluminous pool of wonderful ideas goes unused because of need of proper classification and presentation. Also due to lack of synchronization between solution providers and implementers many ingenious proposals are not employed.

2.1.1 Open Source Solutions

Recent evolution of Computer Technology is turning towards Open Source technology which is a feature offered by cloud in the name of online collaboration. In this the vendors provide source code, included with the

compiled version and modification or customization is actually encouraged. The software developers who support the open source concept believe that by allowing anyone who's interested to modify the source code, the application will be more useful and error-free over the long term. This is a good approach for fast development of software products. The problem here is that even though many contributors have good ideas and also excellent logic for the open problem they may not be able to contribute with the solution due to absence of language and platform knowledge. Also reusing of the source code is less practical.

2.1.2 Example

For instance consider the scenario wherein a user is frustrated by the file searching mechanism of Linux OS where is I search *.cpp, it displays the cpp files and all the folders (whether it contains a cpp file or not) in the current directory. He/she wants to get only the folders containing cpp files and not all files. The logic to solve this may be known to some other person. But both of the actors here may not know how to write a Linux source code. Here an idea (even though can be designed by many) is gone unnoticed just because of lack of coding knowledge which can be easily automated in the current scenario. Due to lack of proper coordination million such ideas may be binned. So we come up with a new approach wherein users an collaborate and design their own logic for exploring the optimal solutions.

2.1.3 Proposed System

To overcome the above drawbacks we propose an elucidation that facilitates the willing people to implement their ideas in their own way. Here, we provide design standards so that the contributors can propose their logical design in a simple manner. We propose design specifications which will be easy to understand by a naïve user. The data-flow diagram portrays the system proposed.

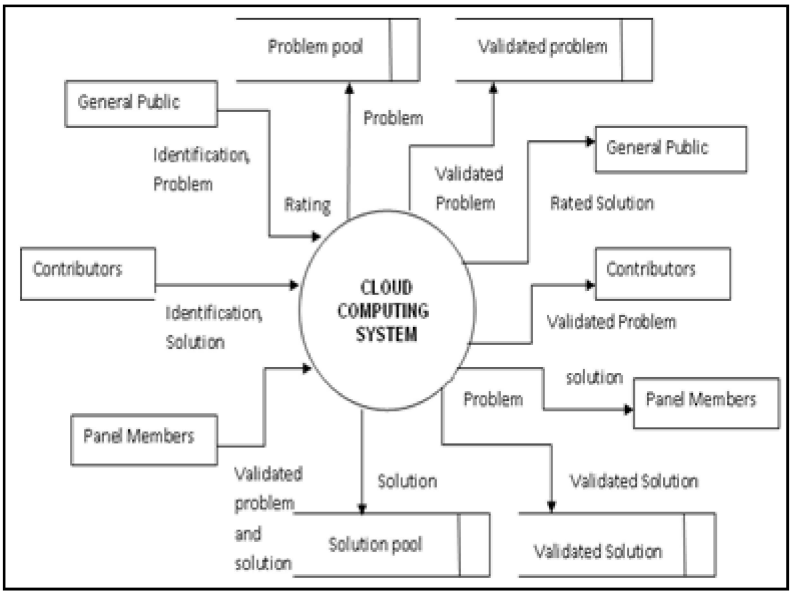

Fig.4 Existing system following cloud computing

2.1.4 Course of Action

3/4 Any problem that can be solved via programs will be posted by the end users who seek optimal solutions for the same.

3/4 The posted problems will be validated by a panel of reliable erudite members and will then be made open to all.

3/4 The contributors who have the solution for the posted problem can post their solution with sample input and output.

3/4 They will be provided with the design specifications through which they can present their logic.

3/4 The best part of the system is the automatic implementer, that is provided, which will convert the design pattern into any of the widely used languages selected by the contributor or the requester or both.

3/4 The given design along with the converted source code will be evaluated automatically by the system by means of empirical or posteriori testing and apriority analysis.

3/4 Now the posted designs will be validated by the panel members based on the correctness of it.
3/4 They make the solutions open to the public.
3/4 The posted solutions will be visible to any authenticated end users who search for it.
3/4 The results will be initially ranked based on the design evaluation and the rating done by the users.

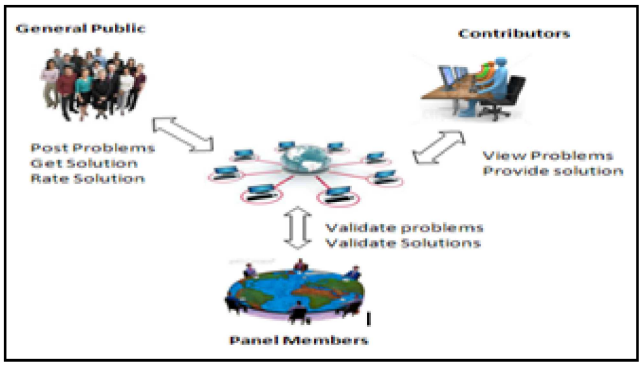

Fig. 5 Pictorial representation of the course of action

2.1.5 Authentication 'N' Authorization

The users who post the problem, the contributors who design the solution and the benefice's who are benefited from the solution all must be properly substantiated. This is because the system must be a reliable source of information and service. The panel members and the contributors are restricted up to their own level of authorized permissions. Though the panel members validate the content posted by any end user, the filtering process becomes too tedious if there is a lot of junk content posted by any untrustworthy users. Also care must be taken such that the one who designs the model must not be able to rate it as an end user. Considering these issues the users are authenticated based on their personal and location identification.

2.2 GUI Enviornment

The contributors can design their solution by making use of the GUI environment. The design models can be simply dragged from the containers and the flow of control will be maintained by keeping the symbols one after the other in the order that will automatically join. A help desk will be provided in the form of tutorial so that the user may be comfortable with the tools provided for designing. For example, if a comment line is to be used, the details about how it can be used can be viewed using the tutorial. This is applicable for all the features offered and design symbols.

2.2.1. Designing In Different Paradigm

The system assists the users to include any formal language concepts in their logic mold. It provides features for designing in any paradigm (pattern) of their choice in which they are familiar with or, the one that is most suitable for the problem, in addition to traditional imperative or object oriented paradigm.

a) Logic Paradigm

In case of designing a logic mold for an AI problem like knowledge based systems, natural language processing, the contributors may need to design in a logic paradigm pattern rather than that of traditional structural one. Designing such a solution may need more patterns apart from the conditional and looping prototypes. This will reduce the burden and effort overhead of designing such logic oriented models with basic notations. So we provide some extra notations for these special purposes.

There will be notations for facts and conditions (that the solution must satisfy) that are key elements of logic programming. The system can figure out for itself how to deduce the solution from the facts given. Also special notation for start and end of inference engine (automated reasoning procedure) will be present. Here knowledge is represented using notations and reasoning is done by calling right procedures at right time. Also layouts for predicate calculus are provided.

b) Functional Paradigm

Similarly, if users prefer functional paradigm for complex computations on complex data that treats computation as the evaluation of mathematical functions and avoids state and mutable data we provide facilities for that too. It emphasizes the application of functions, in contrast to the imperative programming style, which emphasizes changes in state. The users will be able to design in this style by providing patterns for the same. That is, users can evaluate every computation which will be evaluated as mathematical functions, even the operators, keywords and expressions. The arguments of a function too will be evaluated as a function. A notation is provided to denote listener that will be evaluated interactively (Uses a three-step process- read, evaluate and print).

c) Components and Services

Design pattern for the current trend of paradigm such as component based and service oriented style will also be provided. That is symbols will be provided to denote a component or service and related concepts associated with that unit.

2.2.2. Design Tools For Scoping And Indirection

Scoping is an important concept in any program. The tool facilitates scoping option in the design, wherein the scope of the context, where values and expressions are associated, can be fixed. The scoping option is in accordance with the programming language chosen.

The system enables the designers to use the pointer and reference options by providing them with layout.

2.2.3. Reusing Features

Reusing features offered by the system is the automatic design for any aspect predefined in any of the widely used languages. Like predefined functions in C, COBOL, ALL which are structural or predefined classes in Java, Smalltalk which are object-oriented or components/services like security, transactions, session management, memory management in languages like J2EE, .NET which are component-based.

Also the user can specify their preference of data type or size or property attributes for any identifiers they use. They can also use data structure like array, linked list, tree, hash table etc by merely specifying its name and setting attributes.

2.2.4. Customization Facility

Some users may not find it easy to design in the specified pattern. They may be comfortable with their own style. So the system offers them a provision wherein they can map their own prototype with the specified standard and also specify the delimiters used by them for various situations. Thereafter, they can freely design in their own accord. The final model they post will be automatically converted to the standard design. The design model thus posted will be verified and validated by the panel members.

2.2.5. Design Implementer And Evaluator

The best part of the system is the automatic implementer that will convert the design pattern into any of the widely used language selected by the contributor or end user. The given design + the converted source code will be evaluated automatically by the system by means of empirical or posteriori testing and apriority analysis. Also the parameter in which the algorithm is best suited or not suited is analyzed like the average time complexity, time complexity for large number of inputs, for small number of inputs, nature of inputs, language/platform dependency, space complexity etc. The following screenshot gives the idea of how the implementer and evaluator functions and produces the corresponding source code.

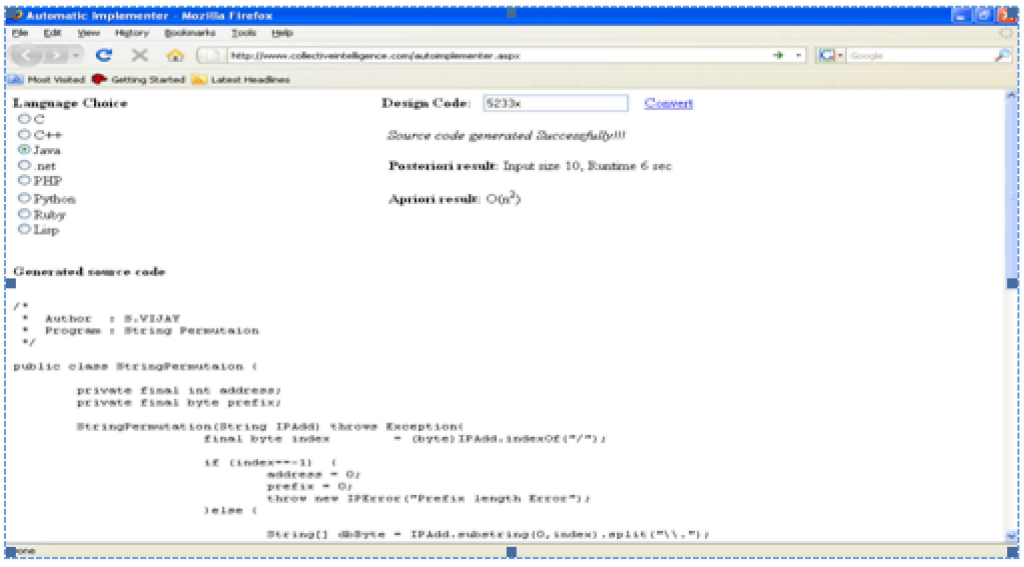

Fig.6 Design implementer and evaluator

2.2.6. Ranking of the Solutions

The posted solutions will be visible to any authenticated end users who search for it. The results will be initially ranked based on the design evaluation. The users can also rate the design. This will boost the ranking for the design posted. The one who rates the design should not be the one who designed it (their identification will be compared). The following screenshot depicts the search results based on the ranking. The problems posted, validated problems, solution provided and the validated solutions will all be saved in a cloud. The ratings too will be stored in cloud which will thereby be made open to public.

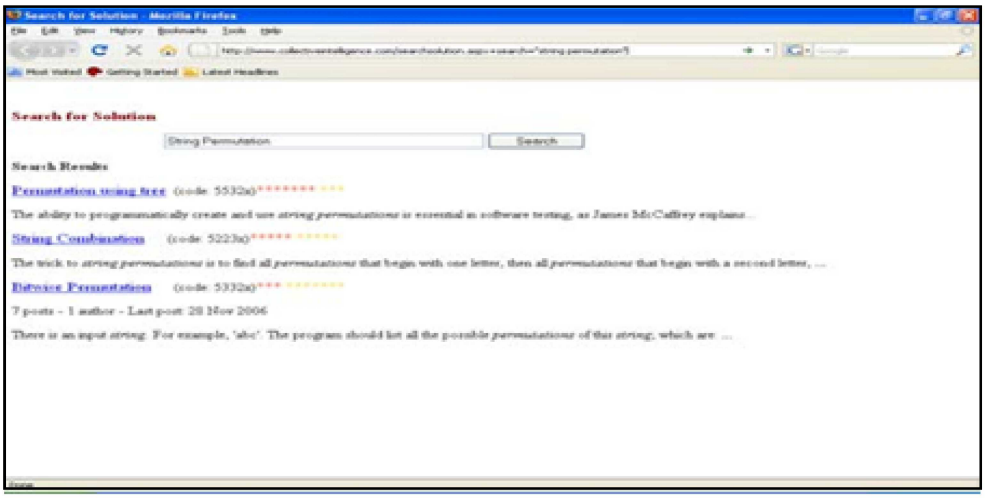

Fig.7 Ranking of the solutions

3. CONCLUSION

This system will bring many ideas to life. It can be used and reused by anyone interested. It will give 'n' number of solutions to any prevailing problem in a simple way and free of cost. It will motivate and also improvise idea provider, designer and the implementer. It paves way for job opportunities too. Builds a healthy network and enlightens the world. If the technique is put into action, this system is expected to bring a new era in the software field.

4. FUTURE ENHANCEMENTS

In the proposed system, the correctness of the design purely depends on the fact that whether the code created runs and gives the expected output. If not, the contributor is expected to correct it. Even a small logical error may collapse the whole design. The system may be enhanced such that it will automatically correct the logical mistakes by using machine learning techniques.

REFERENCES

[1] David A Watt, "Programming Language Design Concepts".
[2] Anthony T.Velty, Toby J.Velte and Robert Elsenpeter, "Cloud Computing A Practical Approach".
[3] Michael Miller, "Cloud Computing: Web-Based Applications That Change The Way You Work And Collaborate Online".
[4] Andrew M.St.Laurent, "Understanding Open Source and Free Software Licensing".
[5] www.opensource.org.
[6] www.socialtext.net.

Optimisation of Plasma Parameters Using Box-Behnken Analysis for Improving Hydrophilicity of Recycled Polyester Knitted Fabric

G. Madhumathi[1] and R. Shanthi[2]

[1]PG Scholar, Apparel Technology and Management, [2]Associate professor, Department Of Fashion Technology, Kumaraguru College of Technology, Coimbatore - 641 049, Tamil Nadu

E-mail:sindhmadhu@gmail.com, shanradkri@gmail.com

Abstract

The current generation of sportswear uses specialized materials to enhance performance of the sports person. Excessive sweat accompanied with increase in weight of the garment during play reduces the performance of the sports person. Hence certain attributes are essential to make sportswear more conducive and comfortable for all types of sports. Polyester (PET) fiber is an invention that can provide many functional attributes far better than the conventional textile materials. Recycled Polyester (RPET) is manufactured from raw material obtained from used PET bottles thereby reducing the raw material used for production of polyester and environmental problems accompanied with the use of virgin polyester. Though polyester has many properties which are suitable for sportswear, basic hydrophilicity is lacking in the fiber. This problem is addressed by subjecting the polyester to oxygen plasma treatment to improve its hydrophilic properties. The plasma parameters like distance between the electrode plates, duration of plasma treatments and applied voltage have been optimized using ox - Behnken analysis. The absorbency, bursting strength and weight loss of single jersey fabrics have been studied to evaluate the effectiveness of plasma treatment. This project aims to develop a hydrophilic sportswear using plasma treated recycled polyester.

Keywords: Box - Behnken analysis, PET bottles, Plasma treatment, Polyester, Recycled polyester.

1. INTRODUCTION

Polyester (PET) fiber is an invention that can provide many functional attributes far better than the conventional textile materials. Many special characteristics have been incorporated in this fiber to cater to the different special and specific needs of the consumer. Polyester alone accounted for approximately 82% of the total MMF consumption in Financial Year 2011 (care-ratings 2012). The plasma technology is considered to be a future oriented process owing to its environmental acceptability and wide range of applications. Recently, plasma treatments have been investigated for producing hydroscopicity in fibers, making them suitable for functional/active wear. The current project aims to develop a hydrophilic sportswear using plasma treated recycled polyester. Though polyester has many properties which are suitable for sportswear, the basic hydrophilicity is lacking in the fiber. This problem is addressed by subjecting the polyester to plasma treatment to improve its hydrophilic properties (Herbet).

2. OBJECTIVES

The effect of plasma treatment on recycled polyester fabric is to be studied and to optimize the plasma parameters using box-behnken analysis.

3. MATERIALS

Recycled polyester fiber was sourced and spun into yarns using ring spinning technology. The spun yarns were knitted into single jersey fabric using Mayer & Cie circular knitting machine of 20" diameter and 24 gauge. Oxygen plasma was used to impart hydrophilic characteristics to the recycled polyester fabric. Treatment time, applied voltage and distance between the two electrode plates are taken as variables for the plasma treatment.

3.1 Material Particulars

The properties of the recycled polyester fiber, yarn and fabric used are given in Table 1.

Table 1 Material Particulars

PROPERTIES		PARTICULARS
FIBER	Fiber denier	1.30
	Fiber length	38mm
YARN	Yarn count	40^s
	Twist per inch	23.1
FABRIC	CPI	45
	WPI	33
	GSM	90
	Thickness	0.34 mm
	BURSTING STRENGTH (kg/cm^2)	6.25
	WVP ($gms/m^2/day$)	242.88
AIR PERMEABILITY (cc/sec/cm)		1.60

4. METHOD

The methodology for experiment is given below in the figure 1.

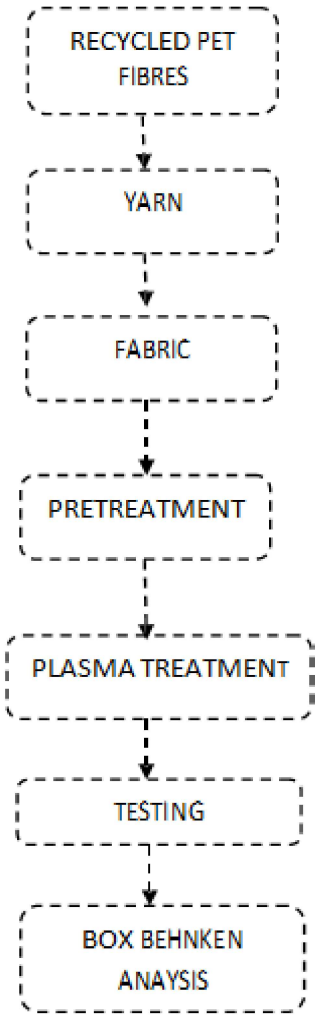

Fig.1 Methodology

4.1 Pre-Treatment Parameters

The fabric pretreatment was done in soft flow machine with following recipe.

- Wetting oil - 1-2gpl
- Lubricating agent - 2gpl
- Soda ash - 1gpl
- Temperature - 95degree
- Time - 30 minutes
- Hot wash
- Cold wash

4.2 PLASMA PARAMETERS

4.2.1. Design of Experiment

Box-Behnken design is a method for developing a mathematical model used to find combinations of factors that yield optimal business performance. Box-Behnken design is a type of response surface method, which provides detailed information about the solution space, allowing researchers to better understand the forces affecting the output of the model. The advantages of Box- Behnken Design include the fact that they are all spherical designs which require factors to be run at only three levels. Box-behnken analysis is an effective statistical method based on a multivariate non-linear

model, and has been widely used for optimizing complex process variables (Liu 2012). This method was adopted to formulate the experimental design, with three variables in three levels to give fifteen different combinations of processing treatments as given in Table 2 and Table 3.

Table 2 Plasma Parameters

LEVEL	ELECTRODE PLATE DISTANCE (CM) X_1	VOLTAGE (VOLTS) X_2	TIME (MINS) X_3
-1	3.5	300	2
0	4.5	350	5
+1	5.5	400	8

Table 3 Details of experiment according to box behnken design of experiment

RUN	Coded Levels of Process Parameters			Experimental Process Parameters		
	X_1	X_2	X_3	X_1	X_2	X_3
1	+1	0	-1	5.5	350	2
2	0	0	0	4.5	350	5
3	0	0	0	4.5	350	5
4	-1	-1	0	3.5	300	5
5	-1	0	+1	3.5	350	8
6	0	+1	+1	4.5	400	8
7	0	+1	-1	4.5	400	2
8	-1	0	-1	3.5	350	2
9	0	0	0	4.5	350	5
10	+1	+1	0	5.5	400	5
11	0	-1	-1	4.5	300	2
12	+1	0	+1	5.5	350	8
13	-1	+1	0	3.5	400	5
14	0	-1	+1	4.5	300	8
15	+1	-1	0	5.5	300	5

All the samples were processed as per the 15 combinations recommended and they were conditioned at standard temperature and relative humidity for further processing. The hydrophilic characteristics of plasma treated recycled polyester fabric was evaluated by the results of sinking time test.

4.3 Statistical Analysis

The optimisation based on the quadratic polynomial to analyse the relationship of each response with the three independent variables is given in the equation 1.

$$Y=B+(B_1*X_1)+(B_2*X_2)+(B_3*X_3)+(B_{12}*X_1*X_2)+(B_{13}*X_1*X_3)+(B_{23}*X_2*X_3)+(B_{11}*X_1*X_1)+(B_{22}*X_2*X_2)+(B_{33}*X_3*X_3)$$

Eq.1 y= predicted response, B= model constant.

B1=slope or linear effect of the input factor *X1*,
B2= quadratic effect of input factor *X2*,
B3= quadratic effect of input factor *X3*,
B12= linear interaction effect between the input factor *Xi* and *Xj*.

Accordingly *Xj* and *Xij* represent the coded independent variables, respectively. Y is represented as sinking time in seconds. The lower the value it reveals with higher hydrophilicity of the material.

4.4 Sinking Time

Sinking method is an indirect measure of transverse wicking of the textile materials. Measurement

of transverse wicking is more important than the measurement of wicking in the longitudinal direction because the fabric is clinging to the body in transverse direction only. AATCC test method 17 – 1994.

5. RESULTS AND DISSCUSSION

5.1 Multiple Regression Equation for Sinking Time

The multiple regression equation for sinking time is given in the equation 2.

$$Y = 8.17 + 0.1125X_1 - 1.675X_2 - 3.10X_3 + 2.1925X_1^2 + 0.0525X_2^2 - 2.0375X_3^3 - 2.815X_1X_2 - 1.035X_1X_3 + 1.65X_2X_3 \quad \text{Eq. 2}$$

The observed values and the predicted values of sinking time calculated using multiple regression equation is given in Table 4.

Table 4 Observed and Predicted Values for Sinking Time

Std Order	Electrode Distance X_1	Time X_2	Voltage X_3	Sinking Time	
				(Observed value)	(Predicted value)
1	5.5	350	2	14.40	12.572
2	4.5	350	5	8.17	8.17
3	4.5	350	5	8.17	8.17
4	3.5	300	5	11.12	9.162
5	3.5	350	8	12.06	10.24
6	**4.5**	**400**	**8**	**3.27**	**3.03**
7	4.5	400	2	4.47	5.96
8	3.5	350	2	9.53	10.277
9	4.5	350	5	8.17	8.17
10	5.5	400	5	5.46	6.037
11	4.5	300	2	11.40	12.61
12	5.5	350	8	5.67	4.302
13	3.5	400	5	4.32	11.442
14	4.5	300	8	4.50	3.11
15	5.5	300	5	14.40	15.017

Table 5 Estimated Regression Coefficients for Sinking Time

Term	Coef	SE coef	T	P
Constant	8.17000	1.0432	7.832	0.001
Electrode Distance	0.11250	0.6388	0.176	0.867
Time	-1.67500	0.6388	-2.622	0.047
Voltage	-3.10000	0.6388	-4.853	0.005
Electrode Distance* electrode distance	2.19250	0.9403	2.332	0.067
Time*time	0.05250	0.9403	0.056	0.958
Voltage*voltage	-2.03750	0.9403	-2.167	0.082
Electrode Distance*time	-2.81500	0.9034	-3.116	0.026
Electrode Distance*voltage	-1.03500	0.9034	-1.146	0.304
Time*voltage	1.65000	0.9034	1.826	0.127

The correlation between the observed and predicted values from the equation was (R^2) 0.918 and the goodness of fit of the model was 91.8%. This indicates good correlation showing that the process variables for the plasma treatment namely 4.5cm electrode distance, 8 minutes duration and 400 voltage are the optimal values for good results of hydrophilicity. From the Table 7 given below, the F value of 6.20 show that the effect of all the parameters taken together was significant at 1% level.

Table 7 Analysis of Variance for Sinking Time

Source	DF	Seq SS	Adj SS	Adj MS	F	P
Regression	9	182.131	182.1314	20.2368	6.20	0.029
Linear	3	99.426	99.4263	33.1421	10.15	0.014
Square	3	35.833	35.8334	11.9445	3.66	0.098
Interaction	3	46.872	46.8718	15.6239	4.79	0.062
Residual Error	5	16.323	16.3233	3.2647		
Lack-of-Fit	3	16.323	16.3233	5.4411	*	*
Pure Error	2	0.0000	0.0000	0.0000		
Total	14	198.455				

5.2 Surface Plot of Sinking Time Vs Voltage, Electrode Distance

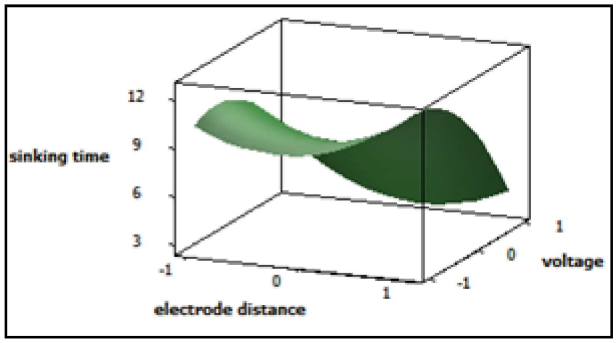

Fig.2 Surface plot of sinking time Vs voltage, electrode distance

From the response surface plot in Figure 2, the minimum sinking time that is the maximum absorbency was observed in (0 level) i.e. 4.5 cm electrode distance and 400 volts, when compared to the (+1) and (-1) levels.

5.3 Surface Plot of Sinking Time Vs Time, Electrode Distance

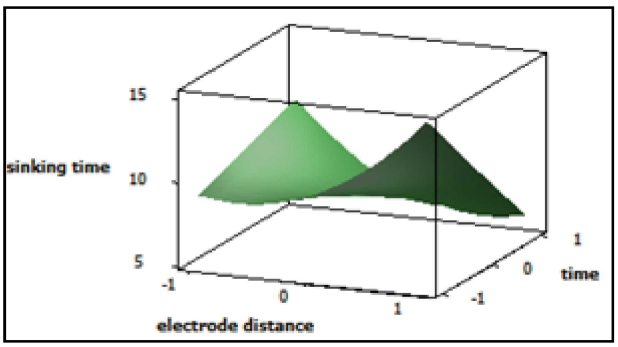

Fig.3 Surface Plot of Sinking Time Vs Time, Electrode Distance

From the response surface plot in Figure 3, when compared to the (+1) and (-1) levels, the maximum absorbency is noted in (0 level) namely 4.5cm electrode distance and with a time duration of 8 mins.

5.4 Surface Plot of Sinking Time Vs Voltage, Time

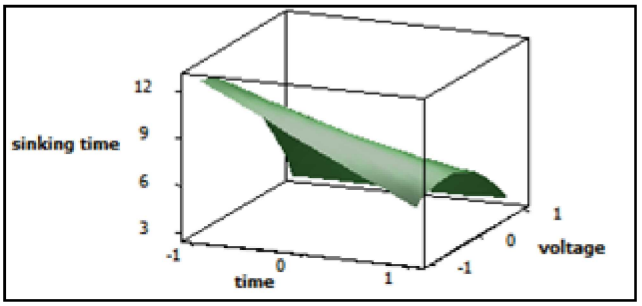

Fig.4 Surface Plot of Sinking Time Vs Voltage, Time

From the response surface plot in Figure 4, the maximum absorbency was noted in (+1 level) namely time duration of 8 minutes and a voltage of 400 volts, when compared to the (0) and (-1) levels.

6. CONCLUSION

The hydrophilicity of the polyester fabric made from recycled polyester fiber has been increased using the oxygen plasma treatment. The optimized processing parameters for plasma treatment of recycled polyester fabric can be taken as 4.5cm electrode distance, 8 minutes duration and a voltage of 400 volts. Box - Behnken model has been used to prove that the optimized process parameters were statistically significant at 1%

level. Recycled polyester fibers from used PET Bottles can be converted to fabric and its absorbency characteristics improved by plasma treatment. The use of Recycled polyester fibers from used PET Bottles can reduce the waste diverted to landfills and the plasma treatment can improve the hydrophilicity of the fabric for comfortable apparels.

7. REFERENCES

[1] T. Herbert, " Atmospheric-pressure Cold Plasma Technology", PLASMA TECHNOLOGIES FOR TEXTILES, SHISOO. pp: 112-119.

[2] Liu G, Guo H, Sun Y, "Optimization of the Extraction of Anthocyanins from the Fruit Skin of Rhodomyrtus Tmentosa (Ait.) Hassk and Identification of Anthocyanins in the Extract Using High-Performance Liquid Chromatography-Electrospray Ionization-Mass Spectrometry (HPLC-ESI- MS)", International Journal of Molecular Sciences, 2012, pp.6292-6302.

[3] MMF – for Masses, for Machines, for Fashion, MMF industry -A Likely Winner", www.careratings.com, (January 2012).

Indian Journal of Engineering, Science, and Technology (IJEST)

(ISSN: 0973-6255)
(A half-yearly refereed research journal)

Information for Authors

1. All papers should be addressed to The Editor-in-Chief, Indian Journal of Engineering, Science, and Technology (IJEST), Bannari Amman Institute of Technology, Sathyamangalam - 638 401, Erode District, Tamil Nadu, India.
2. Two copies of manuscript along with soft copy are to be sent.
3. A CD-ROM containing the text, figures and tables should separately be sent along with the hard copies.
4. Submission of a manuscript implies that : (i) The work described has not been published before; (ii) It is not under consideration for publication elsewhere.
5. Manuscript will be reviewed by experts in the corresponding research area, and their recommendations will be communicated to the authors.

Guidelines for submission

Manuscript Formats

The manuscript should be about 8 pages in length, typed in double space with Times New Roman font, size 12, Double column on A4 size paper with one inch margin on all sides and should include 75-200 words abstract, 5-10 relevant key words, and a short (50-100 words) biography statement. The pages should be consecutively numbered, starting with the title page and through the text, references, tables, figure and legends. The title should be brief, specific and amenable to indexing. The article should include an abstract, introduction, body of paper containing headings, sub-headings, illustrations and conclusions.

References

A numbered list of references must be provided at the end of the paper. The list should be arranged in the order of citation in text, not in alphabetical order. List only one reference per reference number. Each reference number should be enclosed by square brackets.

In text, citations of references may be given simply as "[1]". Similarly, it is not necessary to mention the authors of a reference unless the mention is relevant to the text.

Example

[1] M.Demic, "Optimization of Characteristics of the Elasto-Damping Elements of Cars from the Aspect of Comfort and Handling", International Journal of Vehicle Design, Vol.13, No.1, 1992, pp. 29-46.

[2] S.A.Austin, "The Vibration Damping Effect of an Electro-Rheological Fluid", ASME Journal of Vibration and Acoustics, Vol.115, No.1, 1993, pp. 136-140.

SUBSCRIPTION

The annual subscription for IJEST is Rs.600/- which includes postal charges. To subscribe for IJEST a Demand Draft may be sent in favour of IJEST, payable at Sathyamangalam and addressed to IJEST. Subscription order form can be downloaded from the following link http:// www.bitsathy.ac.in./ ijest.html.

For subscription / further details please contact:

IJEST
Bannari Amman Institute of Technology
Sathyamangalam - 638 401, Erode District, Tamil Nadu Ph: 04295 - 226340 - 44
Fax: 04295 - 226666 E-mail: ijest@bitsathy.ac.in Web:www.bitsathy.ac.in

Indian Journal of Engineering, Science, and Technology

Volume 7, Number 2, July - December 2013

CONTENTS